

DETERMINATION AND IMPROVEMENT OF WEAR AND ABRASION PROPERTIES OF GLASS REINFORCED PLASTIC (GRP) PIPING FOR SLURRY APPLICATIONS

Dissertation submitted in fulfilment of the requirements for the degree of Magister Technologiae:
Metallurgical Engineering

in the
Faculty of Engineering and Technology, Vaal University of Technology

A van der Schyff

9830596



Vaal University of Technology

Supervisor: Prof. P Mendonidis

September, 2014

The financial assistance of Amitech SA, Sasol, Scott Bader, and NCS Resins towards this research is hereby acknowledged. Opinions expressed and conclusions arrived at, are those of the author and are not necessarily to be attributed to Amitech SA, Sasol, Scott Bader, and NCS Resins.

01 November 2013

To Whom It May Concern:

This work has not previously been accepted in substance for any degree and is not being concurrently submitted in candidature for any degree.

This dissertation is being submitted in fulfilment of the requirements for the degree of M-Tech Physical Metallurgical Engineering.

This dissertation is the result of my own independent work/investigation, except where otherwise stated.

Other sources are acknowledged by giving explicit references. A bibliography is appended.

I hereby give consent for my dissertation, if accepted, to be available for photocopying and for interlibrary loans after expiry of a bar on access approved by the Vaal University of Technology.

Signed: _____

Date: _____

ACKNOWLEDGEMENTS

I hereby wish to express my gratitude to the following individuals who enabled this document to be successfully and timeously completed:

- Prof. P Mendonidis
- Mrs. SE van der Westhuizen
- Mr. J Viviers
- Mr. Steve Woodall
- Amitech SA, Sasol, Scott Bader, and NCS Resins

DEDICATION

I dedicate this dissertation to my family, thank you for always believing in me.

ABSTRACT

Glass Reinforced Plastics (GRP) are composite materials comprising a resin matrix reinforced with glass fibers, and are well known for their excellent corrosion resistance and high strength-to-weight ratios. However, their use in slurry transporting pipes is uncertain because the wear resistance of GRP pipe materials is not well documented due to the difficulty encountered in standardizing mechanical properties of GRP pipes. The aim of this project was to identify the main variables that influence the wear and abrasion properties of GRP pipes and the differences of abrasion properties between the continuous and discontinuous filament wound pipes that are manufactured by Amitech SA. In order to achieve the aim of the project, the mechanisms of wear in ductile and brittle matrix GRP composites were investigated. The Pin-on-disk and Jet-impact tests were identified as the best abrasion tests suited for testing GRP composites. Data collected from these tests indicated that the resin type, curing, additive content and- type, fiber content and manufacturing methods are factors affecting wear resistance. It was further found that hard surfaces provided better resistance to abrasive wear, whereas ductile matrices performed better under erosive wear.

TABLE OF CONTENTS

	Page
CHAPTER 1 INTRODUCTION	1
1.1 Introduction	1
1.2 Problem Statement	2
1.3 Motivation for the Research	2
1.4 Aim and Objectives	3
1.5 Importance of the project	4
1.6 Methodology	4
1.7 Lay-out of the Dissertation.....	5
CHAPTER 2 LITERATURE STUDY	6
2.1 GRP Manufacturing Methods.....	6
2.2 Abrasive wear versus Erosive wear	7
2.3 Wear mechanisms of composite materials	8
2.4 Tests used to investigate wear	11
2.4.1 Pin-on-disk test	12
2.4.2 Jet impact test.....	13
2.4.3 Coriolis test	14
2.4.4 Darmstadt Rocker Test.....	16
2.4.5 Semi works tests.....	16
CHAPTER 3 PIN-ON-DISK TEST	18
3.1 Introduction	18
3.2 Factors influencing the wear properties of GRP	18
3.3 Test Apparatus	19
3.4 Test Method	21
3.4.1 Modification of test method	21
3.4.2 Test Parameters	21
3.4.3 Method	22
CHAPTER 4 PIN-ON-DISK TEST –RESULTS	23
4.1 Resin samples	23
4.1.1 Samples Tested.....	23
4.1.2 Sample Appearance	24

4.1.3	Results of resin sample tests.....	25
4.1.4	Discussion of resin sample test results	28
4.2	Pin-on-disk test – Resin samples with fillers	29
4.2.1	Samples Tested.....	29
4.2.2	Results of resin samples with fillers.....	30
4.2.3	Discussion of resin samples with fillers test results.....	32
4.3	Pin-on-disk test – Pipe samples	33
4.3.1	Samples Tested.....	33
4.3.2	Sample Appearance:	33
	Vectus pin.....	33
	Flowtite pin	34
4.3.3	Discussion of Pipe Pin Samples Results.....	34
CHAPTER 5	JET IMPACT TEST.....	44
5.1	Introduction	44
5.2	Test Apparatus	44
5.3	Test Method	45
5.3.1	Test Parameters	46
5.3.2	Test Sand Analysis:	46
5.4	Water absorption test	47
5.5	Method.....	48
5.6	Jet Impact test results	49
5.6.1	Discussion of results.....	49
5.6.2	Difficulties encountered during testing.....	54
CHAPTER 6	CONCLUSIONS AND RECOMMENDATIONS	55
6.1	Variables in GRP pipe construction	55
6.1.1	% Elongation at break of resin.....	55
6.1.2	Post curing of resin and fillers added to resin.....	55
6.1.3	Influence of water absorption.....	56
6.1.4	Influence of impact angle, flow rate and particle size	56
6.2	Recommendations for future research.....	57
REFERENCES	58
APPENDIX A	62
APPENDIX B	NUMERICAL RESULTS - PIN-ON-DISK TEST	63
B1	Test results of resin samples (as-cast samples).....	63
B2	Test results of resin samples (post cured samples)	69

B3 Test results of resin samples with fillers.....72
B4 Test results of GRP pipe samples:.....78
Appendix C.....83
Jet-Impact test results83

LIST OF FIGURES

	Page
Figure 2.1: Typical wall construction of Flowtite pipe.....	6
Figure 2.2: Modified version of Coriolis test apparatus.....	15
Figure 3.1: Configuration of Pin abrasion testing machine used in testing.....	20
Figure 3.2: Test rig used in laboratory for pin-on-disk tests.....	20
Figure 4.1: Resin and catalyst samples with silicon mould.....	24
Figure 4.2: Resin samples cast in the laboratory.....	24
Figure 4.3: Bar chart of average mass loss (g) of the ten as-cast resin types tested.....	26
Figure 4.4: Correlation between EAB and average mass loss (g).....	26
Figure 4.5: Comparison between mass loss (g) of as-cast and post cured resin samples.....	27
Figure 4.6: Absence of correlation between heat deflection temperature and average mass loss (g).....	27
Figure 4.7: Volume loss of flowtite orthophthalic resin samples containing different Amounts of alumina filler.....	31
Figure 4.8: Volume losses of different types of resin samples containing 15% fillers.....	31
Figure 4.9: Volume loss versus abrasion time for Vectus (a) and Flowtite (b) pipe material on 120 grit plate. Steel data plotted for comparison.....	36
Figure 4.10: Volume loss versus abrasion time for Vectus (a) and Flowtite (b) pipe material on 220 grit plate. Steel data plotted for comparison.....	37
Figure 4.11: Volume loss versus abrasion time for Vectus (a) and Flowtite (b) pipe material on 600 grit plate. Steel data plotted for comparison.....	38
Figure 4.12: Comparative volume loss of the Vectus and Flowtite pipe materials on different abrasive grit sizes.....	39
Figure 4.13: Photographs of Vectus and Flowtite pipe material with a magnification of X7. (a) Unabraded flowtite, (b) Unabraded Vectus, (c) Flowtite tested on 600 grit, (d) Vectus tested on 600 grit, (e) Flowtite tested on 220 grit, (f) Vectus tested on 220 grit, (g) Flowtite tested on 120 grit, (h) Vectus tested on 120 grit.....	39
Figure 5.1: Test Apparatus for Jet-Impact Testing.....	45
Figure 5.2: Sand particle size analysis D50=0.622.....	46
Figure 5.3: Sand particle size analysis D50=0.850.....	47
Figure 5.4: Sand particle size analysis D50=1.220.....	47
Figure 5.5: Volume loss on Flowtite material versus slurry velocity using slurries containing sand particles with D50 sizes of 0.622 mm and 0850 mm.....	50

<i>Figure 5.6: Volume loss on Vectus material versus slurry velocity using slurries containing sand particles with D50 sizes of 0.622 mm and 0850 mm.....</i>	<i>50</i>
<i>Figure 5.7: Comparison of wear resistance of Flowtite and Vectus materials using slurries with sand particles size D50 of 0.622 mm.....</i>	<i>51</i>
<i>Figure 5.8: Comparison of wear resistance of Flowtite and Vectus materials using slurries with sand particles size D50 of 0.850 mm.....</i>	<i>51</i>
<i>Figure 5.9: Amount of wear with time during the jet impact test on Flowtite pipe material using slurry with sand with D50 of 0.622 mm.....</i>	<i>52</i>
<i>Figure 5.10: Amount of wear with time during the jet impact test on Vectus pipe material using slurry with sand with D50 of 0.622 mm.....</i>	<i>52</i>
<i>Figure 5.11: Amount of wear with time during the jet impact test on Flowtite pipe material using slurry with sand with D50 of 0.850 mm.....</i>	<i>53</i>
<i>Figure 5.12: Amount of wear with time during the jet impact test on Vectus pipe material using slurry with sand with D50 of 0.850 mm.....</i>	<i>53</i>

LIST OF TABLES

	Page
<i>Table 2.1: Comparison of the wear resistance of Flowtite GRP pipe to that of steel and PE-HD pipe using the Darmstadt Rocker test.....</i>	16
<i>Table 3.1: Comparison of the ASTM standard specification for the pin-on-disk test and parameters used for the pin-on-disk test for GRP pipe samples.....</i>	21
<i>Table 4.1: Resin samples tested with pin-on-disk test.....</i>	23
<i>Table 4.2: Data from numerical results of pin-on-disk test.....</i>	25
<i>Table 4.3: Resin with filler samples tested with pin-on-disk test.....</i>	29
<i>Table 4.4: Densities of resin and fillers used for calculation purposes.....</i>	29
<i>Table 4.5: Average volume loss for resin samples with fillers.....</i>	30
<i>Table 4.6: GRP pipe samples tested with pin-on-disk test.....</i>	33
<i>Table 5.1: Test parameters for Jet-Impact-Test.....</i>	46
<i>Table 5.2: Results of water absorption tests done on (a) Vectus and (b) Flowtite pipe Materials.....</i>	48
<i>Table 5.3: Summary of the variables and result of the 14 jet impact test runs.....</i>	49

LIST OF ANNEXTURES

	Page
<i>APPEDNIX A Post curing schedules of resin samples</i>	62
<i>APPENDIX B Numerical results – Pin-on-disk test</i>	63
<i>Appendix B1 Test results of resin samples (as cast)</i>	63
<i>Appendix B2 Test results of resin samples (post cured samples)</i>	69
<i>Appendix B3 Test results of resin samples (with fillers)</i>	72
<i>Appendix B4 Test results of GRP pipe samples</i>	78
<i>APPENDIX C Numerical results – Jet-Impact test</i>	83

GLOSSARY OF TERMS

Catalyst – a substance that increases the rate of a chemical reaction without itself undergoing any permanent chemical change.

Flowtite – Trade name for GRP pipe manufactured through a continuously advancing mandrel system with chopped strand matt glass fibres and resin.

Glass fibres - A glass thread less than a thousandth of an inch in diameter.

GRP – Glass Reinforced Plastic.

Also known as Fiberglass is a fibre reinforced polymer made of a plastic matrix reinforced by fine fibres of glass. Fiberglass is a lightweight, extremely strong, and robust material.

Mandrel - a shaft to which work is fixed while being turned.

PE-HD – High density Polyethylene.

It is a hydrocarbon polymer prepared from ethylene/petroleum by a catalytic process. It is a kind of thermoplastic which is famous for its tensile strength.

Plastic - A synthetic material made from a wide range of organic polymers such as polyethylene, PVC, nylon, etc., that can be moulded into shape while soft, and then set into a rigid or slightly elastic form.

Resin - a solid or liquid synthetic organic polymer used as the basis of plastics.

Slurry - a semi-liquid mixture, typically of fine particles of solid mixed with water.

Vectus – Trade name for GRP pipe manufactured on a fixed mandrel with continuous glass roving and resin

Wear - Damage, erode, or destroy by friction or use.

CHAPTER 1 INTRODUCTION

1.1 Introduction

Glass Reinforced Plastics (GRP) are composite materials comprising a resin matrix reinforced with glass fibres. The glass fibres can be either continuous filaments or chopped strands. The type of resin is dictated by the intended application of the component in question. Glass reinforced plastics are well known for their excellent corrosion resistance and high strength-to-weight ratios. Thus, pipe manufactured from GRP offers several advantages to pipe manufactured from conventional materials.

Pipelines are extensively used to transport slurries. A slurry is a mixture of a solid and a liquid which do not react with each other chemically and can be mechanically separated (Matousek, 2005; Duraline pipes newsletter, 2004: 3). Generally, two types of slurries can be distinguished: non-settling slurries, in which all particles remain entrained in the liquid, and settling slurries, where suspended particles settle to the lower portion of the pipe. Settling slurries pose problems in terms of flow and pipe wear and need to be transported at a greater critical velocity (Doron et al, 1987; Matousek, 2005). The critical velocity is the minimum velocity required for keeping solids in suspension. The type of flow in a pipe will also influence the abrasive wear resistance of a pipe. Homogeneous flow, usually from fine powder slurries, will result in minimal contact between the solid and the pipe wall and is thus the most desirable from an abrasive wear point of view. In heterogeneous flow, on the other hand, there is a tendency for particles to settle to the bottom of the pipe, but since particles are still not in full contact with the pipe, abrasion is still minimal. Typical examples of slurries that will result in heterogeneous flow are: mine tailings, sand and mineral ores, all with suspended particles of more than 200 micron in size. The successful design a pipeline carrying settling slurries requires prediction of the hydraulic performance of the pipeline. This is given by a relationship between the slurry flow rate and the pressure differential developed over the pipeline at a specific flow rate (Matousek, 2005). For

settling slurries, this implies that a drop in pressure will result in increased friction, which, in turn, will result in higher abrasion and wear losses.

1.2 Problem Statement

This project asks the question:

“Can GRP pipes, with design modifications, be an alternative to High Density Polyethylene (PE-HD) pipe under certain operating conditions?”

PE-HD pipe is currently the preferred material for slurry applications. PE-HD pipe offers several advantages above conventional construction materials such as: polyethylene and PVC; concrete, asbestos-cement; clay, mild steel, rubber-lined steel, metal matrix composites and ductile iron. Specifically, the main advantage is: high abrasive wear resistance, about three to five times longer service life than steel according to a Duraline pipes newsletter (2004: 3) & a US army corps of Engineers publication (1986). Other properties that make PE-HD pipes, specifically the HDPE PE 100 grade, the benchmark for slurry applications are their flexible nature; high impact strength; resilience; high molecular weight; light weight and corrosion resistance (Duraline pipes newsletter (2004: 3)). One disadvantage of PE-HD pipe is its rather limited life span in applications characterized by severe abrasive conditions.

1.3 Motivation for the research

The emphasis on sustainable development, environmental impact and total cost of ownership, has forced companies to source and investigate alternative materials as solutions to the limited life span problem of PE-HD. Large process companies like Sasol, are leaders in the quest for such materials. GRP pipes would be a suitable alternative, if the material could withstand the wear and abrasive conditions commonly encountered when pumping slurry, due to their chemical resistance, and the fact that pipes can be manufactured for specific applications.

Amitech South Africa, one of the largest suppliers of GRP piping to the civil and industrial market has been inundated with enquiries about the possible use of GRP pipes as slurry lines, but very little information on the performance of GRP pipes in slurry applications is available. It is, however, known that GRP pipes are more brittle than PE-HD pipes and not suited for impact loads (Jaeger, et al., 2004). This is a major concern when GRP pipes are installed in pipelines that convey solids at high velocities.

With the above in mind, a joint venture between the Vaal University of Technology, Amitech, Sasol, Scott Bader and NCS Resins was established, to perform small-scale laboratory tests on samples of the GRP piping.

1.4 Aim and Objectives

The aim of the aforementioned tests was to determine the abrasion wear mechanisms and wear rates of the materials, when subjected to varying operating conditions and slurry properties. The tests also helped to identify the main variables in pipe construction that influence the wear and abrasion properties.

The objectives of the project included:

- Identification of the main variables that influence the wear and abrasion properties of GRP pipes;
- Identification of the differences of abrasion properties between the continuous and discontinuous filament wound pipes that are routinely produced by Amitech;
- Comparison of the wear and abrasion data obtained from this study on GRP pipe to those of materials currently considered to be the benchmark in industry.

1.5 Importance of the project

Extensive research has been done on abrasion resistance of non-metallic and composite materials for slurry pipe applications. (Cenna, et al., 2004, Ceschini, et al., 1997, Xu, et al., 2003). These materials include:

- thermoplastic materials such as polyethylene and PVC;
- concrete,
- asbestos-cement;
- clay,
- mild steel,
- rubber lined steel,
- metal matrix composites and
- ductile iron.

Very little research has been done on the wear and abrasion properties of GRP piping. This is probably due to the difficulty encountered in standardizing the mechanical properties of GRP pipe. GRP pipe construction is very application specific, and the intended application will determine the type of resin, the amount and type of glass reinforcement, the type of veiling used and the type and amount of fillers in the matrix, if any. The pipe construction (i.e. continuous or discontinuous winding) will determine the mechanical properties of the pipe (Amianit pipe systems, 2009; Lee, et al., 2001).

This project will provide the opportunity to contribute new knowledge to this field. The test results will provide an indication whether GRP pipe can be used to convey slurry. This will contribute to the development of quality products from the industrial partners, which will enable them to supply competitive products to clients.

1.6 Methodology

The approach to this study was as follows: A literature study was conducted with the aim of identifying the main variables that influence the wear and

abrasion properties of GRP pipes produced through different manufacturing technologies. The literature study covered the following topics:

- Manufacturing processes of GRP-pipes.
- The mechanisms of wear and the different types of wear encountered in pipe systems.
- Mechanisms of wear of ductile and brittle matrix GRP.
- Identification of pipe construction variables that influence wear properties.
- Investigation into- and identification of the different types of abrasion tests suited to the project.

Laboratory testing of the abrasive characteristics of commercially available GRP material was undertaken using abrasion tests identified in the literature. The results emanating from the test work were verified against results published in the literature and with industry specialists. Conclusions drawn from the project were based on verified test results and information from the literature.

1.7 Lay-out of the dissertation

It was decided that the different test methods employed will be addressed in separate chapters. This was due to the fact that the pin-on-disk test evaluated the performance of GRP when abraded, and the jet-impact test evaluated GRP subjected erosion. It was also more logical to discuss the large amount of samples tested using this lay-out. Results from Chapter 4 and 5 was summarised in Chapter 6.

The dissertation will be organized in the following manner:

- Chapter 2: A literature review
- Chapter 3: Pin-on-disk test
- Chapter 4: Pin-on-disk results
- Chapter 5: Jet-impact test and results
- Chapter 6: Conclusions and Recommendations
- Appendices

CHAPTER 2 LITERATURE STUDY

2.1 Introduction

The following chapter provides information on the different manufacturing methods of GRP pipes. Wear and erosion is defined and special attention is given to the wear mechanisms of glass reinforced plastics. This chapter also contains an overview of the different tests available to measure wear and erosion in materials.

2.2 GRP Manufacturing Methods

Amitech South Africa manufactures two types of GRP piping systems: discontinuous filament wound pipes under the trade name Vectus™ and, pipes manufactured through the continuous advancing mandrel process, under the trade name, Flowtite™ (Amianit pipe systems, 2009).

Vectus™ pipes are manufactured from high strength fiberglass filaments and application specific resin systems mainly polyesters and vinyl esters. Vectus™ pipes are produced by the double helix reciprocal filament winding of resin impregnated continuous fiberglass rovings on a rotating mandrel (Amiantit pipe systems, 2009).

Flowtite™ pipe (see figure 2.1) is manufactured from continuous glass fibre reinforcements in the circumferential direction as well as chopped strand and a suitable resin system. The process has the capability of delivering a dual resin system, thus special liner resins can be applied for severe corrosive conditions and less costly resins for the structural, outer portion of the pipe. Isophthalic polyester resin systems are generally used for general applications, but where increased corrosion resistance is required, as in the chemical processing industry, vinyl ester resin systems tend to be used in manufacture. Silica sand may be added to the structure of the pipe to increase the pipe stiffness (Amiantit pipe systems, 2009).

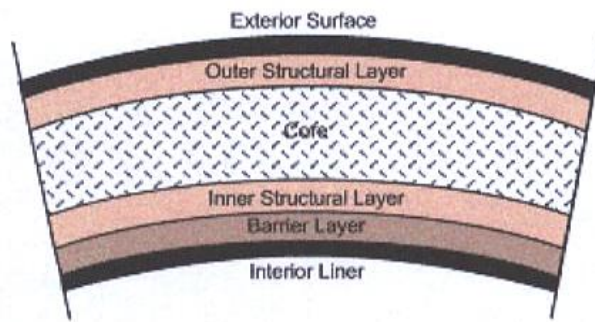


Figure 2.1: Typical wall construction of Flowtite pipe
(Amianit pipe systems, 2009)

The outer structural -, inner structural - and barrier layer consist of application specific resins, the core is a composite of chopped strand matt (glass fibers) and resin and the barrier layer is a composite of veiling and resin.

2.3 Abrasive wear versus erosive wear

To gain a thorough understanding of wear in general and specifically in the more complex context of composite materials requires consideration of the different types of wear encountered. According to Jaeger, et al. (2004), material loss by mechanical means can be divided into abrasive wear and erosive wear. Abrasive wear is described by the American Society for Testing of Materials (1995) as the removal of material due to hard particles or protuberances forced against and moving along a solid surface. On the other hand, erosive wear is defined as material loss resulting from repeated impact of small hard solid particles that are suspended in either a liquid or a gas stream, against a surface.

According to Jaeger, et al., (2004), a more scientific distinction between the two mechanisms is: In abrasion, the force is externally applied and approximately constant over the body, while in erosion the force exerted by the particles on the material is due to their deceleration. Since wear is seen as a loss of material by the process of erosion, this material loss could be

$$\text{expressed by: } m_{loss} = K\rho \left(\frac{mv^2}{2H} \right) \quad (2.1)$$

(Jaeger, et al., 2004)

Where: m is the mass of the material lost through erosion,

v is it's velocity, ($\text{m}\cdot\text{s}^{-1}$)

H is the hardness of the eroded surface, ($\text{kgf}\cdot\text{mm}^2$)

K is a dimensionless factor and

ρ is the density of the material being removed. ($\text{g}\cdot\text{cm}^{-3}$)

The mass loss is thus proportional to the energy provided by the particle, and inversely proportional to the hardness of the eroded material. This relationship is, however, only applicable to ductile materials (Jaeger, et al., 2004).

If we define the ratio of the mass of the material removed to the mass of the sum of all the erosive particles in the slurry, E :

$$E = \frac{K\rho v^2}{2H} \quad (2.2)$$

And we know that a normal load F_N will act on the surface during abrasion,

$$F_N = \frac{\rho v^2}{2} \text{ ie } F_N = \frac{EH}{K} \quad (2.3)$$

We can now define a relationship for abrasive wear:

$$W = \frac{KF_N}{H} \quad (2.4)$$

Where: W is the wear efficiency

According to Jaeger, et al. (2004) the relationship between velocity/energy transfer and wear efficiency makes general sense for composite materials; however the effect of hardness on wear rate of GRP is not as clear. These authors further suggested that either a hard-brittle matrix, or a soft-ductile matrix can exhibit the lowest wear rate, depending whether abrasive or erosive wear conditions persist.

A hard brittle matrix will exhibit a lower wear rate under *abrasive* conditions as it will provide resistance to surface removal from the normal force applied. Thus, the harder the surface the higher the resistance to abrasive wear. Ductile matrix composites will provide little resistance in the aforementioned case. Under *erosive* wear conditions, composites with ductile matrices will provide better resistance to surface removal because the surface will deform

plastically and absorb the impact from entrained particles, whereas, brittle matrices will fracture and break (Jaeger, et al., 2004).

2.4 Wear mechanisms of composite materials

“If we compare fibre reinforced composite materials to monolithic materials, wear resistance can generally be enhanced by introducing a secondary phase into the matrix material” (Lee, et al., 2001). The wear properties can be varied substantially through changes in the microstructure, the morphology, volume fraction and mechanical properties of the reinforcing phase, and the nature of the interface between matrix and reinforcement.

A model for the calculation of abrasion resistance in fibre reinforced composites was proposed by Yen and Dharan (1995), who subdivided wear into 2 stages after it was established that the general rule of mixtures;

$$R_c = \sum_{i=1}^n R_i V_i \quad (2.5)$$

(where: R_c is the wear resistance of the composite in terms of wear resistance R_i , and volume fraction V_i , of each constituent i), did not give an accurate account of wear in fibre reinforced composites.

The two distinct stages proposed by Yen and Dharan (1995) are: Stage 1 where maximum fibre wear resistance occurs and stage 2 where minimum fibre wear resistance occurs.

During the first stage of wear, which is an initial steady state stage, wear in the matrix will be equal to wear in the reinforcement, and the resistance can be described by:

$$R_c = R_m V_m + R_f V_f \quad (2.6)$$

Where: c = composite

m = matrix

f = fibre

The above equation changes if we take the elastic moduli of the fibre and the matrix into account. Increased ductility of the matrix and/or the fibres leads to

lower hardness and yield stress values and higher elasticity of the composite.

$$\frac{E_c}{R_c} = \frac{V_m E_m}{R_m} + \frac{V_f E_f}{R_f} \quad (2.7)$$

This behaviour is, however, only applicable to composites with large diameter fibers (Yen and Dharan, 1995).

The second stage is initiated when the matrix material wears away and the reinforcing fibres are exposed. The matrix will wear away faster than the fibres because the matrix is softer and has lower strength than the fibres. Failure of the fibres will occur by buckling or fracture and it can be assumed that they will not contribute to the overall wear resistance of the composite. The wear resistance during this stage can be described by:

$$R_c = \frac{E_c}{E_m} R_m \quad (2.8)$$

This relationship is applicable to fibre reinforced composites which have very small fibre diameters compared to the matrix diameter, for example: Glass reinforced plastics.

A different approach was followed by Lee et al. (2001). They proposed a physically based abrasive wear model for ductile matrix composites reinforced by hard particles. The authors also made the assumption that the portion of reinforcement removed by wear cannot contribute to the wear resistance of the matrix, but took into account the role of composite microstructure on wear resistance.

Variables influencing the role of the reinforcement in wear resistance are noted as: the relative size and the fracture toughness of the reinforcing particles and the nature of the matrix-reinforcement interface. Wear in composite materials occurs through three possible mechanisms: ploughing, cracking in the reinforcement or at the matrix- reinforcement interface, and particle removal. The wear mechanism encountered will depend on the strength of the matrix- reinforcement interface and the relative size and volume fraction of the reinforcement.

With the above in mind, Lee et al. (2001) proposed a new expression for the abrasive wear rate for particulate reinforced composite:

$$\frac{1}{W_c} = \frac{V_m}{W_m} + C \frac{V_R}{W_R} \quad (2.9)$$

where: C is the contribution coefficient parameter, representing critical reinforcement factors such as fracture toughness and relative size, W is the wear rates of the matrix and the reinforcement respectively and V is the volume fractions of the matrix and the reinforcement.

2.5 Tests used to investigate wear

Extensive research has been done in the field of wear characterization and determination of a variety of different materials including almost all known steels, stainless steels, irons, plastics and polyamides. However, very little research has been done on the study of the wear behaviour of composite materials subjected to abrasive conditions.

The literature presented four types of laboratory tests that are generally performed on materials to determine their wear behaviour:

- The Pin-on-disk test (or pin-on-wheel test and pin-on-drum).
- The Jet-Impact test (liquid impinging test).
- The Coriolis test.
- The Darmstadt Rocker test.

In addition, there is the semi-works test, which is a pilot plant sized simulation method. Infrastructure and funding constraints excluded this test from the test schedule.

Due to the extensive nature of the tests required on the GRP pipe material, it was initially decided to perform all four tests described in the literature. However, due to difficulties encountered during the design of the test equipment as well as time and financial constraints it was decided that the Coriolis test and the Darmstadt rocker test would not be conducted. Both these tests will, nevertheless, be included in the literature study for the sake of

completeness. The Pin-on-disk- and Jet-Impact tests were considered sufficient to provide relevant and valuable data about the behaviour of GRP material, and allow for comparison to steel and PE-HD. The reason for this is that the pin-on-disk method measures abrasive wear whereas the jet-impact test measures erosive wear, so the two methods cover the main two wear mechanisms discussed in the previous sections.

2.5.1 Pin-on-disk test

The first test identified from literature was the pin-on-disk test. (Bijwe et al., 1990; Xu et al., 2003; Indumathi et al., 1999; Iwai et al., 1997). The apparatus is one where a small diametrical specimen of the material (pin) is fixed in a specimen holder (under variable loading) and pressed onto a rotating abrasive disk, rotating at variable angular velocities. The wear of the pin material is determined by measuring the weight of the specimen before rotation and after rotation for a period of time and distance (1996 Annual book of ASTM standards, Section 3). The pins are normally cleaned after each run with acetone, to remove any impurities that might stick to the wear surface. This weight loss is then converted into wear volume using density data.

In the literature, the pin-on-disk apparatus is used extensively to determine the dry sliding wear of materials. Bijwe et al. (1990) made use of this test to determine the wear behaviour of four types of polymers and their fillers-and/or fibre-reinforced composites, while Xu et al. (2003) used a modified version of the apparatus to determine the wear characteristics of thermoset and thermoplastic polymeric materials, used as coatings. Indumathi et al. (1999) investigated the influence of cryo-treatment on wear performance of a series of thermoplastic engineering polymers using the pin-on-disk test. Comparative wear tests, on treated as well as untreated samples under varying loads, were conducted and revealed that cryo-treatment has the potential to increase the wear resistance of some polymers and composites. Wang (1997) investigated the sliding wear behaviour of vanadium carbide coated chrome steels, while El-Raghy et al. (2000) used the pin-on-disk test to determine the wear rate of Ti_3SiC_2 . Other tests similar to the pin-on-disk test are described by Cenna et al. (2000), Zheng et al, (2000) and Ceschini et al. (1997). These include a rotating grinding wheel like apparatus where samples of material are pressed against the outer circumference of the wheel, and a slider-on-cylinder type testing device where a sample of material is pressed against a rotating abrasive cylinder.

The following variables in the pin-on-disk wear apparatus, as outlined in the above mentioned literature, will influence the wear rate of a material:

- Pin loading,
- Rotational speed of abrasive paper disk,
- Grit size of abrasive paper disk,
- Abrasive contact distance between pin and disk,
- Track radius, and
- Contact time.

And, of course, the wear resistance of the material being tested.

The above mentioned parameters were the main variables in the pin-on-disk tests conducted on the GRP pipe, and steel samples. These parameters were recorded and plotted against wear volume.

2.5.2 Jet impact test

The second test method, frequently mentioned in literature, to determine the behaviour of various materials when impinged with a liquid jet, is the jet impact test. This test evaluates the erosive wear characteristics of a material. The test apparatus consists of a specimen holder, a tank and a stirrer to mix the slurry, a nozzle to eject the slurry, a regulator to adjust compressed air pressure and a solenoid valve connected with a timer to control the slurry flow. The flowing stream of slurry, sucked from the tank, is mixed with compressed air in the nozzle, and a slurry jet is ejected at high velocity onto a test specimen, mounted at a certain distance from the nozzle. The jet velocity can be regulated by adjusting the compressed air feed and the impact angle onto the test specimen can be varied to determine the influence of impact angle on wear.

Iwai et al. (1997) used the jet impact test to determine the wear characteristics of tin variants as coatings on a high speed steel substrate. These authors later extended their research to determine the wear properties of 13 different

electrometric liner materials commonly used in slurry pumps, including polymer-, metal- and ceramic coatings.

Rajash et al. (2004) also conducted experiments with the jet impact test apparatus on various polyamides.

The following variables in the jet-impact wear apparatus, as outlined in the above mentioned literature, will influence the wear rate of a material:

- Slurry properties,
- Jet velocity, and
- Impact angle.

These were the main variables considered in the Jet-impact tests conducted on the GRP pipe material in this study.

2.5.3 Coriolis test

The third test identified in literature was the Coriolis test described by Xie et al. (1999) and Hawthorne et al. (2002) (2003). The apparatus is a wheel or disk with a certain diameter containing a diametrical passage, in which two specimen holders are located on either side, equidistant from the rotation centre. The holders each contain a channel with rectangular cross-section, the bottom of which is formed by the test specimen. The slurry, flows from a central chamber outwards through the channels as a rotor is turned. The particles are directed towards the test specimens as a result of Coriolis acceleration. This test was specifically developed to determine particle erosion. The authors conducted tests to determine particle trajectories and particle impact velocities quantitatively. This was done for both diluted and undiluted slurries. The conclusion was that this test mode offers a quick, simple and reproducible means of simulating the wear environment in which particles move rapidly over component surfaces either singly or in a bed. Mcl. Clark et al. (2000) expanded the research done by the above mentioned

authors, to include calculations for the specific energies of the particles moving through the passages of the coriolis tester.

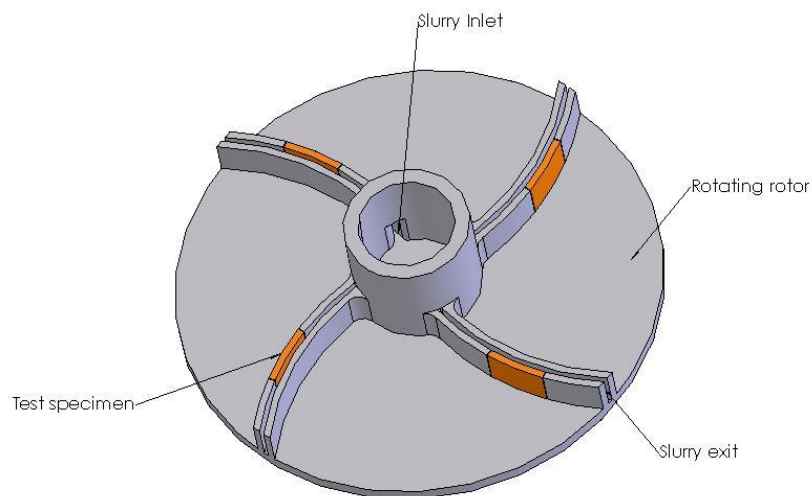


Figure 2.2 Modified version of Coriolis test apparatus

The Coriolis tester was specifically designed to perform wear tests on a wide range of materials. Llewellyn et al, (2004) made use of the Coriolis tester to determine the abrasion resistance of chrome white iron castings typically covered by the ASTM A532 standard, and frequently used in Warman slurry pumps. Hübner et al, (1996) adapted the working principle of the Coriolis tester to determine the erosion-corrosion process of material samples. Solid particles are mixed with a chemical acid and introduced into a similar rotor design as the Coriolis tester. Particles exiting from the rotor impinge on samples of the material, thus producing erosive wear, while the acid produces the corrosive medium.

The following variables in the Coriolis wear apparatus, as outlined in the above mentioned literature, influence the wear rate of materials tested:

- Slurry properties,
- Rotational speed of rotor, and
- Contact and exposure time of slurry with samples.

2.5.4 Darmstadt Rocker Test

In this test, a test specimen one meter long is tilted back and forth with a frequency of 21.6 cycles/minute (Heggemoen and Jonsson, (1997)). The test specimen is a semi-circular channel of pipe which is closed by end plates. The channel pipe contains abrasive slurry of 46% by volume quartz sand (with a particle size of 0.30 mm) in water. The resultant flow rate in the pipe is 0.36 m.s⁻¹. The depth of abrasion is measured at 20 points along the pipe invert over a length of 700 mm, omitting 150 mm at each end of the channel. Measurements are done after 50 000, 100 000, 150 000, and 200 000 cycles. The mean value measured after 100 000 cycles is used as the result of the abrasion test.

Tests conducted by Goddard (1994) and Heggemoen and Jonsson (1997) concluded that Flowtite pipe had an average abrasion loss of 0.34 mm at 100 000 cycles, while PE-HD pipe had an average abrasion loss of 0.3 mm after 400 000 cycles. Steel pipe exhibited a wear rate per unit time of 2.5 times greater than that of PE-HD pipe. These data are presented in Table 2.1.

Table 2.1: Comparison of the wear resistance of Flowtite GRP pipe to that of steel and PE-HD pipe using the Darmstadt Rocker test (Goddard, 1994; Heggemoen and Jonsson, 1997).

GRP Pipe	Steel Pipe	PE-HD Pipe
0.34 mm in 100 000 cycles	0.19 mm in 100 000 cycles	0.075 mm in 100 000 cycles

2.5.5 Semi works tests

A very accurate way of determining the wear rate of pipe is through the semi works tests. These tests comprise a constructed test loop to simulate actual conditions encountered in a plant. Several authors: Goddard (1994), Heggemoen and Jonsson (1997), and the US Army Corps of Engineers (1986), reported on this type of test. A closed loop of test pipe is coupled to a

slurry pump which recirculates suitable slurry. One of the main advantages of this type of testing includes the close simulation of actual plant conditions without the cost implication of failure of the pipe while in operation. A major disadvantage of the method, which excluded it from our testing schedule, is that it requires a very large slurry pump for testing of large diameter pipe, which was beyond the funding and electrical supply resources of the University.

CHAPTER 3 PIN-ON-DISK TEST

3.1 Introduction

The pin-on-disk test is employed when the abrasive sliding wear of materials are to be tested. The sliding wear of a material sample is usually referenced against that of predetermined values, obtained through extensive testing.

The amount of wear on a test specimen is determined by weighing each test sample before and after testing for a set period of time. The recorded mass-loss values of each sample are converted to volume loss values using the best predetermined or calculated material density value. The amount of wear in any system will depend upon a number of system factors, such as: the applied load, machine characteristics, sliding speed, sliding distance, environment and material properties.

3.2 Factors influencing the wear properties of GRP

A very complete overview of all practical aspects related to GRP abrasion can be found in the book: "Corrosion resistant plastic composites in chemical plant design", by Malison John H., (1969). According to the author, factors that affect the abrasion resistance of composites include: the resin, percentage of glass, type of lay-up, toughened matrix, additives to the resin, veiling, impregnated laminates, coupling agents to improve interlaminar adhesion and specialty liners.

It was with the above in mind, and from information gathered during the literature study that test parameters for the pin-on disk test were identified. A very important factor that had to be taken into consideration was the manufacturing method of the pipe. Only manufacturing parameters which could be incorporated into the existing manufacturing process could be altered. Therefore, the effect of percentage of glass, type of lay-up, veiling, impregnated laminates, coupling agents that improve interlaminar adhesion

and specialty liners, were excluded from the test schedule, but will be discussed from a theoretical perspective in the conclusion.

As described in the preceding literature study, the type of resin employed in pipe construction will dictate whether the GRP will have a ductile or a brittle matrix, which in turn will influence the wear properties of the pipe (Jaeger, et al., 2004). The hardness of the matrix will also have an influence on the wear properties. Addition of filler materials to resins will further influence the abrasion resistance of the resin (Malison, 1969 and Friedrich et al., 2005). It was with the above in mind that it was decided to use the pin-on-disk test to evaluate the abrasion resistance of different resin types, resins with increased hardness through post-curing and resin types with fillers. This test would give quick yet accurate results of the behaviour of the material in an abrasive wear situation (Bijwe et al., 1990).

Upon completion of testing of the resin samples and resins samples with fillers, GRP pipe samples were also tested. Testing of Pipe samples were done on different abrasive grit sizes. This gave an indication of the performance of the material when abraded by different sized particles, which may be compared to transporting slurry with different sized particles. The pin-on-disk test of the pipe samples also gave an indication of the wear performance of the different manufacturing technologies used ie. Vectus vs. Flowtite. Results of the pin-on-disk test for GRP were compared to the results for the pin-on-disk test for steel to give an indication of relative abrasion resistance. PE HD samples could not be evaluated with the pin-on-disk test as no measurable material removal took place on the pins with the test parameters used for GRP.

3.3 Test Apparatus

In the pin-on-disk test apparatus (see fig. 3.1), the end of a pin, which may or may not be rotating about its axis, is pressed against an abrasive surface with application of a prescribed normal force while relative motion occurs between

the pin and the abrasive surface. By moving either the abrasive surface or the pin, or both, the pin progressively moves over unused abrasive for a prescribed wear track length (Annual book of ASTM standards, Section 3 1996).

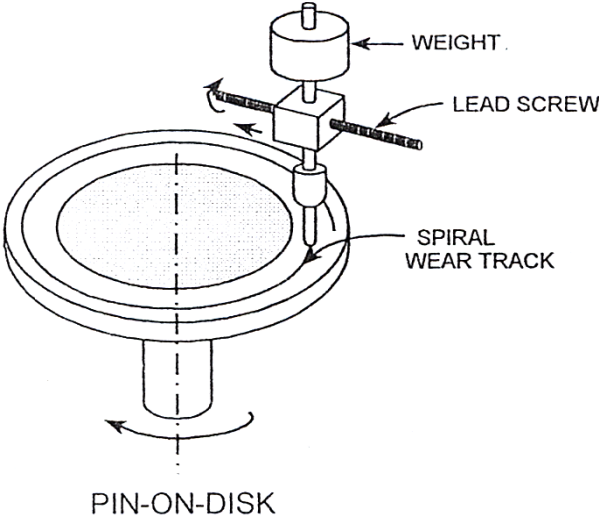


Figure 3.1: Configuration of Pin abrasion testing machine used in testing
(Annual book of ASTM standards, Section 3 1996)

In the test apparatus used for testing in the laboratory, see Fig. 3.2, the end of a resin or GRP disk sample (pin), was held rigidly in a sample holder, and pressed against a silicon carbide abrasive surface. The abrasive surface was rotated to cause relative motion between the pin and the abrasive surface.



Figure 3.2: Test rig used in laboratory for pin-on-disk tests

3.4 Test Method

For the pin-on-disk abrasive tests, the ASTM G132 Standard test method for pin-on-disk abrasion testing was used as reference standard (Annual book of ASTM standards, Section 3, 1996).

During preliminary testing, the pin-on-disc tests were conducted on wet as well as on dry abrasive discs. Samples tested on dry discs exhibited much lower volume loss values as compared to samples tested on wet discs. This was due to the fact that the resin from the GRP clogged the abrasive and caused a polishing action as opposed to a grinding action during testing. All further testing was conducted on wet abrasive disks as it was expected that these conditions would simulate the effect of slurry transportation more accurately.

3.4.1 Modification of test method

Modifications to the ASTM test method were necessary because the ASTM test standard was designed for metal samples with the application of a 66.7 N force. This load leads to very rapid loss of material, which made material loss measurements extremely difficult, especially in thin pipe samples.

It was decided that a test load of 5.078N would be used, as the existing machine in the laboratory could be modified to apply this load.

3.4.2 Test Parameters

Table 3.1: Comparison of the ASTM standard specification for the pin-on-disk test and parameters used for the pin-on-disk test for GRP pipe samples.

	ASTM SPECIFICATION	PARAMETERS USED
Test Load:	66.7 N	5.078 N
Sample diameter:	6.35 mm	14.5 mm
Track length per min.	4 to 16 m	54.98 m

3.4.3 Method

A pin sample of 14.5 mm diameter was placed in a pin holder, onto which a normal force of 5,078 N was applied. The abrasive medium used consisted of a disk with fixed type SiC abrasive particles of 120-, 220-, and 600-grit size respectively. Testing was conducted for 1-minute intervals. The following steps were followed:

- Step 1: A disk sample was cast or cut with a 14.5 mm diameter.
- Step 2: Sample was weighed and initial mass was recorded in grams.
- Step 3: Sample was placed in sample holder and tested for 1 minute.
- Step 4: Sample was removed from sample holder, dried and mass in grams was recorded.
- Step 5: Steps 3 and 4 were repeated until 5 minutes of testing was done.
- Step 6: Mass loss in grams was converted to volume loss in mm³ using the following equation:

$$V_{LOST} = \frac{m_{LOST}}{\rho} \times 1000$$

CHAPTER 4 Pin-on-disk test –RESULTS

4.1 Resin samples

4.1.1 Samples Tested

Ten types of resins were tested; these are listed in Table 4.1.

Table 4.1: Resin samples tested with pin-on-disk test

Sample number	Type of sample tested	%Elongation at break (% EAB)*	Heat deflection temp*	Sample Condition	Grit used
1	Flowtite Orthophthalic Resin – Manufacturer A	3 %	77°C	As-cured**/ Post cured***	220
2	Flowtite Orthophthalic Resin – Manufacturer B	3%	77°C	As-cured	220
3	Isophthalic Liner Resin – Manufacturer A	4 %	75 ± 5°C	As-cured	220
4	Isophthalic Liner Resin – Manufacturer B	4%	75 ± 5°C	As-cured/ Post cured	220
5	Rigid isophthalic thermal resistant core resin - Manufacturer A	2 %	93°C	As-cured	220
6	Orthophthalic Polyester Resin – Manufacturer B	2.3 %	72°C	As-cured	220
7	Urethane Acrylate Modified Isopolyester – Manufacturer B	7 %	65°C	As-cured/ Post cured	220
8	Isophthalic -NPG polyester resin – Manufacturer B	2.5 %	117°C	As-cured	220
9	Epoxy Vinyl Ester 441-400- Manufacturer A	5 %	118°C	As-cured / Post cured	220
10	Epoxy Vinyl Ester 411-350 – Manufacturer A	6%	105°C	As-cured/ Post cured	220

*Data from manufacturers' data sheets (NCS Resins and Scott Bader)

**No heat applied in curing process.

**All resins were post-cured according to schedules provided by manufacturers, (See appendix A).

4.1.2 Sample Appearance

Resin Pin samples of 14.5 mm x 13 mm (see fig. 4.1) were cast in a silicon mould. The resin to catalyst ratio for all samples was 2% (weight) catalyst to resin.



Figure 4.1: Resin and catalyst samples with silicon mould

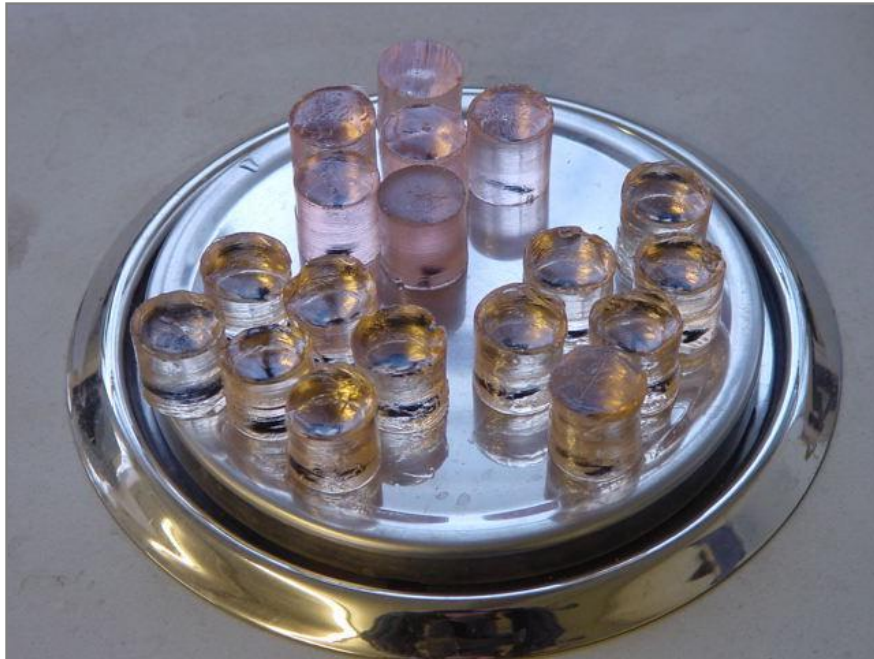


Figure 4.2: Resin samples cast in the laboratory

The density of the resin was approximated to 1 g/cm³ for calculation purposes.

4.1.3 Results of resin sample tests

Six samples of each type of resin were tested on the pin-on-disk method. The numerical results are tabulated in Appendix B1 and summarized in Table 4.2. Figure 4.3 depicts the average mass loss graphically. A reasonable correlation between the average mass loss and the percentage elongation at break was seen (Figure 4.4). All the post cured samples showed less mass loss compared to the as-cast samples (Figure 4.5) There is no correlation between the heat deflection temperature and the average mass loss (Figure 4.6).

Table 4.2: Data from numerical results of pin-on-disk test

Resin number	Resin Type	Average Mass Loss (g)
1	Flowtite Orthophthalic Resin – Manufacturer A	1,213
2	Flowtite Orthophthalic Resin – Manufacturer B	0,784
3	Isophthalic Liner Resin – Manufacturer A	0,840
4	Isophthalic Liner Resin – Manufacturer B	0,628
5	Rigid isophthalic thermal resistant core resin - Manufacturer A	0,897
6	Orthophthalic Polyester Resin – Manufacturer B	0,623
7	Urethane Acrylate Modified Isopolyester – Manufacturer B	0,516
8	Isophthalic -NPG polyester resin – Manufacturer B	0,757
9	Epoxy Vinyl Ester 441-400- Manufacturer A	0,655
10	Epoxy Vinyl Ester 411-350 – Manufacturer A	0,509

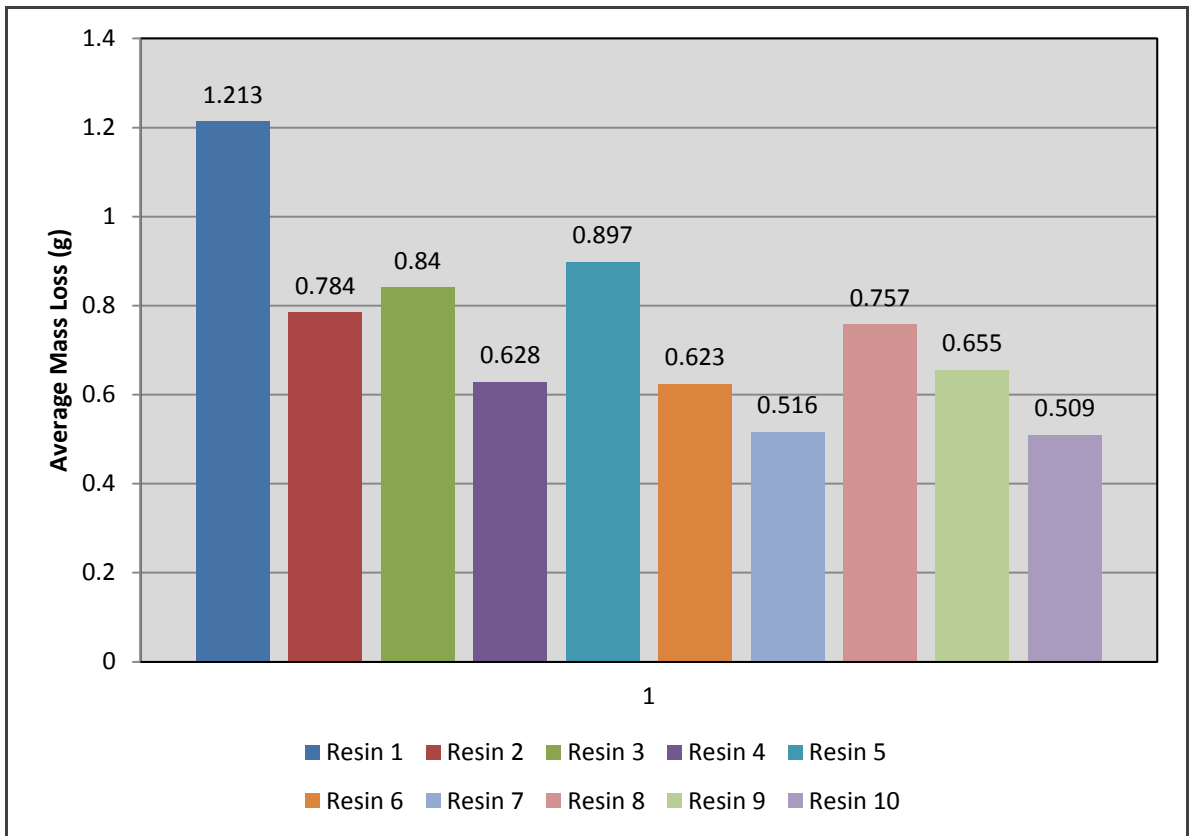


Figure 4.3: Bar chart of average mass loss (g) of the ten as-cast resin types tested.
Data are listed in table 4.2 and Appendix B1

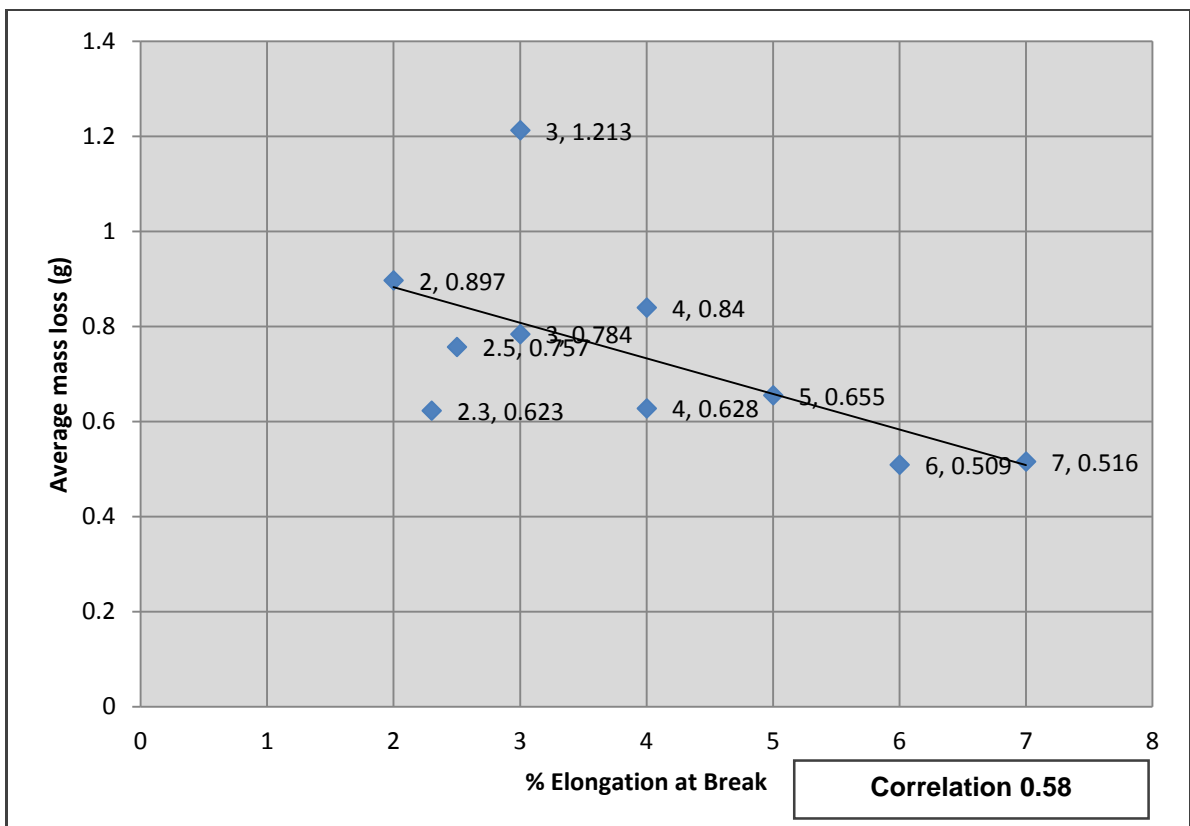


Figure 4.4: Correlation between EAB and Average mass loss (g). Data are listed in table 4.1 and table 4.2

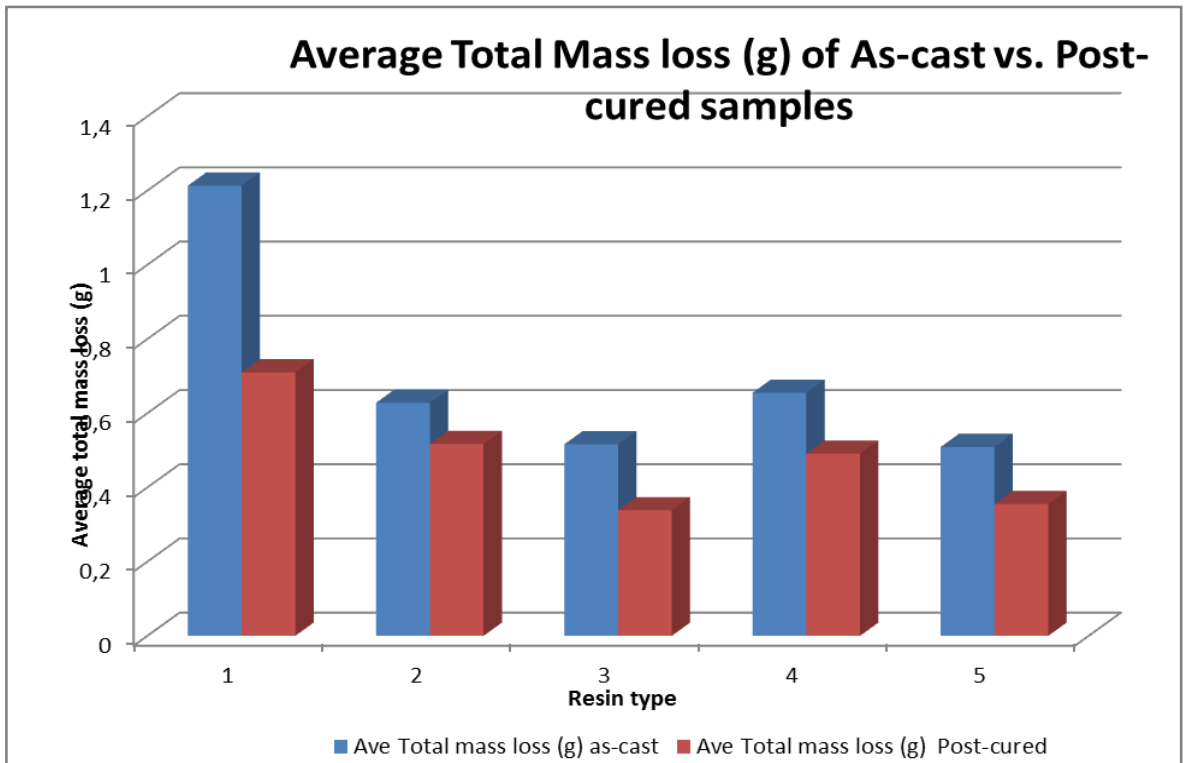


Figure 4.5: Comparison between mass loss (g) of as-cast and post-cured resin samples.

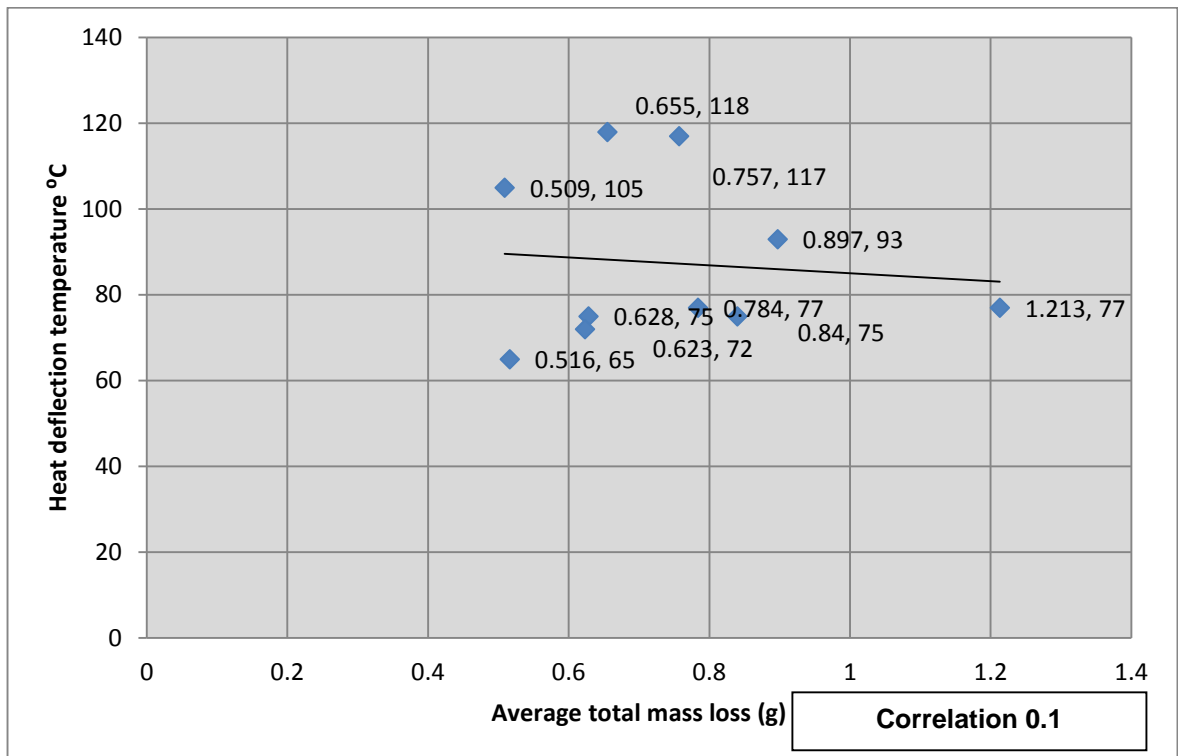


Figure 4.6: Absence of correlation between Heat deflection temperature and Average mass loss (g).

4.1.4 Discussion of resin sample test results

A marked difference in the wear resistance of the different resin types were observed as seen in Figure 4.3. The differences can be explained by the difference in the mechanical properties of the resins. In a sliding wear situation, as simulated in the pin on disk test, resins with higher elongation at break performed better than their counterparts with lower elongation at break (Figure 4.4). This is due to the fact that these materials possess greater toughness and will first plastically deform to absorb some of the force applied. Consequently, material is moved around on the surface of the pin before it is removed. This indicates that the resins with higher elongation at break exhibited lower wear rates, and thus increased wear resistance.

Figure 4.5 illustrates the influence of post curing on the wear resistance of the resin. Only five resins were tested in the post-cured condition due to time constraints. Two resins which are used in the current manufacturing process of GRP-pipe, as well as the three resins which exhibited the highest wear resistance during the pin on disk test were selected. Post curing markedly increased the wear resistance of the resins. Post curing increases the hardness of the material making it more resistant to sliding wear, during initial testing. However, when the hardness of the material is increased, the brittleness is also increased (Jaeger, et al., 2004), which leads to a decrease in toughness, causing higher material removal rates due to chipping and breaking of the resin during the later stages of testing. This can lead to possible problems when there are solids in suspension, as in erosive wear situations.

There was an absence of correlation between the heat deflection temperature and the average mass loss, thus wear resistance. The correlation coefficient was 0.1 (Figure 4.6). This indicates that the heat deflection temperature of the resin is not a factor in wear resistance. However, the wear resistance may still vary with temperature of the material.

4.2 Pin-on-disk test – Resin samples with fillers

4.2.1 Samples Tested

Six samples of each of 3 resin types with different fillers, as summarized in table 4.3, were tested, the data is listed in Appendix B3.

Table 4.3: Resin with filler samples tested with pin-on-disk test.

Sample number	Type of sample tested	Sample Condition	Grit used
1	Flowtite Orthophthalic Resin – Manufacturer A with 5,10,15,20,25,30 % alumina filler	As-Cured	220
2	Isophthalic Liner Resin - 15 % filler Zirconium dioxide	Post-cured	220
3	Isophthalic Liner Resin – 15 % filler Silicon carbide	Post-cured	220
4	Urethane acrylate polyester blend resin 15 % filler Zirconium dioxide	Post-cured	220
5	Urethane acrylate polyester blend resin 15 % filler Silicon carbide	Post-cured	220

Table 4.4: Densities of resin and fillers used for calculation purposes

Density of Resin	
Flowtite Orthophthalic Resin	1.2 g.cm ⁻³
Isophthalic Liner Resin	1.1 g.cm ⁻³
Urethane acrylate polyester blend resin	1.03 g.cm ⁻³
Density of Filler	
Density of Alumina filler	3.98 g.cm ⁻³
Density Silicon carbide	3.21 g.cm ⁻³
Density Zirconium dioxide	5.68 g.cm ⁻³

The following calculations were used to calculate volume loss in the resin samples:

$$V_{LOST} = \frac{m_{LOST}}{\rho} \times 1000 \quad (4.1)$$

$$V_{Lost} = \frac{m_{lost}}{(\rho_{resin} \times fraction) + (\rho_{filler} \times fraction)} \times 1000 \quad (4.2)$$

4.2.2 Results of resin samples with fillers

The average volume loss for each set of samples tested are summarized in table 4.5 and depicted in figures 4.7 and 4.8.

Table 4.5 Average volume loss for resin samples with fillers.

Resin type and filler	Volume loss (cm ⁻³)
Flowtite Orthophthalic Resin – Manufacturer A with alumina filler	
5%	491,79
10%	552,44
15%	619,98
20%	580,39
25%	530,69
30%	460,67
Isophthalic Liner Resin - 15 % filler Zirconium dioxide	422,31
Isophthalic Liner Resin – 15 % filler Silicon carbide	628,43
Urethane acrylate polyester blend resin 15 % filler Zirconium dioxide	467,63
Urethane acrylate polyester blend resin 15 % filler Silicon carbide	525,06

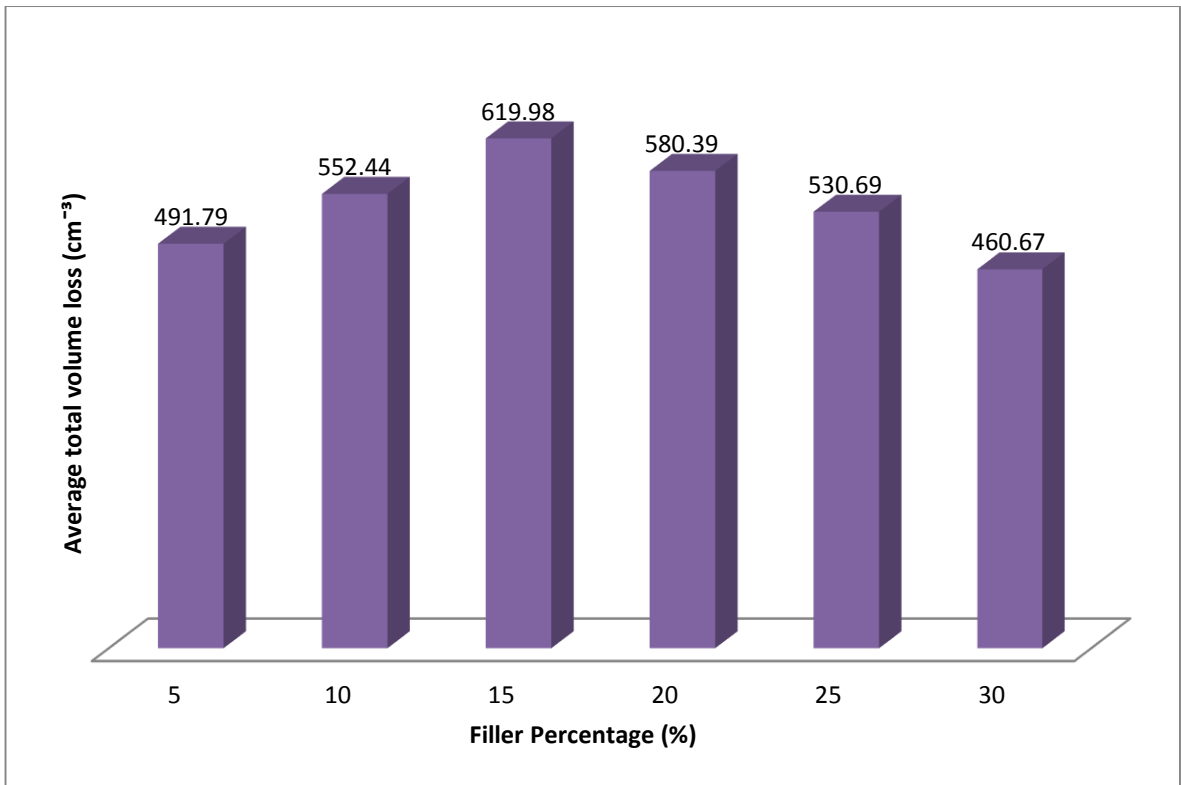


Figure 4.7: Volume loss of flowtite orthophthalic resin samples containing different amounts of alumina filler.

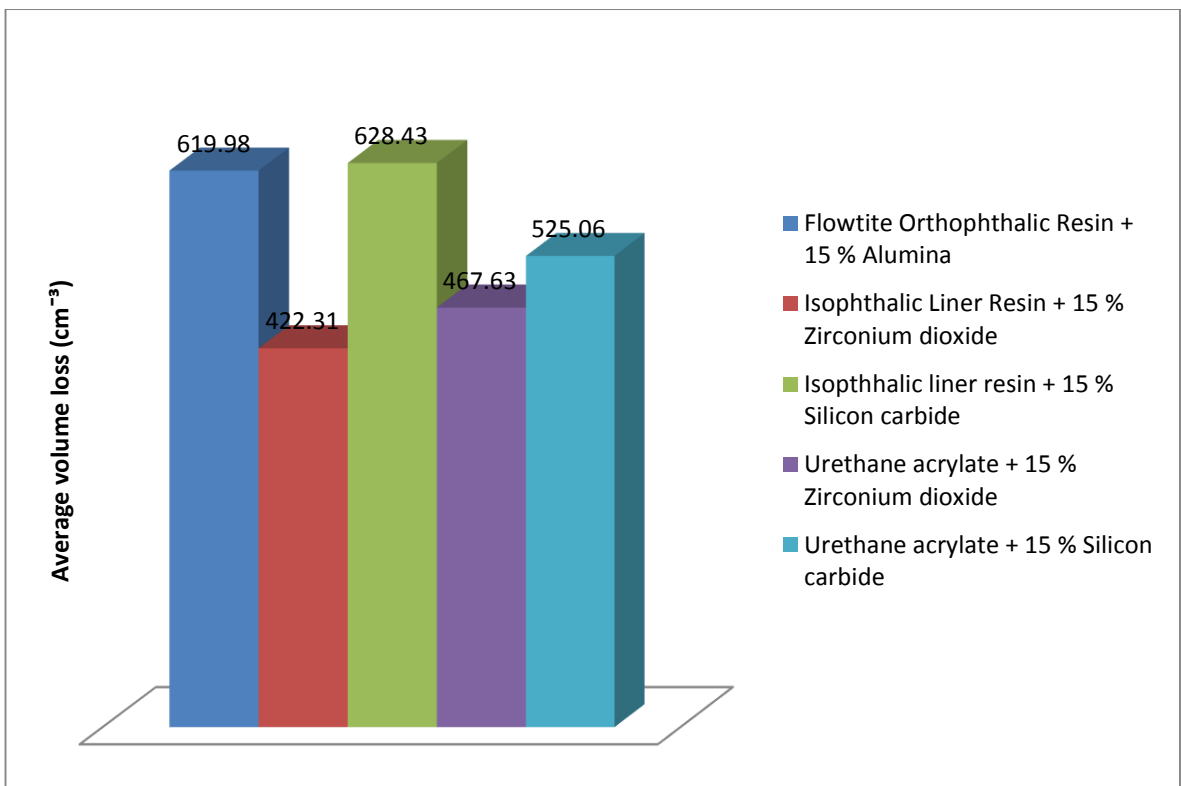


Figure 4.8: Volume losses of different types of resin samples containing 15% fillers.

4.2.3 Discussion of resin samples with fillers test results

It was expected that the fillers would increase the hardness of the composite thus increasing the wear resistance in a sliding wear situation. Increased hardness could however lead to problems when impact is expected in an erosive wear situation as this will also lead to increased brittleness. Malison (1969) discussed the influence of fillers on the tensile strength of laminates and indicated that a decrease in tensile strength was observed when fillers were added in weight percentages of more than 10%, but with no significant effect on the flexural strength or modulus of the laminates.

In this study, fillers added to resins included: alumina, silicon carbide and zirconium dioxide. Alumina was added in weight percentages of 5% up to 30 %, with intervals of 5%. Alumina was used because it is relatively inexpensive and readily available. The above fillers all had hardness values of 9 on the Moh's hardness scale. Figure 4.7 is a plot of volume loss values for samples with 5 weight % to 30 weight % alumina added to the Flowtite Orthophthalic resin in the as cast condition. A steady increase in volume loss could be seen, up to 15%, with a decline in volume loss at higher percentages. The addition of 5 % alumina showed the smallest percentage of volume loss. This may be because all the filler was wetted by resin, thus providing a good bond with the resin, increasing the hardness of the composite which leads to increased wear resistance. For higher percentages of alumina, poor wear resistance can possibly be due to poor wetting of the filler with the resin, or incomplete mixing, causing the filler to fall out during testing, increasing the volume loss of the composite. An increase in wear resistance can be seen in weight percentages of alumina in excess of 20 weight %. This can be because the surface area of the composite comprises mostly of filler material that is hard.

If we compare the effect of different types of fillers with different resin combinations, the best wear resistance, in both cases, were obtained with the addition of zirconium dioxide. The best wear resistance was exhibited by the isophthalic liner resin combined with 15 weight % zirconium dioxide. The urethane resin has a lower elongation at break, leading to a higher hardness,

this combined with high hardness reinforcement, will lead to increased wear resistance.

4.3 Pin-on-disk test – Pipe samples

Both the Vectus and Flowtite commercial varieties of pipe were tested and compared to mild steel, several samples of each were tested using different grit sizes (120,220 and 600 grit) see (Table 4.6). The data is recorded in Appendix B4 and depicted in Figures 4.9 to 4.11.

4.3.1 Samples Tested

Table 4.6: GRP pipe samples tested with pin-on-disk test

Sample number	Type of sample tested	Grit used
1	Vectus pin	120,220,600
2	Flowtite pin	120,220,600
3	Mild steel pin	120

4.3.2 Sample Appearance:

Vectus pin

Samples cut from Vectus pipes with the following construction:

The wall construction consisted of a liner, a structural layer and an outer layer:

Resin – Liner:	DION 272
Resin – Structural:	ULTRASET 242 with continuous roving
Additives:	None
Wall thickness:	7 mm
Density	1.53 g/cm ³

Flowtite pin

Wall construction:

Resin - Liner:	EPS 1
Resin – Structural:	EPS 1 with chopped strand matt
Additives:	Silica Sand
Wall thickness:	5 mm
Density	1.73 g/cm ³

Steel (AISI 1006)* as rolled condition

Carbon composition (wt%)	0.080 %
Tensile strength	330 MPa
Elongation at break	20%
Density	7.87 g/cm ³

(*Data from McGraw-hill.com/Materials Properties Database)

4.3.3 Discussion of Pipe Pin Samples Results

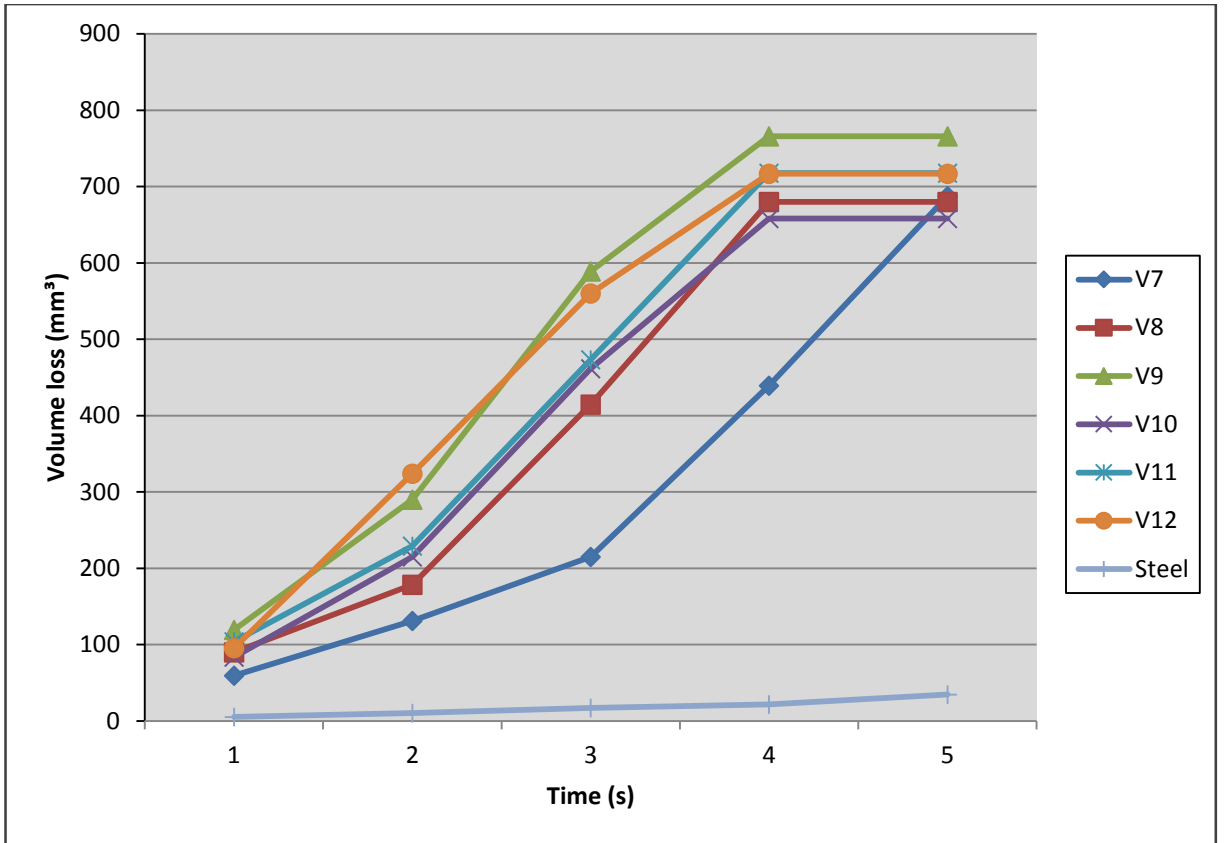
The results plotted in Figures 4.9 to 4.11 show the performance of the GRP pipe in a sliding wear situation. The graphs indicate that data of the Flowtite samples are more consistently distributed than those of the Vectus samples, indicating better precision in the quality of the product, probably because the Flowtite manufacturing process is automated. The performances of the different products on different grit sizes are summarised on a bar chart in figure 4.12. In comparison to the steel samples, the GRP samples demonstrated far greater volume losses, as expected.

A comparison of the volume loss of the GRP to that of HDPE was also attempted; however the pin-on-disk test is not suited to the testing of HDPE. When testing the HDPE on the pin-on-disc apparatus, material removal from the surface in contact with the abrasive could be observed. However, only plastic flow of the material occurred as opposed to material removal in the GRP. Accurate mass loss could thus not be determined.

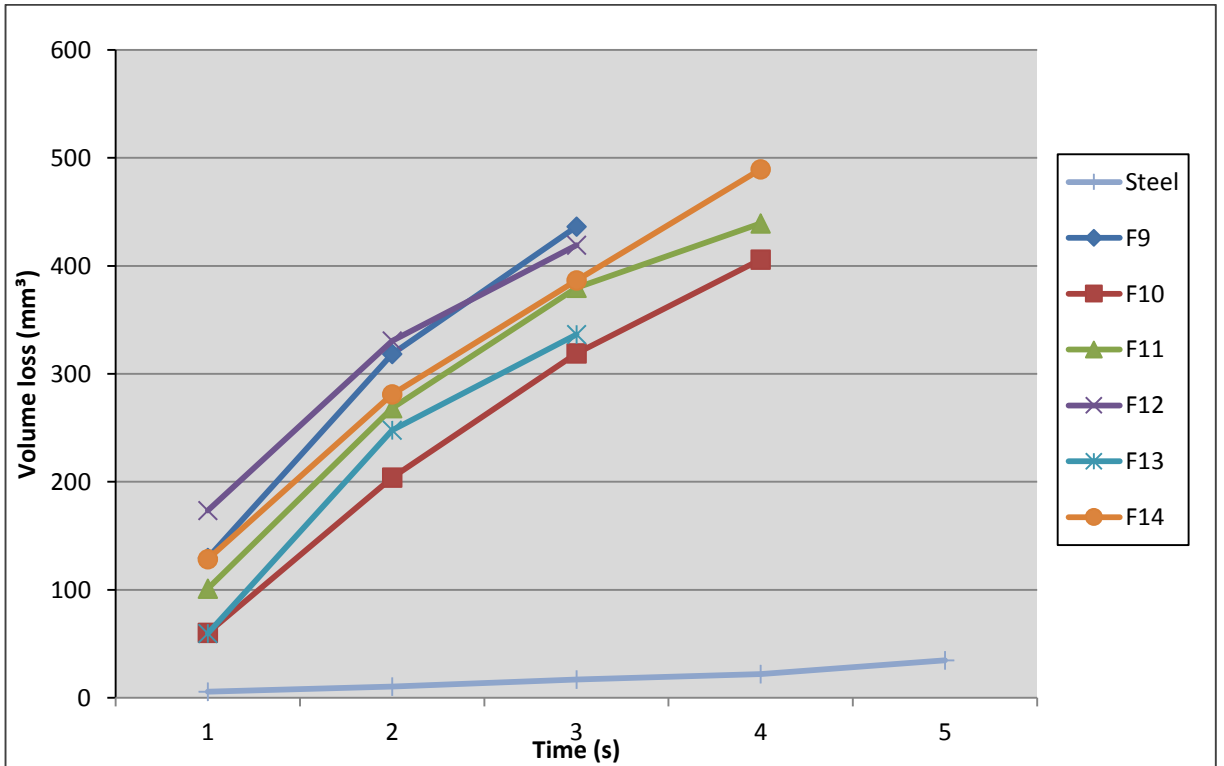
When comparing the volume loss of the Vectus pipe to that of the Flowtite pipe for different abrasive sizes, it was found that the Vectus pipe performed better than the Flowtite pipe on the 600-grit abrasive (Figure 4.11). This is

probably because during this test only the resin, the liner, and the first layer of glass were ground away (Figure 4.13.d). This would lead us to believe that the resin and/ or the resin-glass configuration of the Vectus pipe is more wear resistant than that of the Flowtite.

However, when comparing volume loss values on the 120-, and the 220-grit abrasives, the Flowtite pipe performed better than the Vectus pipe in both cases. This is because the testing continued through to the sand layer of the Flowtite, it is clear that the sand barrier contributes to the wear resistance of the Flowtite pipe.

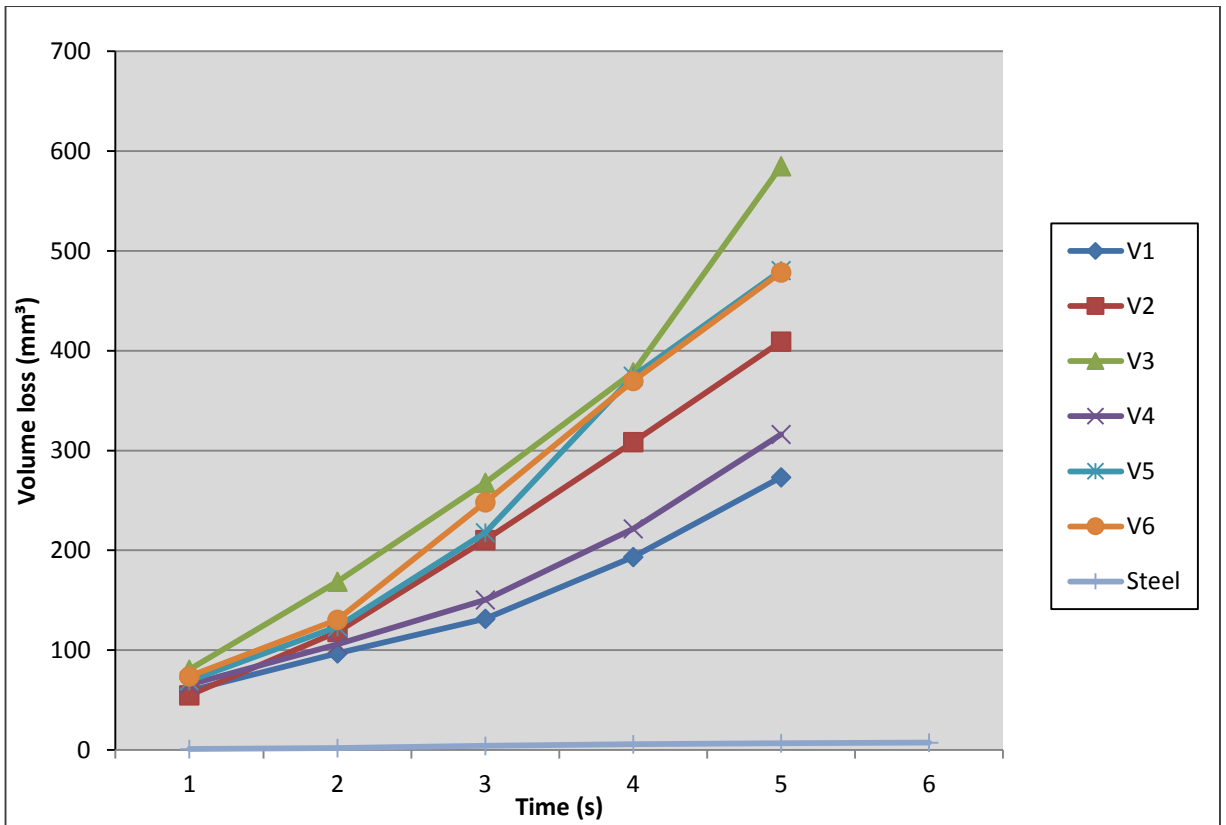


(a)

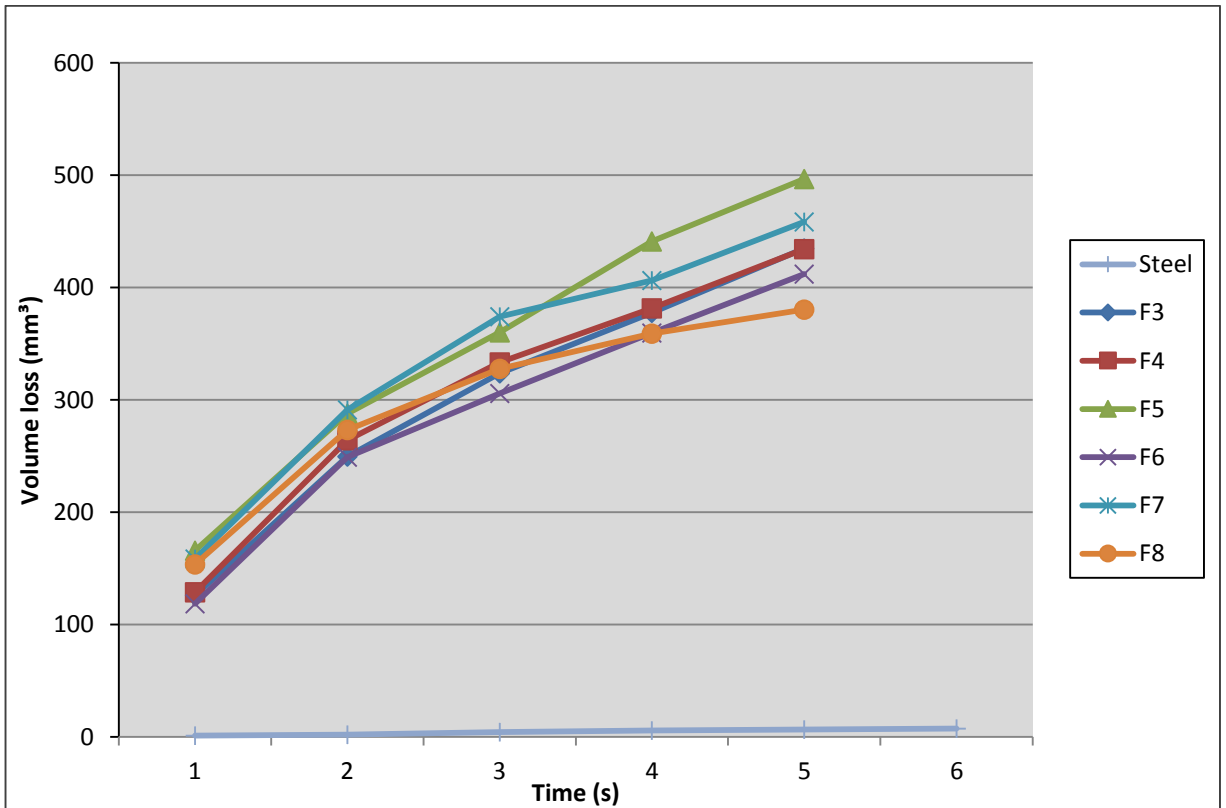


(b)

Figure 4.9: Volume loss versus abrasion time for Vectus (a) and Flowtite (b) pipe material on 120 grit plate. Steel data plotted for comparison

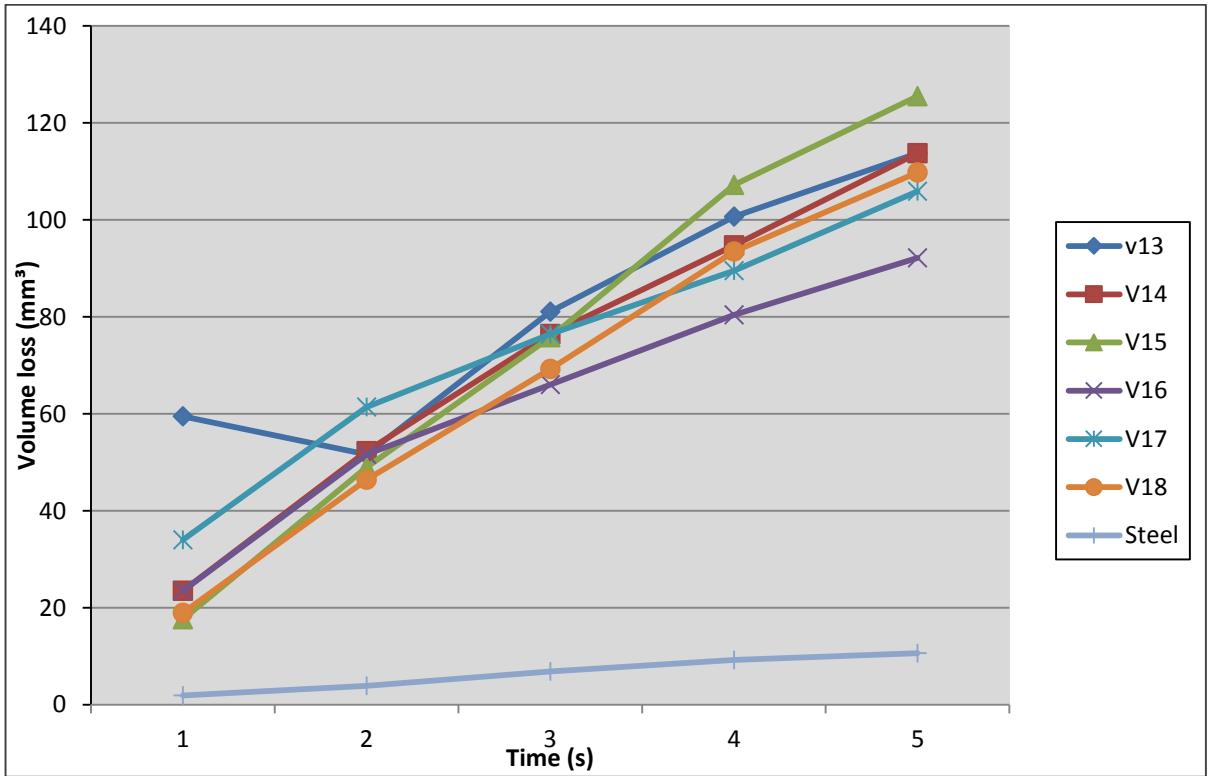


(a)

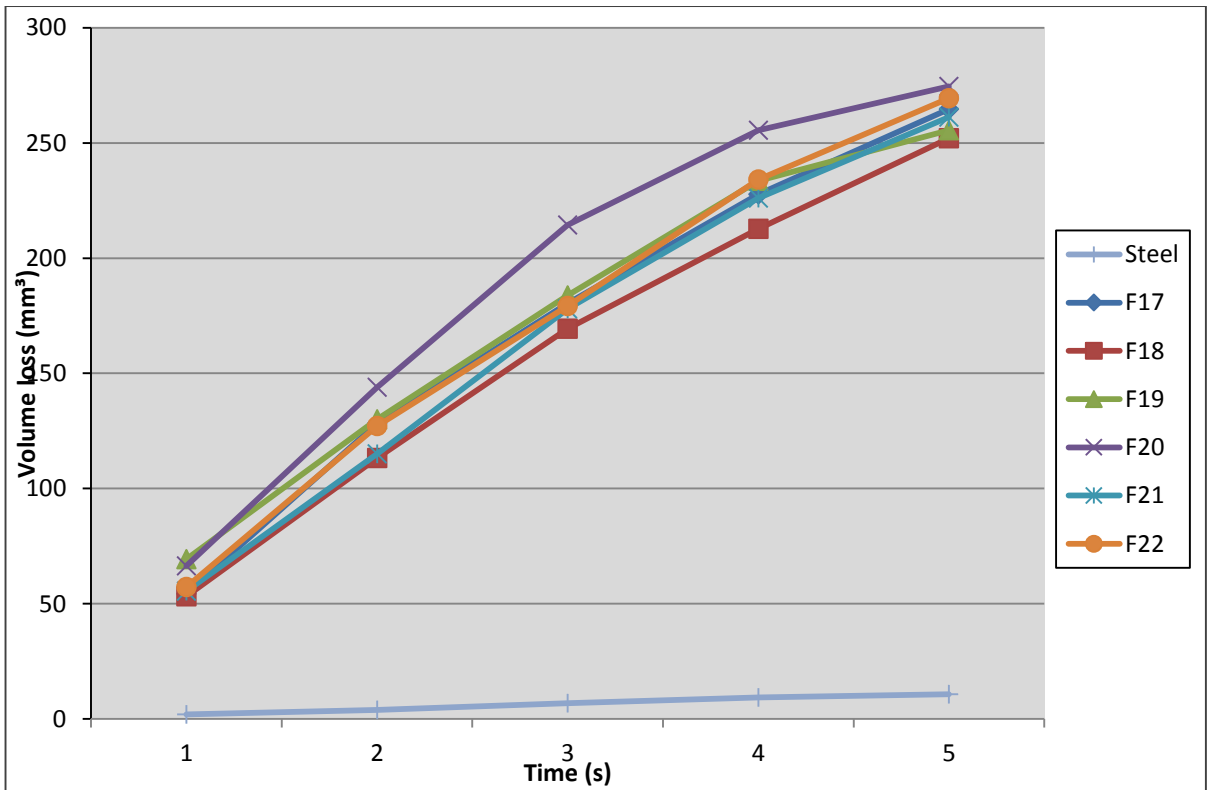


(b)

Figure 4.10: Volume loss versus abrasion time for Vectus (a) and Flowtite (b) pipe material on 220 grit plate. Steel data plotted for comparison



(a)



(b)

Figure 4.11: Volume loss versus abrasion time for Vectus (a) and Flowtite (b) pipe material on 600 grit plate. Steel data plotted for comparison

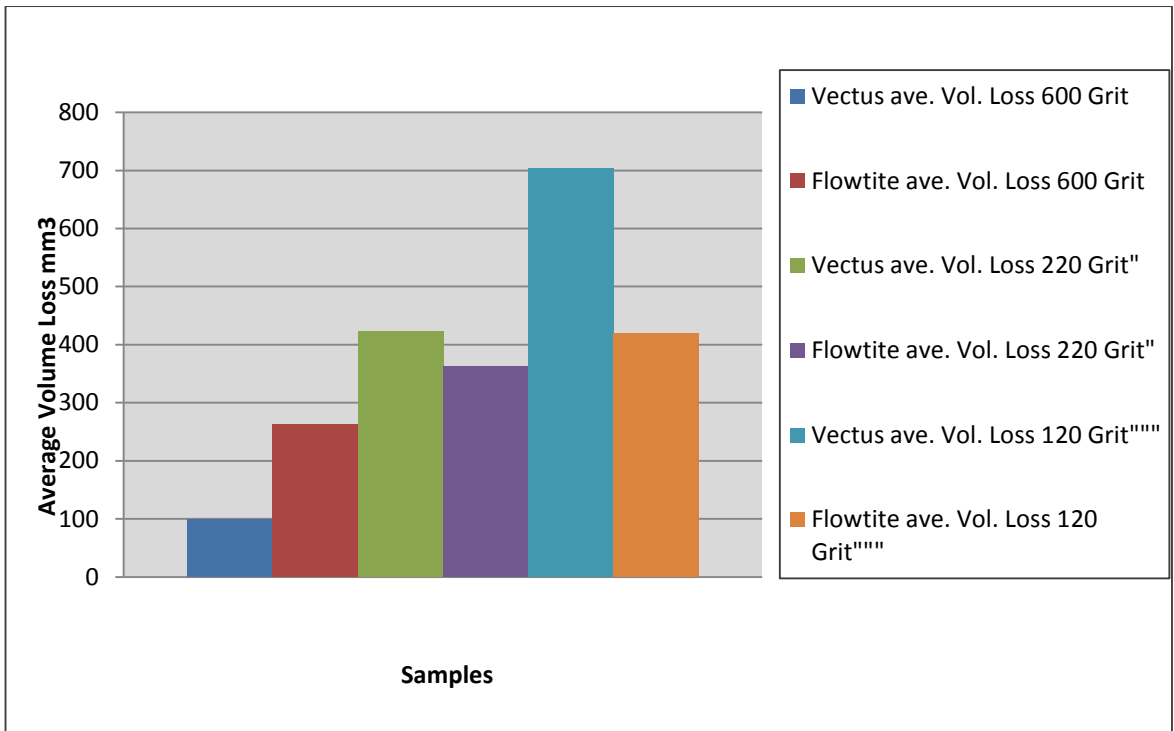
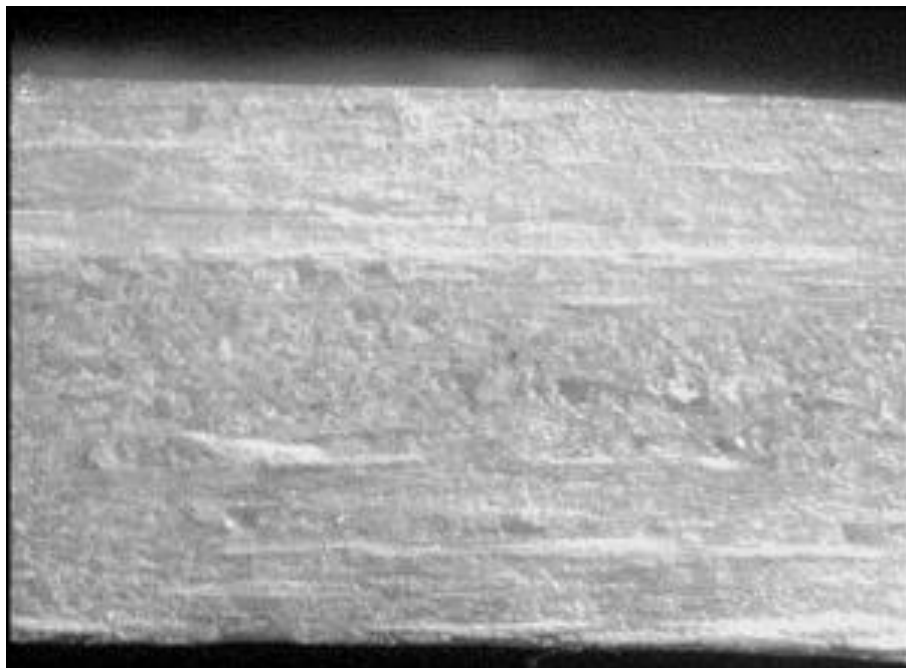
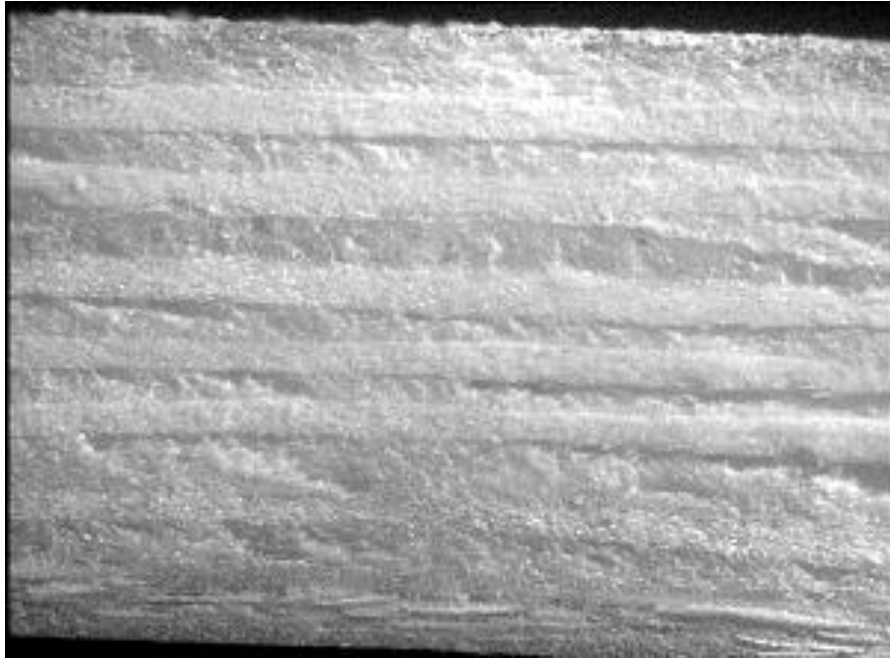


Figure 4.12: Comparative volume loss of the Vectus and Flowtite pipe materials on different abrasive grit sizes

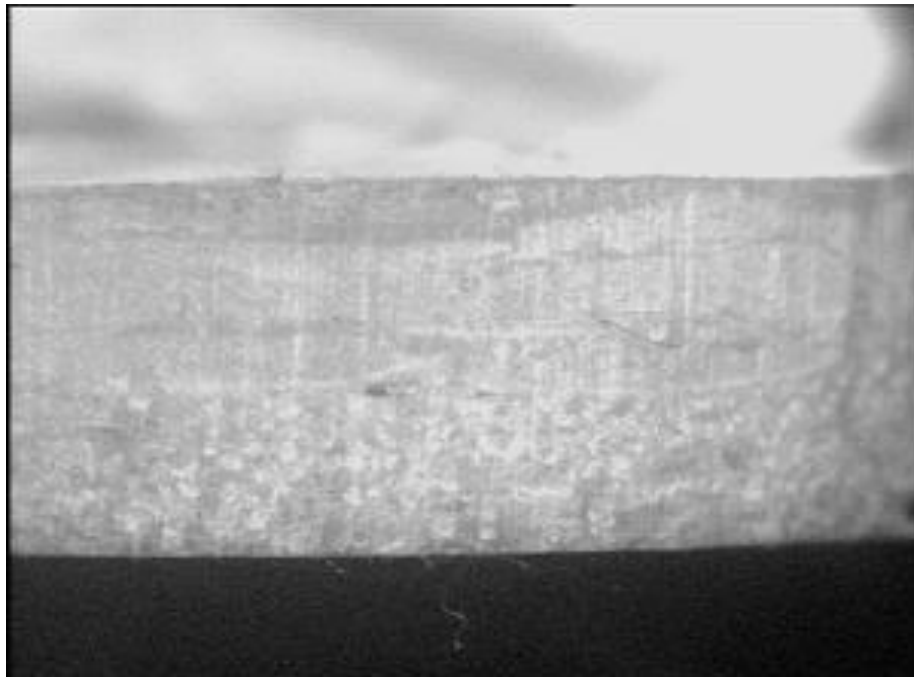
Figures 4.13 (a-h) show that abrasion of the pipe materials is uniform despite the layered nature of the material.



4.13(a)



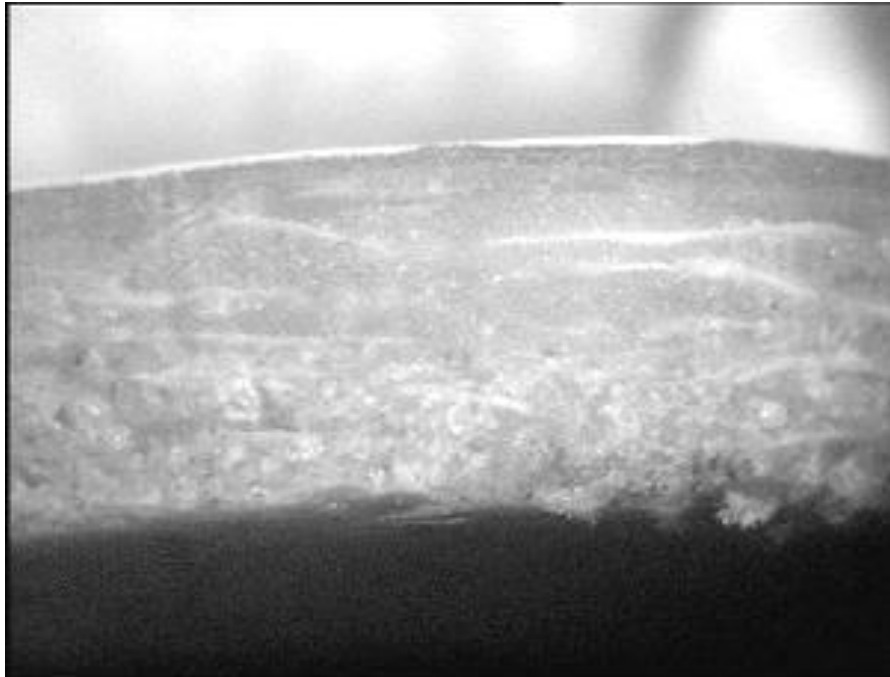
4.13(b)



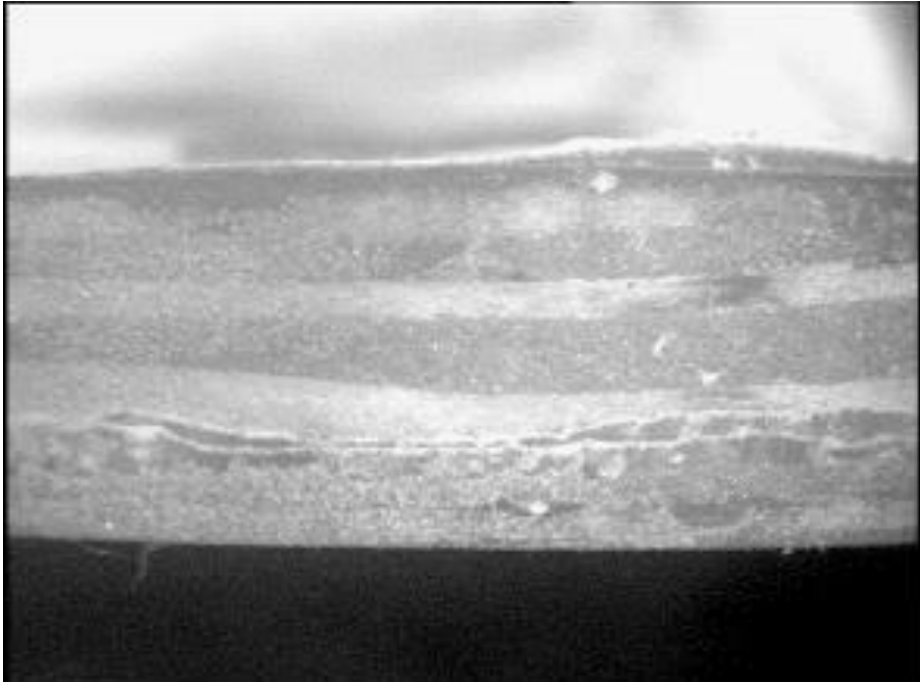
4.13 (c)



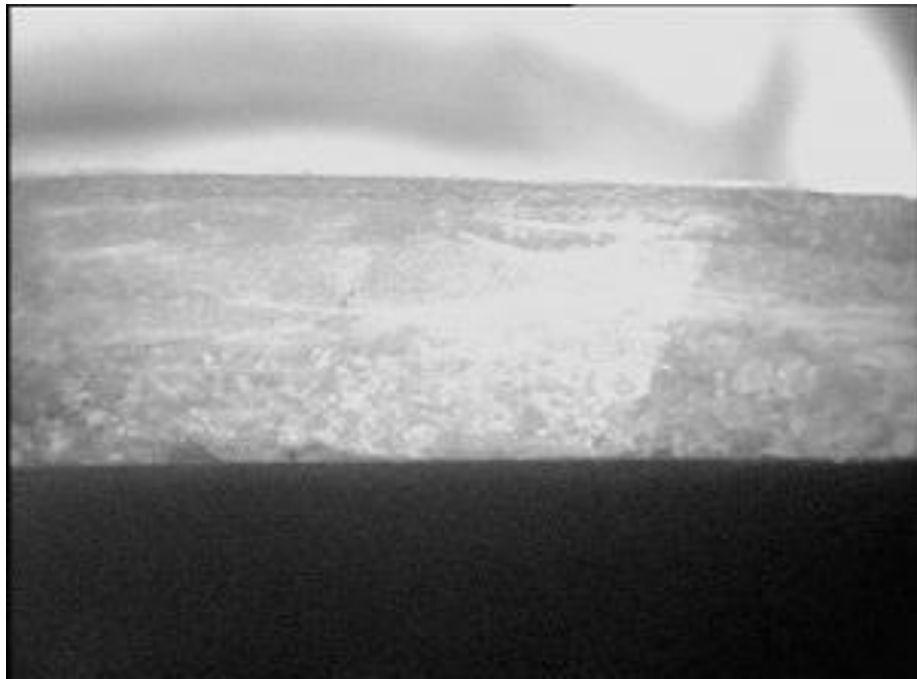
4.13(d)



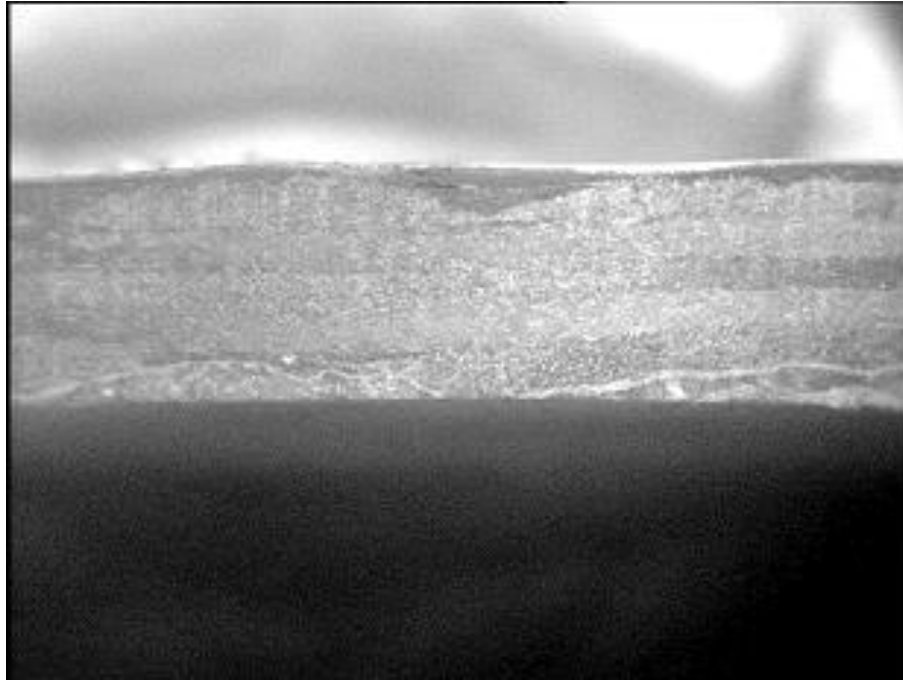
4.13(e)



4.13(f)



4.13(g)



4.13(h)

Figure 4.13: Photographs of Vectus and Flowtite pipe material with a magnification of X7. (a) Unabraded flowtite, (b) Unabraded Vectus, (c) Flowtite tested on 600 grit, (d) Vectus tested on 600 grit, (e) Flowtite tested on 220 grit, (f) Vectus tested on 220 grit, (g) Flowtite tested on 120 grit, (h) Vectus tested on 120 grit.

CHAPTER 5 JET IMPACT TEST

5.1 Introduction

The Jet impact test, was the second test conducted during the GRP wear characterisation tests. This test gave a good indication of the performance of the GRP pipe under erosive wear conditions. During testing sand and water were mixed in a nozzle and ejected onto a sample of GRP piping mounted a certain distance away from the nozzle.

The following variables were varied in the Jet impact wear apparatus:

Slurry properties (sand particle size)

Jet velocity, and

Impact angle. (Testing was conducted at 90°)

5.2 TEST APPARATUS

The test consisted of a specimen holder, a tank, a nozzle to eject the test liquid and sand, a gravity sand feeder, and a regulator to adjust water flow. (Figure 5.1) The flowing stream of water, was mixed with sand in the nozzle, and a slurry jet ejected at high velocity into atmosphere, onto the test specimen, which was mounted a distance of 10 mm from the nozzle. The jet velocity was regulated by adjusting the water feed. The impact angle onto the test specimen could also be varied to determine the influence of impact angle on wear, but was kept at 90°.



Figure 5.1: Test Apparatus for Jet-Impact Testing

5.3 TEST METHOD

The test apparatus consisted of two GRP tanks, one mounted inside the other. The tanks were separated by a sieve which allows water flow between them. A stainless steel nozzle was fixed onto a piping system with valves and a flow meter to regulate water flow to the nozzle. The nozzle was located inside the centre tank; when the apparatus was assembled. Sand was fed manually through a funnel into the nozzle, where it was mixed with water and the slurry was then ejected onto a GRP sample that was fixed in a sample holder ± 10 mm from the nozzle.

5.3.1 Test Parameters

Test were undertaken on both Flowtite and Vectus pipe material using different sand particle sizes and nozzle velocities, as indicated in Table 5.1. A total of 14 tests were done.

Table 5.1: Test parameters for Jet-Impact-Test

Sand Particle Sizes	Nozzle Velocities	Impact Angle
D 50 = 0.622 mm	4.72 m.s ⁻¹	90°
D 50 = 0.850 mm	3.34 m.s ⁻¹	
D 50 = 1.220 mm	2.46 m.s ⁻¹	
Nozzle distance from sample:	± 10 mm	

5.3.2 Test Sand Analysis:

Sand samples were obtained from the Eggo sand mine near Rustenburg. Sand was acquired in bags already sieved with known particle size distributions (Figures 5.2 – 5.4). The sand was checked under the microscope to determine whether the particle shapes were uniform.

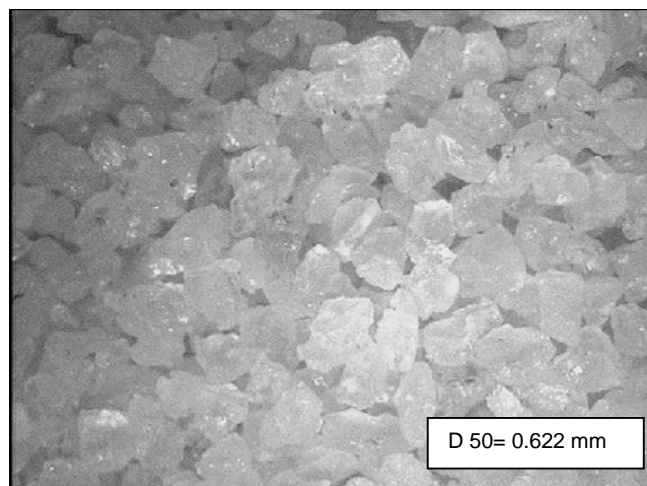


Figure 5.2: Sand particle size analysis D50=0.622

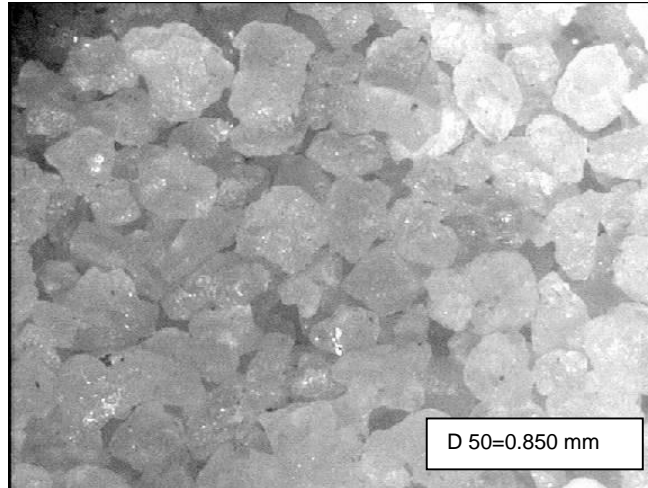


Figure 5.3: Sand particle size analysis D50=0.850

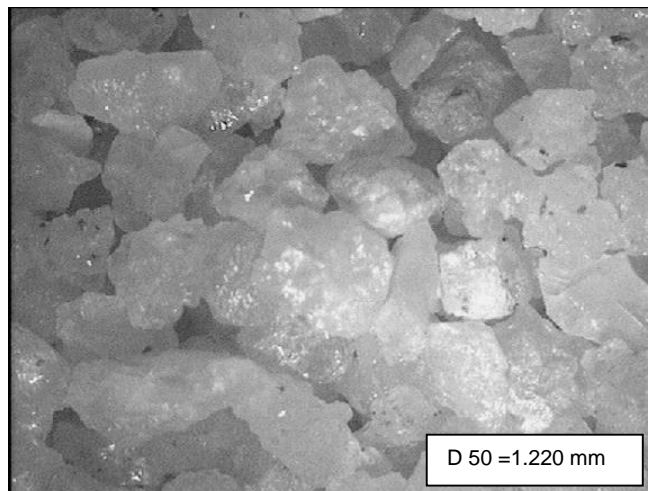


Figure 5.4: Sand particle size analysis D50=1.220

5.4 Water absorption test

Test samples of GRP pipe were immersed in water for 34 days and the increase in sample weight recorded until all samples were saturated. The results are shown in Table 5.2.

Table 5.2: Results of water absorption tests done on (a) Vectus and (b) Flowtite pipe materials.

(a) Vectus pipe:

Duration Day(s)	Mass (g)	Mass increase (g)
1	10.494	0
4	10.519	0.025
6	10.523	0.004
15	10.538	0.015
18	10.551	0.013
34	10.551	0

(b) Flowtite pipe:

Duration Day(s)	Mass (g)	Mass increase (g)
1	10.949	0
4	11.058	0.109
6	11.074	0.016
15	11.098	0.024
18	11.124	0.026
34	11.13	0.006

It was expected that water will act as a plasticizer and this will change the properties of the matrix, causing the matrix to act in a more ductile fashion. The above data indicate that water absorption was minimal.

5.5 Method

- The sample was placed in the sample holder.
- The water flow was switched on and the flow rate set.
- 1000 g of sand was weighed and fed through funnel into nozzle.
- The time to feed sand through nozzle was measured and recorded.
- The water flow was closed and the wear depth measured and recorded.
- Steps 2 to 6 was repeated until sample failure.

5.6 Jet Impact test results

A total of 14 test runs were done using the parameters outlined in Table 5.1. The test runs were labelled samples A to N, and the results of the tests are listed in Appendix C and summarised in Table 5.3.

Table 5.3: Summary of the variables and result of the 14 jet impact test runs

Material Type	Sample	Sand particle size, D50 (mm)	Slurry velocity (m/s ⁻¹)	Volume loss mm ³ /s ⁻¹
Flowtite	A	0.622	4.72	0.007171
	C	0.622	3.34	0.002836
	E	0.622	2.46	0.000957
	G	0.850	4.72	0.008082
	I	0.850	3.34	0.002466
	K	0.850	2.46	0.000141
	M	1.268	4.72	0.01098
Vectus	B	0.622	4.72	0.007475
	D	0.622	3.34	0.002428
	F	0.622	2.46	0.001104
	H	0.850	4.72	0.009506
	J	0.850	3.34	0.002563
	L	0.850	2.46	0.000933
	N	1.268	4.72	0.009306

5.6.1 Discussion of results

Greater wear is produced by coarser sand particle sizes in the slurry only at higher slurry velocities for both the Flowtite and Vectus materials (Figures 5.5 and 5.6).

At high slurry velocities the, Flowtite material has greater wear resistance than the Vectus material, but the converse is true at lower flow rates (Figures 5.7 and 5.8). This is true for sand particles sizes (D 50) of 0.622 mm and 0.850 mm, although it is more pronounced with the 0.850 mm particle sizes.

Figures 5.9 – 5.12 depict plots of the data listed in Appendix C showing the decrease of the wall thicknesses with time due to the slurry impact. These data show that the rate of abrasion (wall thickness decrease) increases with increasing slurry velocity. Figures 5.9 – 5.12 show that the rate of material

loss is not constant, probably a result of the composite nature of the material with the glass fibres having greater resistance to abrasion than the matrix. The sand layers of the Flowtite material and the outer (post-cured) layers of the Vectus material also showed slower rates of volume loss.

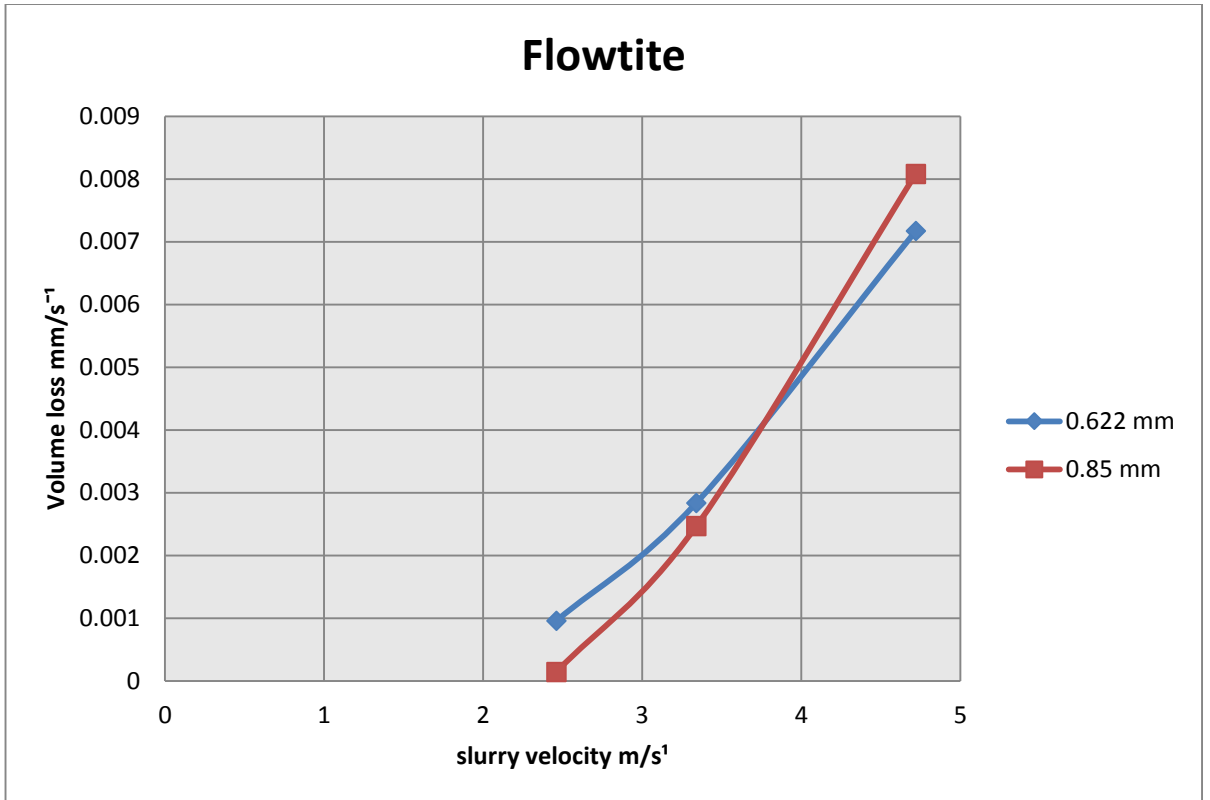


Figure 5.5: Volume loss on Flowtite material versus slurry velocity using slurries containing sand particles with D50 sizes of 0.622 mm and 0850 mm

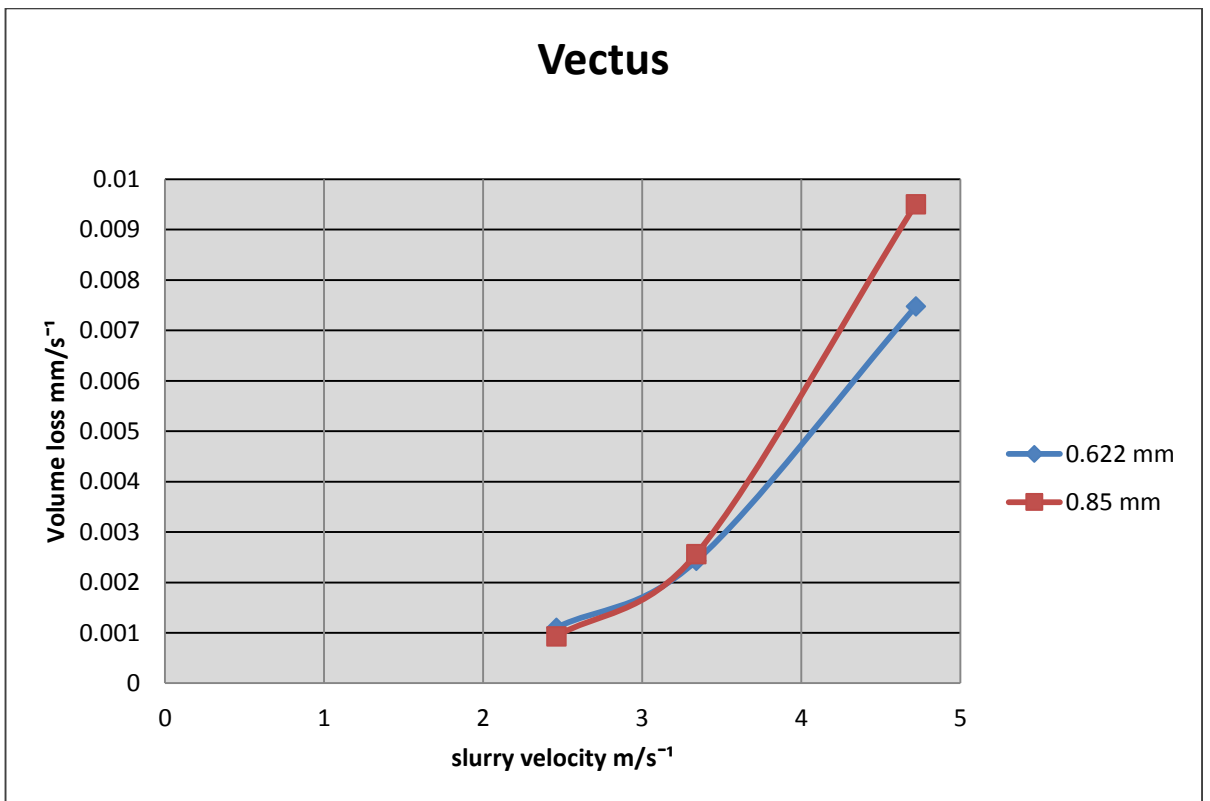


Figure 5.6: Volume loss on Vectus material versus slurry velocity using slurries containing sand particles with D50 sizes of 0.622 mm and 0850 mm

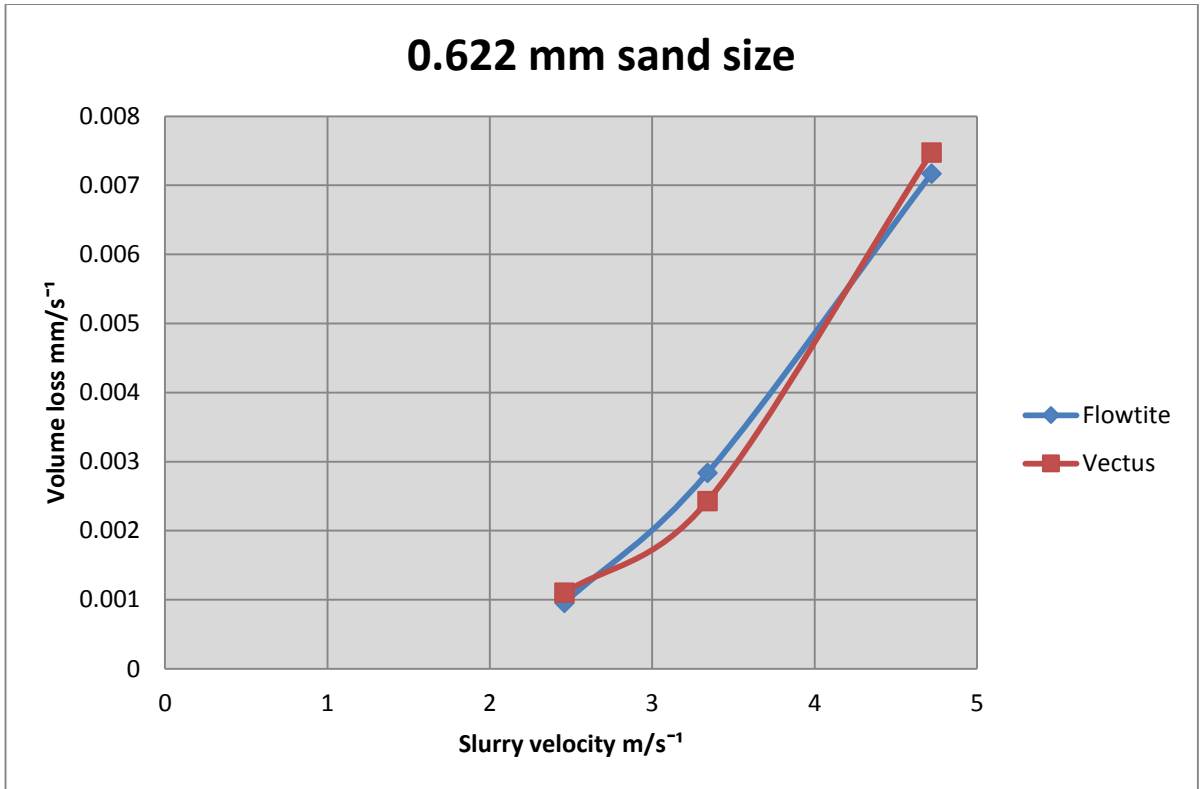


Figure 5.7: Comparison of wear resistance of Flowtite and Vectus materials using slurries with sand particles size D50 of 0.622 mm

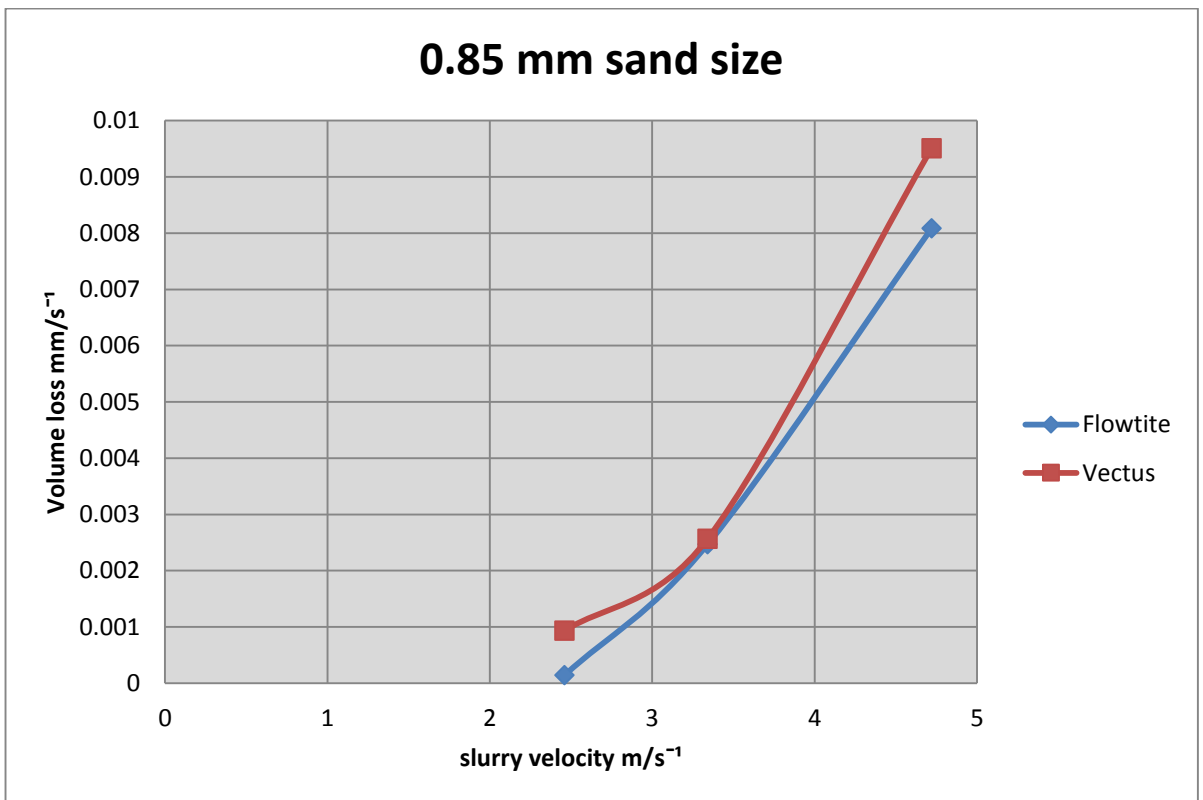


Figure 5.8: Comparison of wear resistance of Flowtite and Vectus materials using slurries with sand particles size D50 of 0.850 mm

Flowtite 0.622 mm Sand Results

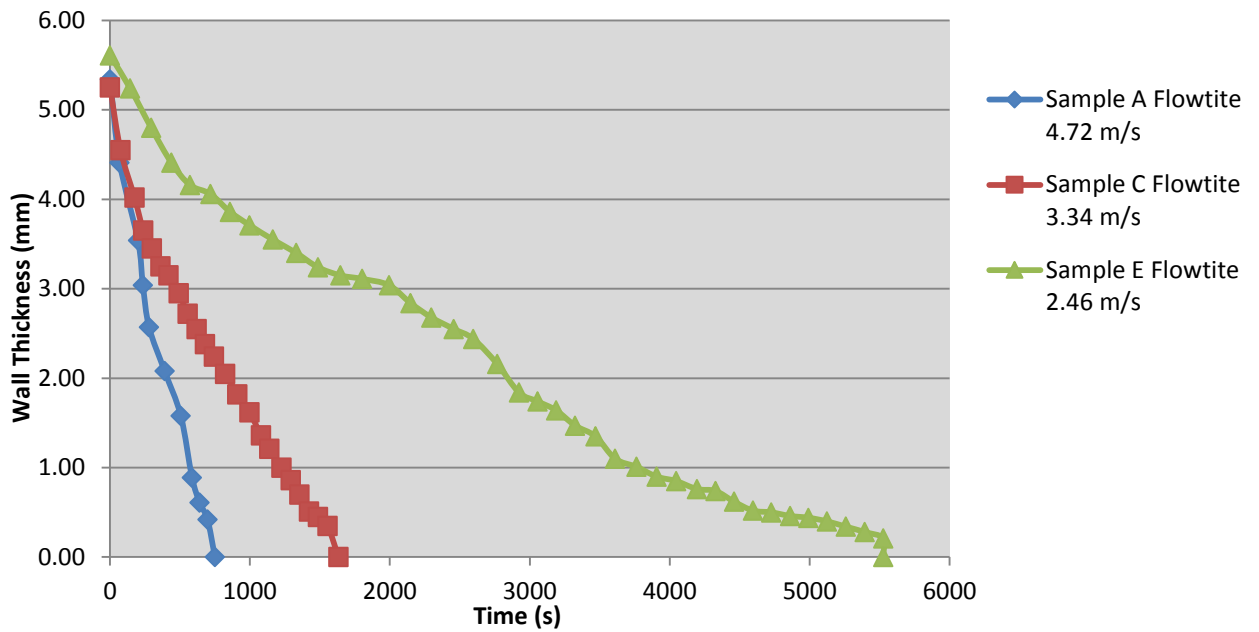


Figure 5.9: Amount of wear with time during the jet impact test on Flowtite pipe material using slurry with sand with D50 of 0.622 mm

Vectus 0.622 mm Particle Results

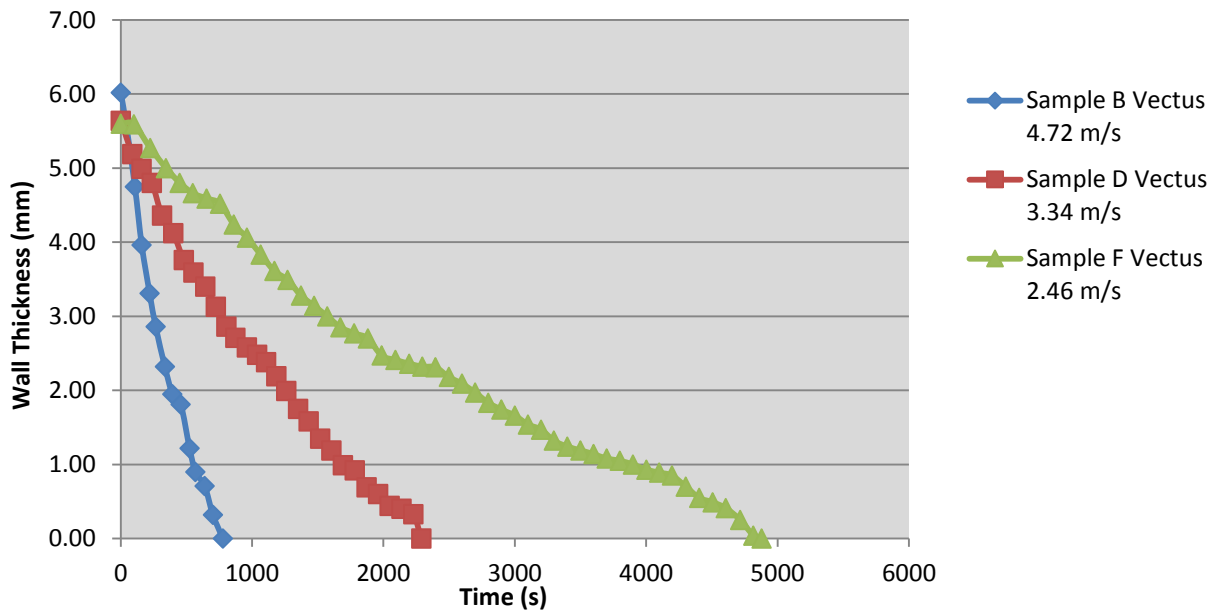


Figure 5.10: Amount of wear with time during the jet impact test on Vectus pipe material using slurry with sand with D50 of 0.622 mm

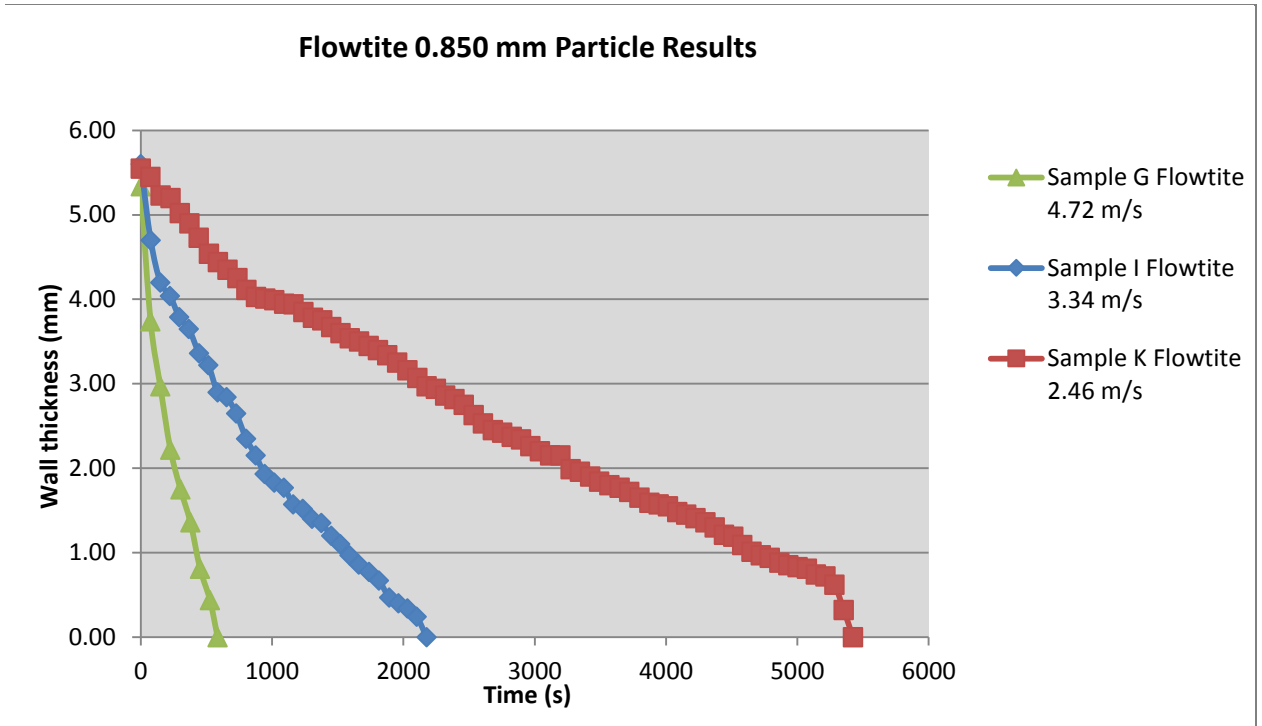


Figure 5.11: Amount of wear with time during the jet impact test on Flowtite pipe material using slurry with sand with D50 of 0.850 mm

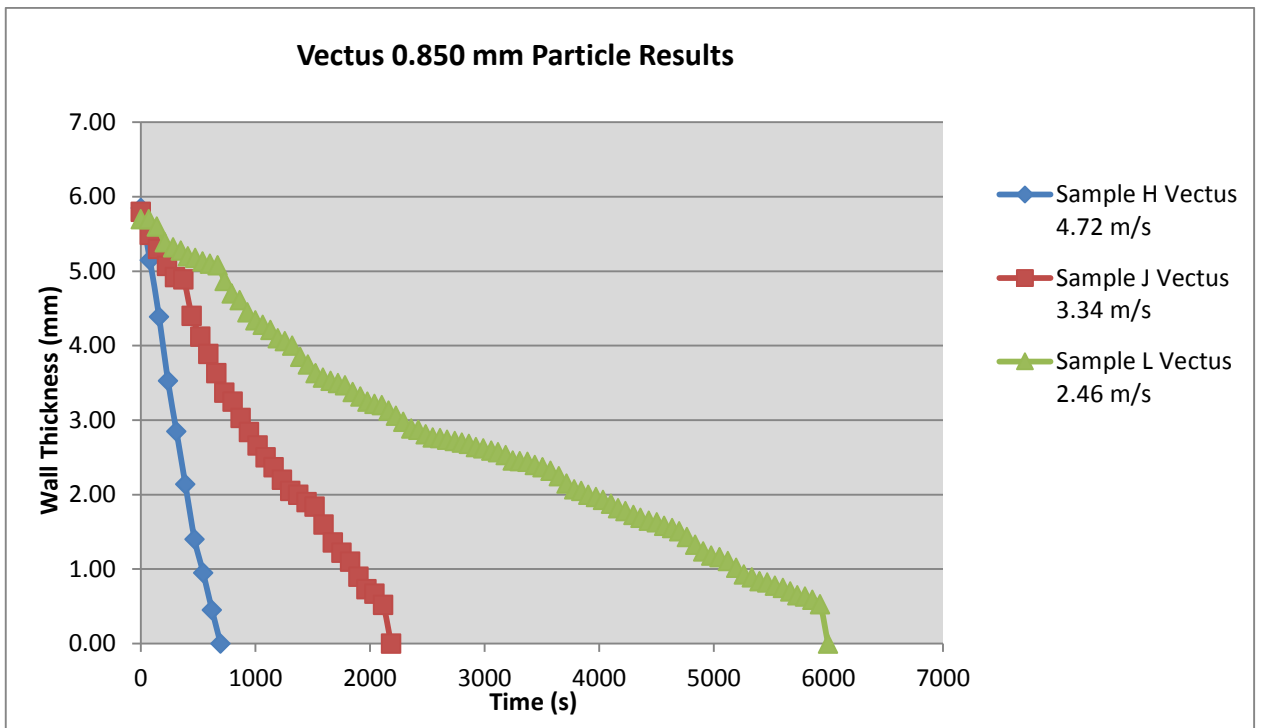


Figure 5.12: Amount of wear with time during the jet impact test on Vectus pipe material using slurry with sand with D50 of 0.850 mm

Samples were tested using slurries with particle sizes of $D_{50}=1.220$ mm at $4.72 \text{ m}\cdot\text{s}^{-1}$. Wear from these particles were very severe, see results from samples M and N in appendix C. Problems were also experienced with clogging of the nozzle. It was concluded that it would not be feasible to test samples at this particle size.

5.6.2 Difficulties encountered during testing

During testing, wear occurred in the carbon steel nozzle of the testing machine. The wear increased the diameter of the nozzle leading to a less concentrated water jet stream, possibly causing the lower wear rates as exhibited by the last samples tested. Wear of the pump impeller also occurred. Although care was taken to keep the water and sand separate, contamination of the recirculated water occurred, leading to lower nozzle velocities. Because the sand was manually fed into the nozzle feeding did not occur at a constant rate and this lead to inaccurate test results.

CHAPTER 6 CONCLUSIONS AND RECOMMENDATIONS

6.1 Introduction

The project asked the question “Can GRP pipe be an alternative to PE-HD pipe, and if so under which operating conditions?” The answer to this question is more complex than a simple yes or no. The easiest way to answer the question is to look at the variables in GRP pipe construction that will influence the wear resistance of the pipe and the type of flow in the pipe.

If an abrasive wear situation is present in the pipe, low flow rates with particles scraping against the bottom of the pipe, hard surfaces will be preferred. Under erosive wear situations, higher flow rates with particle-pipe wall collisions, a more ductile pipe matrix will be of benefit because the matrix will deform plastically and absorb particle collisions, reducing the wear rate significantly, Malison, (1969).

6.2 Variables in GRP pipe construction

6.2.1 % Elongation at break of resin

Under erosive wear conditions, resins with high elongation at break will perform better than their counter parts, as the resins will deform and absorb the particle collisions, providing better resistance to wear. This was evident from the results of the pin on disk test where the resins with the higher elongation at break values exhibited smaller mass loss values.

6.2.2 Post curing of resin and fillers added to resin

Subjecting resin to post curing (as evident from figure 4.5), as well as the addition of fillers increases the wear resistance of the composite under abrasive (sliding) wear conditions, Malison, (1969). This increase in wear resistance may be due to an increase in the hardness of the composite, Ota et al. (2002). The results of the pin on disk tests verified this. A harder composite will also be more brittle. Under erosive wear conditions hard, brittle composites are not preferable because suspended and saltating particles impacting on the surface of the pipe will chip and break small pieces of brittle resin from the pipe wall, which will be carried away with the effluent, resulting in an increased wear rate of the GRP pipe (Malison, 1969). This was evident from the jet impact test where, initially, pipes with post curing exhibited lower wear rates. Pipes with an added sand layer also showed a marked decrease in the wear rate, reinforcing the fact that fillers will increase the wear resistance.

6.2.3 Influence of water absorption

Water absorption tests conducted in this study indicated insignificant amounts of water absorption. Over longer exposure periods, it is expected that water acts as a plasticiser of the matrix, which will cause the resin to act in a more ductile manner, allowing it to absorb collisions of particles during erosion situations, but will lead to decreased resistance to sliding wear.

6.2.4 Influence of impact angle, flow rate and particle size

The effect of impact angle on the wear rate of the pipe was not investigated due to difficulties encountered with the equipment (see discussion 5.6.2). From literature (Malison, 1969), it was evident that the maximum wear rate will be experienced at 90° impact angle and all testing was done accordingly. In agreement with the findings of Malison (1969), the wear rate of samples increased with increased slurry velocity, for all particle sizes tested. From the test results it was found that the assumption made that wear rate will increase

with an increase in sand particle size, was proved wrong, at low slurry velocities. However, errors could possibly have been introduced due to differing testing conditions such as different nozzle to sample distances. Impact is proportional to the momentum (mv^2) of the striking particle. Therefore the effect of particle mass will be more pronounced at higher velocities. Also, for the same reason, errors will affect the results more markedly at the lower velocities. Consequently, the difficulties encountered during testing with the apparatus leads to the conclusion that the results from the jet impact test were not accurate and thus should not be accepted as conclusive.

6.3 Recommendations for future research

Standard manufactured pipes were evaluated during this study. Future projects should include the manufacture of test pipes, using the findings from this study to improve the wear resistance (e.g. post curing and the use of fillers). A complete redesign of GRP pipe can also be done to investigate the effect of pipe construction variables on wear resistance. These include: the percentage of glass, the type of lay-up, the veiling used, coupling agents to improve interlaminar adhesion and speciality liners.

References

AMIANIT PIPE SYSTEMS, *Vectus and Flowtite product guide* (2009)

BIJWE J., LOGANI C. M., TEWARI U. S., (1990). *Influence of fillers and fibre reinforcement on abrasive wear resistance of some polymeric composites*. *Wear*, (1990), 138: 77-92.

CENNA A. A., DOYLE J., PAGE N. W., BEEHAG A., DASTOOR P. *Wear mechanisms in polymer matrix composites abraded by bulk solids*. *Wear*, (2000), 240: 207-214.

CESCHINI L., DAEHN G. S., GARAGNANI G. L., MARTINI C. *Friction and wear behaviour of $C^4Al_2O_3/Al$ composites under dry sliding conditions*. *Wear*, (1997), 216: 229-238.

DORON P, GRANICA D, BARNEA D, (1987) *Slurry flow in horizontal pipes – experimental and modeling*. *International journal of multiphase flow* Vol 13, No 4: (1987) 535-547.

DURALINE PIPES NEWS LETTER, (2004). Q4/2004. 1-4

EL-RAGHY T., BLAU P., BARSOUM M. W., (2000). *Effect of grain size on friction and wear behaviour of Ti_3SiC_2* . *Wear*, (2000), 238: 125-130.

FRIEDRICH K., ZHANG Z., SCHLARB A., K., (2005) *Effects of various fillers on the sliding wear of polymer composites*. *Composites Science and Technology* ,(2005), 65: 2329-2343.

GODDARD JB, (1994) *Abrasion resistance of piping systems*. ADS Pipe technical notes.

HAWTHORNE H. M., XIE Y., YICK S. K., (2002). *A study of single particle-target surface interactions along a specimen in the Coriolis slurry erosion tester*. *Wear*, (2002), 253: 403-410.

HAWTHORNE H. M., XIE Y., YICK S. K., (2003). *A new Coriolis slurry erosion tester designed for improved slurry dynamics*. *Wear*, (2003), 255: 170-180.

HAWTHORNE H. M., (2002). *Some Coriolis slurry erosion test developments*. *Tribology International*, (2002), 35: 625-630.

HEGGEMOEN V AND JONSSON H, (1997) *Flowtite test report: T-97-113-B*, Owens Corning Pipe Systems

HÜBNER W., LEITEL E. (1996). *Peculiarities of erosion-corrosion processes*. *Tribology International*, (1996), 29(3): 199-206.

IWAI Y., HONDA T., YAMADE H., MATSUBARA T., LARSSON M., HOGMARK, S., (2001).

Evaluation of wear resistance of thin hard coatings by a new solid particle impact test. *Wear*, (2001), 251: 861-867.

IWAI Y., NAMBU K. K., (1997). *Slurry wear properties of pump lining materials*. *Wear*, (1997), 210:

211-219.

INDUMATHI J., BIJWE J., GHOSH A. K., FAHIM M., KRISHNARAJ N., (1999). *Wear Of cryo-treated engineering polymers and composites*. *Wear*, (1999), 225-229: 343-353.

JAEGER M., SCHNEIDER G., GAUTHIER C.(2004), *Abrasion resistance of fiberglass reinforced vinyl ester composites*. Conference proceedings^{2nd} Biennial International Composites Africa (2004) 291-303.

KARNATAKA COASTAL PROJECT. (2004) *Duraline Pipes Newsletter*. (2004), :Q4, 3

LEE G., Y., DHARAN C., K., H., RITCHIE R., O. (2001). *A physically based abrasive wear model for composite materials*. *Wear*, (2002), 252: 322-331.

LLEWELLYN R. J., YICK S. K., DOLMAN K. F., (2004). *Scouring erosion resistance of metallic materials used in slurry pump service*. *Wear*, (2004), XX: 1-4.

MALISON JOHN H., (1969) *Corrosion resistant plastic composites in chemical plant design*. Chapter 9: 417-439.

MATOUSEK V, (2005) *Research developments in pipeline transport of settling slurries*. *Powder technology* 156 (2005): 43-51

McI. CLARK H., TUZSON J., WONG K. K., (2000). *Measurements of specific energies for erosive wear using a Coriolis erosion tester*. *Wear*, (2000), 241: 1-9.

OTA, T, MATSUOKA T, SAKAGUSHI K, *Effect of post cure on flexural properties of plain woven glass fabric vinyl ester composites*: Proceedings of Tenth U.S.-Japan Conference on Composite Materials, (2002), 454:461

RAJESH J. J., BIJWE J., VENKATARAMA B., TEWARI U. S., (2004). *Effect of impinging velocity on the erosive wear behaviour of polyamides*. *Tribology International*, (2004), 37: 219-226.

US ARMY CORPS OF ENGINEERS, (1986), *Field applications of Polyethylene pipe in dredging*. www.asace.army.mil/publications/eng-tech/trs/etl1110-2-530. (1986)

WANG G. B., (1997). *Wear mechanisms in vanadium carbide coated steels*. *Wear*, (1997), 212: 25-32.

XIE Y., McI.CLARK H., HAWTHORNE H. M., (1999). *Modelling slurry particle dynamics in the Coriolis erosion tester*. *Wear*, (1999), 225: 405-416.

XU Y. M., MELLOR B. G., (2003). *A comparative study of the wear resistance of thermoplastic and thermoset coatings*. *Wear*, (2003), 255: 722-733.

YEN B. K., DHARAN C. K. H., (1995) *A model for the abrasive wear of fiber-reinforced polymer composites*. *Wear*, (1996), 195: 123-127

ZENG Y. G., YAO Z. M., KE W., (2000). *Erosion-corrosion resistant alloy development for aggressive slurry flows*. *Materials letters*, (2000), 46: 362-368.

1995 Annual book of ASTM standards, G40-94, p 145 – 148.

1996 Annual book of ASTM standards, Section 3 Metals Test Methods and Analytical Procedures, p 385 – 389.

1996 Annual book of ASTM standards, Section 3 Metals Test Methods and Analytical Procedures, p 382 – 384.

http://highered.mcgraw-hill.com/sites/dl/free/0072953586/240416/Materials_Properties_Database.xls

Appendix A

Postcuring Schedules of Resin samples

1. Crystic 196 (orthophthalic standard filament winding resin)
2. Crystic 272 (isophthalic standard filament winding resin and the one used by Amiantit for liners in Vectus pipes)
3. Crystic EPS1 (Flowtite orthophthalic resin)
4. Crestomer 1220PA (urethane acrylic modified isopolyester - high impact strength)
5. Crystic 397PA (high HDT, high elongation iso-NPG filament winding resin)

Resins 1-4 had a post cure schedule as follows:

24h at 25 ° C

1 hr at 40 ° C

1 hr at 60 ° C

3 hr at 80 ° C

Resin 5 was post cured further as follows:

1hr at 90 ° C

1hr at 100 ° C

1hr at 110 ° C

2hr at 120 ° C

Appendix B Numerical Results - Pin-on-disk test

B1 Test results of resin samples (as-cast samples)

Resin 1: Flowtite Orthophthalic Resin – Manufacturer A												
		1 min elapsed		2 min elapsed		3 min elapsed		4 min elapsed		5 min elapsed		
Sample number	Initial Mass (g)	Mass (g)	Loss (g)	Mass (g)	Loss (g)	Mass (g)	Loss (g)	Mass (g)	Loss (g)	Mass (g)	Loss (g)	Total Mass Loss (g)
1	2.569	2.441	0.128	2.177	0.264	1.918	0.259	1.673	0.245	1.43	0.243	1.139
2	2.521	2.247	0.274	1.984	0.263	1.735	0.249	1.48	0.255	1.237	0.243	1.284
3	2.689	2.406	0.283	2.138	0.268	1.898	0.240	1.663	0.235	1.43	0.233	1.259
4	2.55	2.317	0.233	2.074	0.243	1.844	0.230	1.614	0.230	1.407	0.207	1.143
5	2.666	2.404	0.262	2.151	0.253	1.900	0.251	1.663	0.237	1.423	0.240	1.243
6	2.833	2.568	0.265	2.327	0.241	2.077	0.250	1.849	0.228	1.626	0.223	1.207

Resin 2: Flowtite Orthophthalic Resin – Manufacturer B												
		1 min elapsed		2 min elapsed		3 min elapsed		4 min elapsed		5 min elapsed		
Sample number	Initial Mass (g)	Mass (g)	Loss (g)	Mass (g)	Loss (g)	Mass (g)	Loss (g)	Mass (g)	Loss (g)	Mass (g)	Loss (g)	Total Mass Loss (g)
1	2.751	2.625	0.126	2.482	0.143	2.339	0.143	2.198	0.141	2.049	0.149	0.702
2	2.675	2.536	0.139	2.377	0.159	2.234	0.143	2.087	0.147	1.929	0.158	0.746
3	2.735	2.580	0.155	2.42	0.160	2.262	0.158	2.109	0.153	1.947	0.162	0.788
4	2.710	2.542	0.168	2.373	0.169	2.213	0.160	2.014	0.199	1.863	0.151	0.847
5	2.757	2.604	0.153	2.424	0.180	2.280	0.144	2.120	0.160	1.950	0.170	0.807
6	2.809	2.648	0.161	2.0480	0.168	2.329	0.151	2.179	0.15	1.994	0.185	0.815

Resin 3: Isophthalic Liner Resin – Manufacturer A												
		1 min elapsed		2 min elapsed		3 min elapsed		4 min elapsed		5 min elapsed		
Sample number	Initial Mass (g)	Mass (g)	Loss (g)	Mass (g)	Loss (g)	Mass (g)	Loss (g)	Mass (g)	Loss (g)	Mass (g)	Loss (g)	Total Mass Loss (g)
1	2.288	2.111	0.177	1.940	0.171	1.772	0.168	1.609	0.163	1.439	0.170	0.849
2	2.095	1.927	0.168	1.759	0.168	1.591	0.168	1.422	0.169	1.257	0.165	0.838
3	2.279	2.107	0.172	1.932	0.175	1.766	0.166	1.591	0.175	1.424	0.167	0.855
4	2.454	2.285	0.169	2.158	0.127	1.984	0.174	1.815	0.169	1.638	0.177	0.816
5	2.458	2.293	0.165	2.124	0.169	1.953	0.171	1.785	0.168	1.610	0.175	0.848
6	2.345	2.188	0.157	2.019	0.169	1.856	0.163	1.684	0.172	1.511	0.173	0.834

Resin 4: Isophthalic Liner Resin – Manufacturer B												
		1 min elapsed		2 min elapsed		3 min elapsed		4 min elapsed		5 min elapsed		
Sample number	Initial Mass (g)	Mass (g)	Loss (g)	Mass (g)	Loss (g)	Mass (g)	Loss (g)	Mass (g)	Loss (g)	Mass (g)	Loss (g)	Total Mass Loss (g)
1	2.784	2.638	0.146	2.498	0.140	2.358	0.140	2.211	0.137	2.089	0.132	0.695
2	2.688	2.539	0.149	2.389	0.150	2.224	0.165	2.060	0.164	1.896	0.164	0.792
3	2.595	2.436	0.159	2.264	0.172	2.098	0.166	2.017	0.081	19.16	0.101	0.679
4	2.598	2.492	0.106	2.386	0.106	2.274	0.112	2.168	0.106	2.060	0.108	0.538
5	2.696	2.587	0.109	2.490	0.097	2.380	0.110	2.287	0.093	2.170	0.117	0.526
6	2.792	2.685	0.170	20582	0.103	2.475	0.170	2.367	0.108	2.257	0.110	0.535

Resin 5: Rigid isophthalic thermal resistant core resin - Manufacturer A												
		1 min elapsed		2 min elapsed		3 min elapsed		4 min elapsed		5 min elapsed		
Sample number	Initial Mass (g)	Mass (g)	Loss (g)	Mass (g)	Loss (g)	Mass (g)	Loss (g)	Mass (g)	Loss (g)	Mass (g)	Loss (g)	Total Mass Loss (g)
1	2.448	2.256	0.192	2.057	0.199	1.853	0.204	1.653	0.200	1.452	0.201	0.996
2	2.954	2.751	0.203	2.539	0.212	2.329	0.21	2.127	0.202	1.906	0.221	1.048
3	2.462	2.279	0.183	2.085	0.194	1.874	0.211	1.663	0.211	1.455	0.208	1.007
4	2.572	2.415	0.157	2.250	0.165	2.092	0.158	1.927	0.165	1.766	0.161	0.806
5	2.429	2.294	0.135	2.136	0.158	1.981	0.155	1.825	0.156	1.663	0.162	0.766
6	2.700	2.559	0.141	2.409	0.150	2.249	0.160	2.092	0.157	1.942	0.150	0.758

Resin 6: Orthophthalic Polyester Resin – Manufacturer B												
		1 min elapsed		2 min elapsed		3 min elapsed		4 min elapsed		5 min elapsed		
Sample number	Initial Mass (g)	Mass (g)	Loss (g)	Mass (g)	Loss (g)	Mass (g)	Loss (g)	Mass (g)	Loss (g)	Mass (g)	Loss (g)	Total Mass Loss (g)
1	2.723	2.602	0.121	2.488	0.114	2.377	0.111	2.272	0.105	2.174	0.098	0.549
2	2.795	2.694	0.101	2.593	0.101	2.488	0.105	2.380	0.108	2.259	0.121	0.536
3	2.780	2.660	0.120	2.536	0.124	2.408	0.128	2.266	0.142	2.144	0.122	0.636
4	2.754	2.629	0.125	2.491	0.138	2.355	0.136	2.212	0.143	2.077	0.135	0.677
5	2.680	2.554	0.126	2.424	0.130	2.280	0.144	2.132	0.148	1.996	0.136	0.684
6	2.685	2.552	0.133	2.430	0.122	2.320	0.110	2.171	0.149	2.030	0.141	0.655

Resin 7: Urethane Acrylic Modified Isopolyester – Manufacturer B												
		1 min elapsed		2 min elapsed		3 min elapsed		4 min elapsed		5 min elapsed		
Sample number	Initial Mass (g)	Mass (g)	Loss (g)	Mass (g)	Loss (g)	Mass (g)	Loss (g)	Mass (g)	Loss (g)	Mass (g)	Loss (g)	Total Mass Loss (g)
1	2.320	2.226	0.094	2.118	0.108	2.006	0.112	1.908	0.098	1.825	0.083	0.495
2	2.498	2.413	0.085	2.312	0.101	2.205	0.107	2.102	0.103	1.993	0.109	0.505
3	2.461	2.379	0.082	2.272	0.107	2.168	0.104	2.063	0.105	1.954	0.109	0.507
4	2.374	2.280	0.094	2.174	0.106	2.062	0.112	1.946	0.116	1.855	0.091	0.519
5	2.286	2.191	0.095	2.73	0.118	1.947	0.126	1.828	0.119	1.701	0.127	0.585
6	2.245	2.153	0.092	2.058	0.095	1.962	0.096	1.86	0.102	1.762	0.098	0.483

Resin 8: Isophthalic -NPG polyester resin – Manufacturer B												
		1 min elapsed		2 min elapsed		3 min elapsed		4 min elapsed		5 min elapsed		
Sample number	Initial Mass (g)	Mass (g)	Loss (g)	Mass (g)	Loss (g)	Mass (g)	Loss (g)	Mass (g)	Loss (g)	Mass (g)	Loss (g)	Total Mass Loss (g)
1	2.697	2.579	0.118	2.419	0.160	2.252	0.167	2.096	0.156	1.952	0.144	0.745
2	2.430	2.280	0.150	2.134	0.146	1.982	0.152	1.822	0.160	1.658	0.164	0.772
3	2.587	2.459	0.128	2.292	0.167	2.143	0.149	1.969	0.174	1.841	0.128	0.746
4	2.533	2.407	0.126	2.248	0.159	2.097	0.151	1.946	0.151	1.791	0.155	0.742
5	2.490	2.364	0.126	2.202	0.162	2.045	0.157	1.891	0.154	1.737	0.154	0.753
6	2.544	2.416	0.128	2.266	0.150	2.099	0.167	1.932	0.167	1.760	0.172	0.784

Resin 9: Epoxy Vinyl Ester 441-400- Manufacturer A												
		1 min elapsed		2 min elapsed		3 min elapsed		4 min elapsed		5 min elapsed		
Sample number	Initial Mass (g)	Mass (g)	Loss (g)	Mass (g)	Loss (g)	Mass (g)	Loss (g)	Mass (g)	Loss (g)	Mass (g)	Loss (g)	Total Mass Loss (g)
1	2.409	2.322	0.087	2.186	0.136	2.043	0.143	1.903	0.140	1.764	0.139	0.645
2	2.463	2.382	0.081	2.242	0.140	2.102	0.140	1.959	0.143	1.813	0.146	0.650
3	2.381	2.280	0.101	2.137	0.143	1.992	0.145	1.859	0.133	1.710	0.149	0.671
4	2.387	2.242	0.145	2.098	0.144	1.951	0.147	1.838	0.113	1.707	0.131	0.680
5	2.455	2.336	0.119	2.208	0.128	2.080	0.128	1.955	0.125	1.830	0.125	0.625
6	2.420	2.322	0.098	2.183	0.139	2.028	0.155	1.878	0.150	1.760	0.118	0.660

Resin 10: Epoxy Vinyl Ester411-350 – Manufacturer A												
		1 min elapsed		2 min elapsed		3 min elapsed		4 min elapsed		5 min elapsed		
Sample number	Initial Mass (g)	Mass (g)	Loss (g)	Mass (g)	Loss (g)	Mass (g)	Loss (g)	Mass (g)	Loss (g)	Mass (g)	Loss (g)	Total Mass Loss (g)
1	2.523	2.451	0.072	2.345	0.106	2.248	0.097	2.156	0.092	2.062	0.094	0.461
2	2.450	2.360	0.090	2.247	0.113	2.139	0.108	2.038	0.101	1.940	0.098	0.510
3	2.428	2.368	0.060	2.264	0.104	2.158	0.106	1.991	0.167	1.884	0.107	0.544
4	2.360	2.300	0.060	2.200	0.100	2.093	0.107	1.991	0.102	1.884	0.107	0.476
5	2.511	2.441	0.070	2.334	0.107	2.221	0.113	2.098	0.123	1.978	0.120	0.533
6	2.510	2.431	0.079	2.308	0.123	2.197	0.111	2.082	0.115	1.981	0.101	0.529

B2 Test results of resin samples (post cured samples)

Resin 1: Flowtite Orthophthalic Resin – Manufacturer A												
		1 min elapsed		2 min elapsed		3 min elapsed		4 min elapsed		5 min elapsed		
Sample number	Initial Mass (g)	Mass (g)	Loss (g)	Mass (g)	Loss (g)	Mass (g)	Loss (g)	Mass (g)	Loss (g)	Mass (g)	Loss (g)	Total Mass Loss (g)
1	2.605	2.497	0.108	2.378	0.119	2.258	0.120	2.156	0.102	2.028	0.128	0.577
2	2.665	2.549	0.116	2.427	0.122	2.305	0.122	2.175	0.130	2.052	0.123	0.613
3	2.463	2.345	0.118	2.211	0.134	2.083	0.128	1.956	0.127	1.834	0.122	0.629
4	2.575	2.457	0.118	2.299	0.158	2.152	0.147	1.997	0.155	1.837	0.160	0.738
5	2.541	2.393	0.148	2.223	0.170	2.056	.167	1.888	0.168	1.713	0.175	0.828
6	2.640	2.475	0.165	2.296	0.179	2.122	0.174	1.942	0.180	1.763	0.179	0.877

Resin 4: Isophthalic Liner Resin – Manufacturer B												
		1 min elapsed		2 min elapsed		3 min elapsed		4 min elapsed		5 min elapsed		
Sample number	Initial Mass (g)	Mass (g)	Loss (g)	Mass (g)	Loss (g)	Mass (g)	Loss (g)	Mass (g)	Loss (g)	Mass (g)	Loss (g)	Total Mass Loss (g)
1	2.667	2.556	0.111	2.467	0.089	2.362	0.105	2.285	0.077	2.167	0.118	0.500
2	2.705	2.589	0.116	2.479	0.110	2.356	0.123	2.214	0.142	2.093	0.121	0.612
3	2.487	2.375	0.112	2.266	0.109	2.163	0.103	2.117	0.046	2.005	0.112	0.482
4	2.730	2.624	0.106	2.510	0.114	2.400	0.110	2.298	0.102	2.185	0.113	0.545
5	2.534	2.441	0.093	2.353	0.088	2.256	0.097	2.199	0.057	2.099	0.100	0.435
6	2.609	2.504	0.105	2.397	0.107	2.290	0.107	2.173	0.117	2.081	0.092	0.528

Resin 7: Urethane Acrylate Modified Isopolyester – Manufacturer B												
		1 min elapsed		2 min elapsed		3 min elapsed		4 min elapsed		5 min elapsed		
Sample number	Initial Mass (g)	Mass (g)	Loss (g)	Mass (g)	Loss (g)	Mass (g)	Loss (g)	Mass (g)	Loss (g)	Mass (g)	Loss (g)	Total Mass Loss (g)
1	2.300	2.225	0.075	2.163	0.062	2.088	0.075	2.017	0.071	1.944	0.073	0.356
2	2.427	2.359	0.068	2.290	0.069	2.218	0.072	2.148	0.070	2.080	0.068	0.347
3	2.614	2.537	0.077	2.470	0.067	2.400	0.070	2.343	0.057	2.268	0.075	0.346
4	2.527	2.463	0.064	2.388	0.075	2.333	0.055	2.265	0.068	2.196	0.069	0.331
5	2.592	2.531	0.061	2.468	0.063	2.403	0.065	2.337	0.066	2.268	0.069	0.324
6	2.548	2.486	0.062	2.411	0.075	2.354	0.057	2.277	0.077	2.222	0.055	0.326

Resin 9: Epoxy Vinyl Ester 441-400- Manufacturer A												
		1 min elapsed		2 min elapsed		3 min elapsed		4 min elapsed		5 min elapsed		
Sample number	Initial Mass (g)	Mass (g)	Loss (g)	Mass (g)	Loss (g)	Mass (g)	Loss (g)	Mass (g)	Loss (g)	Mass (g)	Loss (g)	Total Mass Loss (g)
1	2.519	2.421	0.098	2.309	0.112	2.205	0.104	2.112	0.093	2.053	0.059	0.466
2	2.476	2.386	0.090	2.267	0.119	2.146	0.121	2.059	0.087	1.955	0.104	0.521
3	2.510	2.442	0.068	2.326	0.116	2.212	0.114	2.119	0.093	2.003	0.116	0.507
4	2.595	2.519	0.076	2.435	0.084	2.326	0.109	2.236	0.090	2.137	0.099	0.458
5	2.581	2.501	0.080	2.403	0.098	2.307	0.096	2.201	0.106	2.105	0.096	0.476
6	2.532	2.442	0.090	2.334	0.108	2.218	0.116	2.109	0.109	2.017	0.092	0.515

Resin 10: Epoxy Vinyl Ester 411-350 – Manufacturer A												
		1 min elapsed		2 min elapsed		3 min elapsed		4 min elapsed		5 min elapsed		
Sample number	Initial Mass (g)	Mass (g)	Loss (g)	Mass (g)	Loss (g)	Mass (g)	Loss (g)	Mass (g)	Loss (g)	Mass (g)	Loss (g)	Total Mass Loss (g)
1	2.546	2.497	0.049	2.422	0.075	2.342	0.080	2.309	0.033	2.230	0.079	0.316
2	2.389	2.330	0.059	2.245	0.085	2.159	0.086	2.074	0.085	1.989	0.085	0.400
3	2.465	2.398	0.067	2.310	0.088	2.218	0.092	2.131	0.087	2.058	0.073	0.407
4	2.466	2.408	0.058	2.339	0.069	2.262	0.077	2.205	0.057	2.140	0.065	0.326
5	2.615	2.558	0.057	2.484	0.074	2.408	0.076	2.341	0.067	2.257	0.084	0.358
6	2.465	2.422	0.043	2.392	0.030	2.305	0.087	2.228	0.077	2.140	0.088	0.325

B3 Test results of resin samples with fillers

Resin: Flowtite Orthophthalic Resin – Manufacturer A with 5% Alumina filler – As cured condition												
		1 min elapsed		2 min elapsed		3 min elapsed		4 min elapsed		5 min elapsed		
Sample number	Initial Mass (g)	Mass (g)	Loss (g)	Mass (g)	Loss (g)	Mass (g)	Loss (g)	Mass (g)	Loss (g)	Mass (g)	Loss (g)	Total Mass Loss (g)
1	2.765	2.653	0.112	2.46	0.193	2.346	0.114	2.256	0.09	2.144	0.112	0.621
2	2.814	2.702	0.112	2.518	0.184	2.426	0.092	2.316	0.11	2.247	0.069	0.567
3	2.519	2.327	0.192	2.224	0.103	2.124	0.1	2.016	0.108	1.903	0.113	0.616
4	2.688	2.494	0.194	2.368	0.126	2.247	0.121	2.117	0.13	1.987	0.13	0.701
5	2.734	2.533	0.201	2.410	0.123	2.280	0.130	2.140	0.140	1.963	0.177	0.771
6	2.513	2.319	0.194	2.193	0.126	2.065	0.128	1.956	0.109	1.838	0.118	0.675

Resin: Flowtite Orthophthalic Resin – Manufacturer A with 10% Alumina filler – As-cured condition												
		1 min elapsed		2 min elapsed		3 min elapsed		4 min elapsed		5 min elapsed		
Sample number	Initial Mass (g)	Mass (g)	Loss (g)	Mass (g)	Loss (g)	Mass (g)	Loss (g)	Mass (g)	Loss (g)	Mass (g)	Loss (g)	Total Mass Loss (g)
1	2.691	2.515	0.176	2.377	0.138	2.227	0.15	2.095	0.132	1.970	0.125	0.721
2	2.650	2.492	0.158	2.333	0.159	2.187	0.146	2.045	0.142	1.899	0.146	0.751
3	2.578	2.392	0.186	2.233	0.159	2.086	0.147	1.947	0.139	1.807	0.140	0.771
4	2.762	2.585	0.177	2.388	0.197	2.228	0.160	2.074	0.154	1.913	0.161	0.849
5	2.700	2.537	0.163	2.345	0.192	2.183	0.162	2.031	0.152	1.865	0.166	0.835
6	2.555	2.380	0.175	2.184	0.196	2.008	0.175	1.807	0.201	1.583	0.224	0.972

Resin: Flowtite Orthophthalic Resin – Manufacturer A with 15% Alumina filler – As-cured condition												
		1 min elapsed		2 min elapsed		3 min elapsed		4 min elapsed		5 min elapsed		
Sample number	Initial Mass (g)	Mass (g)	Loss (g)	Mass (g)	Loss (g)	Mass (g)	Loss (g)	Mass (g)	Loss (g)	Mass (g)	Loss (g)	Total Mass Loss (g)
1	2.766	2.565	0.201	2.300	0.265	2.062	0.238	1.869	0.193	1.653	0.216	1.113
2	2.897	2.694	0.203	2.357	0.337	2.113	0.244	1.894	0.219	1.755	0.139	1.142
3	2.762	2.501	0.261	2.200	0.301	1.975	0.225	1.826	0.149	1.683	0.143	1.079
4	2.759	2.585	0.174	2.333	0.252	2.186	0.147	2.034	0.152	1.885	0.149	0.874
5	2.915	2.736	0.179	2.476	0.260	2.319	0.157	2.162	0.157	2.009	0.153	0.906
6	3.003	2.812	0.191	2.542	0.270	2.389	0.153	2.235	0.154	2.102	0.133	0.901

Resin: Flowtite Orthophthalic Resin – Manufacturer A with 20% Alumina filler – As-cured condition												
		1 min elapsed		2 min elapsed		3 min elapsed		4 min elapsed		5 min elapsed		
Sample number	Initial Mass (g)	Mass (g)	Loss (g)	Mass (g)	Loss (g)	Mass (g)	Loss (g)	Mass (g)	Loss (g)	Mass (g)	Loss (g)	Total Mass Loss (g)
1	3.269	3.073	0.196	2.84	0.233	2.384	0.456	2.090	0.294	1.838	0.252	1.431
2	2.852	2.539	0.313	2.64	0.175	2.199	0.165	2.041	0.158	1.822	0.159	0.970
3	3.110	2.918	0.192	2.599	0.319	2.391	0.208	2.249	0.142	2.098	0.151	1.012
4	2.995	2.830	0.165	2.522	0.308	2.335	0.187	2.180	0.155	2.028	0.152	0.967
5	2.923	2.651	0.272	2.505	0.146	2.351	0.154	2.199	0.152	2.052	0.147	0.871
6	2.862	2.576	0.286	2.427	0.149	2.274	0.153	2.128	0.146	1.998	0.130	0.864

Resin: Flowtite Orthophthalic Resin – Manufacturer A with 25% Alumina filler – As-cured condition												
		1 min elapsed		2 min elapsed		3 min elapsed		4 min elapsed		5 min elapsed		
Sample number	Initial Mass (g)	Mass (g)	Loss (g)	Mass (g)	Loss (g)	Mass (g)	Loss (g)	Mass (g)	Loss (g)	Mass (g)	Loss (g)	Total Mass Loss (g)
1	3.044	2.710	0.334	2.473	0.237	2.304	0.169	2.128	0.176	1.950	0.178	1.094
2	3.191	2.999	0.192	2.814	0.185	2.495	0.319	2.282	0.213	2.114	0.168	1.077
3	2.999	2.687	0.312	2.409	2.078	2.348	0.061	2.198	0.150	2.041	0.157	0.958
4	3.043	2.769	0.274	2.541	0.228	2.376	0.165	2.208	0.168	2.047	0.161	0.996
5	3.176	2.865	0.311	2.611	0.254	2.421	0.190	2.258	0.163	2.110	0.148	1.066
6	2.832	2.579	0.253	2.485	0.094	2.320	0.165	2.150	0.170	1.989	0.161	0.843

Resin: Flowtite Orthophthalic Resin – Manufacturer A with 30% Alumina filler – As-cured condition												
		1 min elapsed		2 min elapsed		3 min elapsed		4 min elapsed		5 min elapsed		
Sample number	Initial Mass (g)	Mass (g)	Loss (g)	Mass (g)	Loss (g)	Mass (g)	Loss (g)	Mass (g)	Loss (g)	Mass (g)	Loss (g)	Total Mass Loss (g)
1	3.488	3.292	0.196	3.102	0.19	2.802	0.300	2.530	0.272	2.353	0.177	1.135
2	3.239	3.043	0.196	2.825	0.218	2.589	0.236	2.454	0.135	2.299	0.155	0.940
3	3.098	2.794	0.304	2.557	0.237	2.433	0.124	2.292	0.141	2.143	0.149	0.955
4	3.057	2.993	0.064	2.718	0.275	2.537	0.181	2.399	0.138	2.269	0.130	0.788
5	3.038	2.875	0.163	2.598	0.277	2.383	0.215	2.243	0.140	2.108	0.135	0.930
6	3.092	2.940	0.152	2.683	0.257	2.483	0.200	2.399	0.084	2.218	0.181	0.874

Resin: Isophthalic Liner Resin – 15% filler – Zirconium dioxide - Post-cured condition												
		1 min elapsed		2 min elapsed		3 min elapsed		4 min elapsed		5 min elapsed		
Sample number	Initial Mass (g)	Mass (g)	Loss (g)	Mass (g)	Loss (g)	Mass (g)	Loss (g)	Mass (g)	Loss (g)	Mass (g)	Loss (g)	Total Mass Loss (g)
1	2.846	2.67	0.176	2.51	0.16	2.349	0.161	2.197	0.152	2.151	0.046	0.695
2	2.781	2.597	0.184	2.442	0.155	2.283	0.159	2.111	0.172	2.034	0.077	0.747
3	2.823	2.659	0.164	2.495	0.164	2.414	0.081	2.253	0.191	2.230	0.053	0.593
4	2.828	2.681	0.147	2.545	0.136	2.373	0.172	2.215	0.158	2.071	0.144	0.757
5	2.778	2.585	0.193	2.404	0.131	2.224	0.180	2.071	0.153	1.911	0.160	0.867
6	2.741	2.556	0.185	2.368	0.188	2.188	0.180	2.047	0.141	1.072	0.173	0.869

Resin: Isophthalic Liner Resin – 15% filler – Silicon carbide - Post-cured condition												
		1 min elapsed		2 min elapsed		3 min elapsed		4 min elapsed		5 min elapsed		
Sample number	Initial Mass (g)	Mass (g)	Loss (g)	Mass (g)	Loss (g)	Mass (g)	Loss (g)	Mass (g)	Loss (g)	Mass (g)	Loss (g)	Total Mass Loss (g)
1	2.822	2.605	0.217	2.414	0.191	2.232	0.182	2.053	0.179	1.875	0.173	0.947
2	2.95	2.756	0.194	2.560	0.196	2.382	0.173	2.200	0.182	2.027	0.173	0.923
3	2.95	2.759	0.191	2.570	0.189	2.396	0.175	2.222	0.173	2.060	0.162	0.890
4	2.989	2.788	0.201	2.598	0.190	2.417	0.181	2.239	0.178	2.060	0.179	0.929
5	2.938	2.735	0.203	2.541	0.194	2.361	0.130	2.215	0.146	2.111	0.104	0.827
6	2.871	2.665	0.206	2.473	0.192	2.282	0.191	2.163	0.114	2.048	0.122	0.825

Resin: Urethane acrylate polyester blend Resin – 15% filler – Silicon carbide - Post-cured condition												
		1 min elapsed		2 min elapsed		3 min elapsed		4 min elapsed		5 min elapsed		
Sample number	Initial Mass (g)	Mass (g)	Loss (g)	Mass (g)	Loss (g)	Mass (g)	Loss (g)	Mass (g)	Loss (g)	Mass (g)	Loss (g)	Total Mass Loss (g)
1	2.618	2.501	0.117	2.373	0.128	2.244	0.129	2.130	0.114	2.044	0.086	0.574
2	2.704	2.572	0.132	2.475	0.097	2.351	0.124	2.219	0.132	2.163	0.050	0.535
3	2.634	2.532	0.102	2.366	0.166	2.204	0.182	2.045	0.159	1.883	0.159	0.748
4	2.558	2.404	0.154	2.224	0.180	2.043	0.181	1.893	0.15	1.760	0.133	0.798
5	2.523	2.348	0.175	2.194	0.154	2.019	0.175	1.833	0.136	1.731	0.152	0.792
6	2.641	2.482	0.159	2.314	0.168	2.158	0.156	1.975	0.183	1.813	0.162	0.828

Resin: Urethane acrylate polyester blend Resin – 15% filler – Zirconium dioxide - Post-cured condition												
		1 min elapsed		2 min elapsed		3 min elapsed		4 min elapsed		5 min elapsed		
Sample number	Initial Mass (g)	Mass (g)	Loss (g)	Mass (g)	Loss (g)	Mass (g)	Loss (g)	Mass (g)	Loss (g)	Mass (g)	Loss (g)	Total Mass Loss (g)
1	2.968	2.780	0.188	2.625	0.155	2.441	0.184	2.323	0.118	2.166	0.157	0.802
2	2.968	2.777	0.191	2.587	0.190	2.417	0.170	2.230	0.187	2.048	0.182	0.920
3	2.853	2.659	0.194	2.466	0.193	2.297	0.169	2.159	0.138	2.017	0.142	0.838
4	2.821	2.655	0.166	2.489	0.166	2.324	0.165	2.191	0.133	2.031	0.160	0.790
5	2.855	2.672	0.183	2.563	0.109	2.512	0.051	2.346	0.164	2.189	0.159	0.665
6	2.784	2.605	0.179	2.429	0.176	2.272	0.157	2.101	0.171	1.952	0.149	0.832

Resin: Flowtite Orthophthalic Resin – Manufacturer A with 15% Alumina filler – Post-cured condition												
		1 min elapsed		2 min elapsed		3 min elapsed		4 min elapsed		5 min elapsed		
Sample number	Initial Mass (g)	Mass (g)	Loss (g)	Mass (g)	Loss (g)	Mass (g)	Loss (g)	Mass (g)	Loss (g)	Mass (g)	Loss (g)	Total Mass Loss (g)
1	3.001	2.847	0.154	2.686	0.161	2.518	0.168	2.346	0.172	2.173	0.173	0.828
2	3.008	2.810	0.198	2.615	0.195	2.435	0.180	2.246	0.189	2.065	0.181	0.943
3	3.093	2.888	0.205	2.679	0.209	2.489	0.190	2.302	0.187	2.106	0.196	0.987
4	3.016	2.813	0.203	2.601	0.212	2.413	0.188	2.218	0.195	2.020	0.198	0.996
5	3.018	2.830	0.251	2.611	0.219	2.402	0.209	2.201	0.201	2.004	0.197	1.077
6	3.056	2.829	0.227	2.788	0.041	2.576	0.212	2.369	0.207	2.163	0.206	0.893

B4 Test results of GRP pipe samples:

VECTUS PIPE ON 120 GRIT SiC ABRASIVE												
		1 min elapsed		2 min elapsed		3 min elapsed		4 min elapsed		5 min elapsed		
Sample number	Initial Mass (g)	Mass (g)	Loss (g)	Mass (g)	Loss (g)	Mass (g)	Loss (g)	Mass (g)	Loss (g)	Mass (g)	Loss (g)	Total Mass Loss (g)
V7	2.024	1.873	0.151	1.823	0.05	1.695	0.128	1.352	0.343	0.972	0.38	1.052
V8	1.933	1.795	0.138	1.660	0.135	1.299	0.361	0.893	0.406			1.040
V9	1.943	1.76	0.183	1.499	0.261	1.042	0.457	0.771	0.271			1.172
V10	1.729	1.601	0.128	1.400	0.201	1.023	0.377	0.722	0.301			1.007
V11	1.853	1.694	0.159	1.502	0.192	1.129	0.373	0.755	0.374			1.098
V12	1.83	1.684	0.146	1.334	0.35	0.973	0.361	0.733	0.24			1.097

FLOWTITE PIPE ON 120 GRIT SiC ABRASIVE												
		1 min elapsed		2 min elapsed		3 min elapsed		4 min elapsed		5 min elapsed		
Sample number	Initial Mass (g)	Mass (g)	Loss (g)	Mass (g)	Loss (g)	Mass (g)	Loss (g)	Mass (g)	Loss (g)	Mass (g)	Loss (g)	Total Mass Loss (g)
F9	1.545	1.519	0.026	1.392	0.127	1.100	0.292	0.982	0.118			0.639
F10	1.497	1.393	0.104	1.144	0.249	0.945	0.199	0.795	0.15			1.497
F11	1.555	1.380	0.175	1.091	0.289	0.898	0.193	0.795	0.103			1.555
F12	1.517	1.217	0.300	0.945	0.272	0.792	0.153	0.792				1.517
F13	1.374	1.271	0.103	0.945	0.326	0.792	0.153	0.792				1.374
F14	1.589	1.367	0.222	1.103	0.264	0.920	0.183	0.742	0.178			1.589

STEEL PIPE ON 120 GRIT SiC ABRASIVE												
		1 min elapsed		2 min elapsed		3 min elapsed		4 min elapsed		5 min elapsed		
Sample number	Initial Mass (g)	Mass (g)	Loss (g)	Mass (g)	Loss (g)	Mass (g)	Loss (g)	Mass (g)	Loss (g)	Mass (g)	Loss (g)	Total Mass Loss (g)
S1	9.29	9.246	0.044	9.209	0.037	9.156	0.053	9.118	0.038	9.017	0.101	0.273

VECTUS PIPE ON 220 GRIT SiC ABRASIVE												
		1 min elapsed		2 min elapsed		3 min elapsed		4 min elapsed		5 min elapsed		
Sample number	Initial Mass (g)	Mass (g)	Loss (g)	Mass (g)	Loss (g)	Mass (g)	Loss (g)	Mass (g)	Loss (g)	Mass (g)	Loss (g)	Total Mass Loss (g)
V1	1.853	1.762	0.091	1.705	0.057	1.652	0.053	1.557	0.095	1.435	0.122	0.418
V2	1.910	1.826	0.084	1.729	0.097	1.588	0.141	1.438	0.150	1.284	0.154	0.626
V3	1.939	1.816	0.123	1.681	0.135	1.529	0.152	1.360	0.169	1.044	0.316	0.895
V4	1.947	1.847	0.100	1.785	0.062	1.717	0.068	1.608	0.109	1.463	0.145	0.484
V5	1.863	1.757	0.106	1.674	0.083	1.530	0.144	1.290	0.240	1.128	0.162	0.735
V6	1.776	1.663	0.113	1.576	0.087	1.395	0.180	1.210	0.186	1.044	0.166	0.732

FLOWTITE PIPE ON 220 GRIT SiC ABRASIVE												
		1 min elapsed		2 min elapsed		3 min elapsed		4 min elapsed		5 min elapsed		
Sample number	Initial Mass (g)	Mass (g)	Loss (g)	Mass (g)	Loss (g)	Mass (g)	Loss (g)	Mass (g)	Loss (g)	Mass (g)	Loss (g)	Total Mass Loss (g)
F3	1.545	1.327	0.218	1.113	0.214	0.985	0.128	0.892	0.093	0.793	0.099	0.752
F4	1.542	1.319	0.223	1.085	0.234	0.965	0.120	0.822	0.083	0.791	0.091	0.751
F5	1.608	1.321	0.287	1.110	0.211	0.985	0.125	0.845	0.140	0.749	0.096	0.859
F6	1.430	1.225	0.205	0.999	0.226	0.901	0.098	0.808	0.093	0.717	0.091	0.713
F7	1.545	1.271	0.274	1.041	0.230	0.898	0.143	0.842	0.056	0.752	0.090	0.793
F8	1.457	1.191	0.266	0.984	0.207	0.890	0.094	0.836	0.054	0.799	0.037	0.658

STEEL PIPE ON 220 GRIT SiC ABRASIVE												
		1 min elapsed		2 min elapsed		3 min elapsed		4 min elapsed		5 min elapsed		
Sample number	Initial Mass (g)	Mass (g)	Loss (g)	Mass (g)	Loss (g)	Mass (g)	Loss (g)	Mass (g)	Loss (g)	Mass (g)	Loss (g)	Total Mass Loss (g)
S2	9.376	9.367	0.009	9.360	0.007	9.342	0.018	9.330	0.012	9.324	0.006	0.052

VECTUS PIPE ON 600 GRIT SiC ABRASIVE												
		1 min elapsed		2 min elapsed		3 min elapsed		4 min elapsed		5 min elapsed		
Sample number	Initial Mass (g)	Mass (g)	Loss (g)	Mass (g)	Loss (g)	Mass (g)	Loss (g)	Mass (g)	Loss (g)	Mass (g)	Loss (g)	Total Mass Loss (g)
V13	1.883	1.852	0.031	1.804	0.048	1.759	0.045	1.729	0.03	1.709	0.020	0.174
V14	1.936	1.900	0.036	1.856	0.044	1.819	0.037	1.791	0.028	1.762	0.029	0.174
V15	1.927	1.900	0.027	1.852	0.048	1.811	0.041	1.763	0.048	1.735	0.028	0.192
V16	1.730	1.694	0.036	1.651	0.043	1.629	0.022	1.607	0.022	1.589	0.018	0.141
V17	1.935	1.883	0.052	1.841	0.042	1.818	0.023	1.798	0.02	1.773	0.025	0.162
V18	1.875	1.846	0.029	1.804	0.042	1.769	0.035	1.732	0.037	1.707	0.025	0.168

FLOWTITE PIPE ON 600 GRIT SiC ABRASIVE												
		1 min elapsed		2 min elapsed		3 min elapsed		4 min elapsed		5 min elapsed		
Sample number	Initial Mass (g)	Mass (g)	Loss (g)	Mass (g)	Loss (g)	Mass (g)	Loss (g)	Mass (g)	Loss (g)	Mass (g)	Loss (g)	Total Mass Loss (g)
F17	1.562	1.468	0.094	1.340	0.128	1.250	0.090	1.168	0.082	1.104	0.064	0.452
F18	1.555	1.463	0.092	1.359	0.104	1.262	0.097	1.187	0.075	1.119	0.068	0.436
F19	1.394	1.274	1.169	1.169	0.105	1.076	0.093	0.990	0.086	0.952	0.038	0.422
F20	1.486	1.371	0.115	1.237	0.134	1.115	0.122	1.044	0.071	1.011	0.033	0.475
F21	1.54	1.444	0.096	1.341	0.103	1.232	0.109	1.149	0.083	1.088	0.061	0.452
F22	1.551	1.452	0.099	1.331	0.121	1.241	0.090	1.146	0.095	1.085	0.061	0.466

STEEL PIPE ON 600 GRIT SiC ABRASIVE												
		1 min elapsed		2 min elapsed		3 min elapsed		4 min elapsed		5 min elapsed		
Sample number	Initial Mass (g)	Mass (g)	Loss (g)	Mass (g)	Loss (g)	Mass (g)	Loss (g)	Mass (g)	Loss (g)	Mass (g)	Loss (g)	Total Mass Loss (g)
S3	9.09	9.075	0.015	9.059	0.016	9.036	0.023	9.017	0.019	9.006	0.011	0.084

Appendix C

Jet-Impact test results

Sample A								
Test date								
Type	Flowtite							
Water flow rate (L/hr)	480							
Water flow rate (g/s)	133.296							
Operating pressure (kPa)								
Sample thickness (mm)	5.34							
Impact angle (deg)	90							
Particle batch size	0.4-0.85							
D50 distribution (mm)	0.622							
Particle impact velocity (m/s)	4.72							
Sand mass (g)	Time increment (s)	Elapsed time (s)	Sand flow-rate (g/s)	Sand to water wt%	Hole depth (mm)	Wear (mm)	Sample wall thickness (mm)	Sample wear rate (mm/s)
0	0	0	0.000	0.000	0	0.00	5.34	0.000000
1000	69	69	14.493	9.806	0.93	0.93	4.41	0.013478
2000	131	200	7.634	5.417	1.80	0.87	3.54	0.006641
3000	35	235	28.571	17.651	2.30	0.50	3.04	0.014286
4000	44	279	22.727	14.567	2.77	0.47	2.57	0.010682

5000	111	390	9.009	6.331	3.26	0.49	2.08	0.004414
6000	116	506	8.621	6.074	3.76	0.50	1.58	0.004310
7000	80	586	12.500	8.574	4.45	0.69	0.89	0.008625
8000	54	640	18.519	12.198	4.73	0.28	0.61	0.005185
9000	57	697	17.544	11.631	4.92	0.19	0.42	0.003333
10000	53	750	18.868	12.400	5.34	0.42	0.00	0.007925
			14.408	9.513		0.485		0.007171

Minimum wear rate	0.003333
Average wear rate	0.007171
Maximum wear rate	0.014286
Total time	750

Sample B	
Test date	
Type	Vectus
Water flow rate (L/hr)	480
Water flow rate (g/s)	133.296
Operating pressure (kPa)	
Sample thickness (mm)	6.02
Impact angle (deg)	90
Particle batch size	0.4-0.85

D50 distribution (mm)	0.622							
Particle impact velocity (m/s)	4.72							
Sand mass (g)	Time increment (s)	Elapsed time (s)	Sand flow-rate (g/s)	Sand to water wt%	Hole depth (mm)	Wear (mm)	Sample wall thickness (mm)	Sample wear rate (mm/s)
0	0	0	0.000	0.000	0.00	0.00	6.02	0.000000
1000	43	43	23.256	14.855	0.45	0.45	5.57	0.010465
2000	65	108	15.385	10.347	1.27	0.82	4.75	0.012615
3000	52	160	19.231	12.608	2.06	0.79	3.96	0.015192
4000	60	220	16.667	11.114	2.71	0.65	3.31	0.010833
5000	46	266	21.739	14.022	3.16	0.45	2.86	0.009783
6000	70	336	14.286	9.680	3.70	0.54	2.32	0.007714
7000	58	394	17.241	11.453	4.07	0.37	1.95	0.006379
8000	63	457	15.873	10.641	4.21	0.14	1.81	0.002222
9000	67	524	14.925	10.070	4.80	0.59	1.22	0.008806
10000	45	569	22.222	4.425	5.12	0.32	0.90	0.007111
11000	70	639	14.286	9.680	5.31	0.19	0.71	0.002714
12000	63	702	15.873	10.641	5.70	0.39	0.32	0.006190
13000	75	777	13.333	9.093	6.02	0.32	0.00	0.004267
			16.023	9.902		0.430		0.007450

Minimum wear rate	0.002222
Average wear rate	0.007450

Maximum wear rate	0.015192
Total time	777

Sample C								
Test date								
Type	Flowtite							
Water flow rate (L/hr)	340							
Water flow rate (g/s)	94.418							
Oppering pressure (kPa)								
Sample thickness (mm)	5.25							
Impact angle (deg)	90							
Particle batch size	0.4-0.85							
D50 distribution (mm)	0.622							
Particle impact velocity (m/s)	3.34							
Sand mass (g)	Time increment (s)	Elapsed time (s)	Sand flow-rate (g/s)	Sand to water wt%	Hole depth (mm)	Wear (mm)	Sample wall thickness (mm)	Sample wear rate (mm/s)
0	0	0	0.000	0.000	0.00	0.00	5.25	0.000000
1000	75	75	13.333	12.374	0.70	0.70	4.55	0.009333
2000	100	175	10.000	9.577	1.23	0.53	4.02	0.005300
3000	63	238	15.873	14.392	1.60	0.37	3.65	0.005873
4000	60	298	16.667	15.004	1.80	0.20	3.45	0.003333
5000	63	361	15.873	14.392	2.00	0.20	3.25	0.003175

6000	56	417	17.857	15.905	2.10	0.10	3.15	0.001786
7000	75	492	13.333	12.374	2.30	0.20	2.95	0.002667
8000	63	555	15.873	14.392	2.53	0.23	2.72	0.003651
9000	64	619	15.625	14.199	2.70	0.17	2.55	0.002656
10000	60	679	16.667	15.004	2.87	0.17	2.38	0.002833
11000	63	742	15.873	14.392	3.01	0.14	2.24	0.002222
12000	80	822	12.500	11.691	3.20	0.19	2.05	0.002375
13000	89	911	11.236	10.635	3.43	0.23	1.82	0.002584
14000	86	997	11.628	10.965	3.63	0.20	1.62	0.002326
15000	83	1080	12.048	11.316	3.89	0.26	1.36	0.003133
16000	59	1139	16.949	15.219	4.04	0.15	1.21	0.002542
17000	86	1225	11.628	10.965	4.25	0.21	1.00	0.002442
18000	67	1292	14.925	13.650	4.39	0.14	0.86	0.002090
19000	62	1354	16.129	14.590	4.55	0.16	0.70	0.002581
20000	69	1423	14.493	13.307	4.74	0.19	0.51	0.002754
21000	64	1487	15.625	14.199	4.80	0.06	0.45	0.000937
22000	68	1555	14.706	13.476	4.90	0.10	0.35	0.001471
23000	78	1633	12.821	11.955	5.25	0.00	0.00	0.000000
			13.819	12.666		0.204		0.002836

Minimum wear rate	0.000937
Average wear rate	0.0028360

Maximum wear rate	0.0093330
Total time	1633

Sample D								
Test date								
Type	Vectus							
Water flow rate (L/hr)	340							
Water flow rate (g/s)	94.418							
Operating pressure (kPa)								
Sample thickness (mm)	5.64							
Impact angle (deg)	90							
Particle batch size	0.4-0.85							
D50 distribution (mm)	0.622							
Particle impact velocity (m/s)	3.34							
Sand mass (g)	Time increment (s)	Elapsed time (s)	Sand flow-rate (g/s)	Sand to water wt%	Hole depth (mm)	Wear (mm)	Sample wall thickness (mm)	Sample wear rate (mm/s)
0	0	0	0.000	0.000	0.00	0.00	5.64	0.000000
1000	89	89	11.236	10.635	0.45	0.45	5.19	0.005056
2000	71	160	14.085	12.981	0.65	0.20	4.99	0.002817
3000	77	237	12.987	12.092	0.84	0.19	4.80	0.002468
4000	77	314	12.987	12.092	1.28	0.44	4.36	0.005714
5000	86	400	11.628	10.965	1.52	0.24	4.12	0.002791

6000	80	480	12.500	11.691	1.88	0.36	3.76	0.004500
7000	75	555	13.333	12.374	2.05	0.17	3.59	0.002267
8000	88	643	11.364	10.743	2.24	0.19	3.40	0.002159
9000	81	724	12.346	11.564	2.51	0.27	3.13	0.003333
10000	80	804	12.500	11.691	2.78	0.27	2.86	0.003375
11000	70	874	14.286	13.142	2.93	0.15	2.71	0.002143
12000	88	962	11.364	10.743	3.06	0.13	2.58	0.001477
13000	76	1038	13.158	12.231	3.16	0.10	2.48	0.001316
14000	68	1106	14.706	13.476	3.26	0.10	2.38	0.001471
15000	80	1186	12.500	11.691	3.45	0.19	2.19	0.002375
16000	74	1260	13.514	12.520	3.65	0.20	1.99	0.002703
17000	90	1350	11.111	10.529	3.89	0.24	1.75	0.002667
18000	82	1432	12.195	11.439	4.06	0.17	1.58	0.002073
19000	86	1518	11.628	10.965	4.29	0.23	1.35	0.002674
20000	85	1603	11.765	11.080	4.45	0.16	1.19	0.001882
21000	89	1692	11.236	10.635	4.65	0.20	0.99	0.002247
22000	90	1782	11.111	10.529	4.72	0.07	0.92	0.000778
23000	90	1872	11.111	10.529	4.95	0.23	0.69	0.002556
24000	88	1960	11.364	10.743	5.04	0.09	0.60	0.001023
25000	87	2047	11.494	10.853	5.20	0.16	0.44	0.001839
26000	91	2138	10.989	10.425	5.24	0.04	0.40	0.000440
27000	90	2228	11.111	10.529	5.31	0.07	0.33	0.000778

27446	60	2288	7.433	7.298	5.64	0.33	0.00	0.005500
			11.622	10.903		0.194		0.002428

Minimum wear rate	0.000440
Average wear rate	0.002428
Maximum wear rate	0.005714
Total time	2288

Sample E								
Test date								
Type	Flowtite							
Water flow rate (L/hr)	250							
Water flow rate (g/s)	69.425							
Oppering pressure (kPa)								
Sample thickness (mm)	5.61							
Impact angle (deg)	90							
Particle batch size	0.4-0.85							
D50 distribution (mm)	0.622							
Particle impact velocity (m/s)	2.46							
Sand mass (g)	Time increment (s)	Elapsed time (s)	Sand flow-rate (g/s)	Sand to water wt%	Hole depth (mm)	Wear (mm)	Sample wall thickness (mm)	Sample wear rate (mm/s)
0	0	0	0.000	0.000	0.00	0.00	5.61	0.000000

1000	147	144	6.803	8.924	0.37	0.37	5.24	0.002517
2000	144	294	6.944	9.093	0.81	0.44	4.80	0.003056
3000	150	438	6.667	8.761	1.20	0.39	4.41	0.002600
4000	144	571	6.944	9.093	1.45	0.25	4.16	0.001736
5000	133	717	7.519	9.772	1.55	0.10	4.06	0.000752
6000	146	858	6.849	8.980	1.75	0.20	3.86	0.001370
7000	141	998	7.092	9.269	1.90	0.15	3.71	0.001064
8000	140	1163	7.143	9.329	2.06	0.16	3.55	0.001143
9000	165	1331	6.061	8.029	2.21	0.15	3.40	0.000909
10000	168	1486	5.952	7.897	2.37	0.16	3.24	0.000952
11000	155	1646	6.452	8.503	2.46	0.09	3.15	0.000581
12000	160	1802	6.250	8.259	2.50	0.04	3.11	0.000250
13000	156	1994	6.410	8.453	2.57	0.07	3.04	0.000449
14000	192	2148	5.208	6.979	2.77	0.20	2.84	0.001042
15000	154	2296	6.494	8.553	2.93	0.16	2.68	0.001039
16000	148	2457	6.757	8.869	3.06	0.13	2.55	0.000878
17000	161	2596	6.211	8.212	3.17	0.11	2.44	0.000683
18000	139	2767	7.194	9.390	3.45	0.28	2.16	0.002014
19000	171	2923	5.848	7.769	3.77	0.32	1.84	0.001871
20000	156	3057	6.410	8.453	3.87	0.10	1.74	0.000641
21000	134	3189	7.463	9.706	3.97	0.10	1.64	0.000746
22000	132	3324	7.576	9.839	4.14	0.17	1.47	0.001288
23000	135	3470	7.407	9.641	4.26	0.12	1.35	0.000889

24000	146	3610	6.849	8.980	4.51	0.25	1.10	0.001712
25000	140	3762	7.143	9.329	4.60	0.09	1.01	0.000643
26000	152	3906	6.579	8.656	4.71	0.11	0.90	0.000724
27000	144	4046	6.944	9.093	4.76	0.05	0.85	0.000347
28000	140	4196	7.143	9.329	4.85	0.09	0.76	0.000643
29000	150	4327	6.667	8.761	4.87	0.02	0.74	0.000133
30000	131	4460	7.634	9.906	4.99	0.12	0.62	0.000916
31000	133	4595	7.519	9.772	5.09	0.10	0.52	0.000752
32000	135	4727	7.407	9.641	5.11	0.02	0.50	0.000148
33000	132	4861	7.576	9.839	5.15	0.04	0.46	0.000303
34000	134	4992	7.463	9.706	5.17	0.02	0.44	0.000149
35000	131	5124	7.634	9.906	5.21	0.04	0.40	0.000305
36000	132	5260	7.576	9.839	5.27	0.06	0.34	0.000455
37000	136	5395	7.353	9.577	5.33	0.06	0.28	0.000441
38000	135	5526	7.407	9.641	5.40	0.07	0.21	0.000519
39000	131	5526	7.634	9.906	5.61	0.21	0.00	0.001603
			6.755	8.841		0.140		0.000957

Minimum wear rate	0.000133
Average wear rate	0.000957
Maximum wear rate	0.003056
Total time	5526

.Sample F								
Test date								
Type	Vectus							
Water flow rate (L/hr)	250							
Water flow rate (g/s)	69.425							
Operating pressure (kPa)								
Sample thickness (mm)	5.6							
Impact angle (deg)	90							
Particle batch size	0.4-0.85							
D50 distribution (mm)	0.622							
Particle impact velocity (m/s)	2.46							
Sand mass (g)	Time increment (s)	Elapsed time (s)	Sand flow-rate (g/s)	Sand to water wt%	Hole depth (mm)	Wear (mm)	Sample wall thickness (mm)	Sample wear rate (mm/s)
0	0	0	0.000	0.000	0.00	0.00	5.60	0.000000
1000	100	100	10.000	12.590	0.01	0.01	5.59	0.000100
2000	125	225	8.000	10.333	0.33	0.32	5.27	0.002560
3000	120	345	8.333	10.717	0.60	0.27	5.00	0.002250
4000	105	450	9.524	12.063	0.80	0.20	4.80	0.001905
5000	100	550	10.000	12.590	0.94	0.14	4.66	0.001400
6000	105	655	9.524	12.063	1.01	0.07	4.59	0.000667
7000	100	755	10.000	12.590	1.08	0.07	4.52	0.000700
8000	105	860	9.524	12.063	1.36	0.28	4.24	0.002667

9000	102	962	9.804	12.374	1.54	0.18	4.06	0.001765
10000	104	1066	9.615	12.165	1.77	0.23	3.83	0.002212
11000	105	1171	9.524	12.063	1.99	0.22	3.61	0.002095
12000	100	1271	10.000	12.590	2.11	0.12	3.49	0.001200
13000	101	1372	9.901	12.481	2.32	0.21	3.28	0.002079
14000	100	1472	10.000	12.590	2.46	0.14	3.14	0.001400
15000	101	1573	9.901	12.481	2.60	0.14	3.00	0.001386
16000	100	1673	10.000	12.590	2.75	0.15	2.85	0.001500
17000	105	1778	9.524	12.063	2.83	0.08	2.77	0.000762
18000	103	1881	9.709	12.269	2.90	0.07	2.70	0.000680
19000	105	1986	9.524	12.063	3.13	0.23	2.47	0.002190
20000	105	2091	9.524	12.063	3.19	0.06	2.41	0.000571
21000	106	2197	9.434	11.963	3.24	0.05	2.36	0.000472
22000	100	2297	10.000	12.590	3.28	0.04	2.32	0.000400
23000	100	2397	10.000	12.590	3.29	0.01	2.31	0.000100
24000	101	2498	9.901	12.481	3.42	0.13	2.18	0.001287
25000	100	2598	10.000	12.590	3.51	0.09	2.09	0.000900
26000	101	2699	9.901	12.481	3.63	0.12	1.97	0.001188
27000	100	2799	10.000	12.590	3.77	0.14	1.83	0.001400
28000	100	2899	10.000	12.590	3.86	0.09	1.74	0.000900
29000	101	3000	9.901	12.481	3.94	0.08	1.66	0.000792
30000	100	3100	10.000	12.590	4.06	0.12	1.54	0.001200

31000	100	3200	10.000	12.590	4.13	0.07	1.47	0.000700
32000	99	3299	10.101	12.702	4.28	0.15	1.32	0.001515
33000	102	3401	9.804	12.374	4.36	0.08	1.24	0.000784
34000	100	3501	10.000	12.590	4.41	0.05	1.19	0.000500
35000	98	3599	10.204	12.815	4.46	0.05	1.14	0.000510
36000	100	3699	10.000	12.590	4.52	0.06	1.08	0.000600
37000	100	3799	10.000	12.590	4.55	0.03	1.05	0.000300
38000	100	3899	10.000	12.590	4.60	0.05	1.00	0.000500
39000	102	4001	9.804	12.374	4.67	0.07	0.93	0.000686
40000	98	4099	10.204	12.815	4.71	0.04	0.89	0.000408
41000	97	4196	10.309	12.930	4.75	0.04	0.85	0.000412
42000	107	4303	9.346	11.865	4.90	0.15	0.70	0.001402
43000	100	4403	10.000	12.590	5.05	0.15	0.55	0.001500
44000	104	4507	9.615	12.165	5.11	0.06	0.49	0.000577
45000	100	4607	10.000	12.590	5.19	0.08	0.41	0.000800
46000	110	4717	9.091	11.578	5.35	0.16	0.25	0.001455
47000	100	4817	10.000	12.590	5.56	0.21	0.04	0.002100
48000	63	4880	15.873	18.609	5.60	0.04	0.00	0.000635
			9.702	12.218		0.114		0.001104

Minimum wear rate	0.000100
Average wear rate	0.001104

Maximum wear rate	0.002100
Total time	4880

Sample G								
Test date								
Type	Flowtite							
Water flow rate (L/hr)	480							
Water flow rate (g/s)	133.296							
Operating pressure (kPa)								
Sample thickness (mm)	5.34							
Impact angle (deg)	90							
Particle batch size	0.6-1.2							
D50 distribution (mm)	0.85							
Particle impact velocity (m/s)	4.72							
Sand mass (g)	Time increment (s)	Elapsed time (s)	Sand flow-rate (g/s)	Sand to water wt%	Hole depth (mm)	Wear (mm)	Sample wall thickness (mm)	Sample wear rate (mm/s)
0	0	0	0.000	0.000	0	0.00	5.34	0.000000
1000	75	75	13.333	9.093	1.60	1.60	3.74	0.021333
2000	74	149	13.514	9.205	2.37	0.77	2.97	0.010405
3000	77	226	12.987	8.878	3.12	0.75	2.22	0.009740
4000	77	303	12.987	8.878	3.59	0.47	1.75	0.006104
5000	75	378	13.333	9.093	3.98	0.39	1.36	0.005200
6000	74	452	13.514	9.205	4.53	0.55	0.81	0.007432

7000	75	527	13.333	9.093	4.90	0.37	0.44	0.004933
7789	58	585	13.603	9.260	5.34	0.44	0.00	0.007586
			11.845	8.078		0.593		0.008082

Minimum wear rate	0.004933
Average wear rate	0.008082
Maximum wear rate	0.021333
Total time	585

Sample H								
Test date								
Type	Vectus							
Water flow rate (L/hr)	480							
Water flow rate (g/s)	133.296							
Operating pressure (kPa)								
Sample thickness (mm)	5.85							
Impact angle (deg)	90							
Particle batch size	0.6-1.2							
D50 distribution (mm)	0.85							
Particle impact velocity (m/s)	4.72							
Sand mass (g)	Time increment (s)	Elapsed time (s)	Sand flow-rate (g/s)	Sand to water wt%	Hole depth (mm)	Wear (mm)	Sample wall thickness (mm)	Sample wear rate (mm/s)
0	0	0	0.000	0.000	0.00	0.00	5.85	0.000000

1000	80	80	12.500	8.574	0.70	0.70	5.15	0.008750
2000	77	160	12.987	8.878	1.46	0.76	4.39	0.009870
3000	75	237	13.333	9.093	2.32	0.86	3.53	0.011467
4000	77	312	12.987	8.878	3.00	0.68	2.85	0.008831
5000	81	389	12.346	8.477	3.71	0.71	2.14	0.008765
6000	75	470	13.333	9.093	4.45	0.74	1.40	0.009867
7000	77	545	12.987	8.878	4.90	0.45	0.95	0.005844
8000	75	622	13.333	9.093	5.40	0.50	0.45	0.006667
8165	18	697	9.167	6.434	5.85	0.45	0.00	0.025000
			11.297	7.740			0.585	0.009506

Minimum wear rate	0.005844
Average wear rate	0.009506
Maximum wear rate	0.025000
Total time	697

Sample I	
Test date	
Type	Flowtite
Water flow rate (L/hr)	340
Water flow rate (g/s)	94.418
Oppering pressure (kPa)	
Sample thickness (mm)	5.6

Impact angle (deg)	90							
Particle batch size	0.6-1.2							
D50 distribution (mm)	0.85							
Particle impact velocity (m/s)	3.34							
Sand mass (g)	Time increment (s)	Elapsed time (s)	Sand flow-rate (g/s)	Sand to water wt%	Hole depth (mm)	Wear (mm)	Sample wall thickness (mm)	Sample wear rate (mm/s)
0	0	0	0.000	0.000	0	0.00	5.60	0.000000
1000	76	76	13.158	12.231	0.90	0.90	4.70	0.011842
2000	74	150	13.514	12.520	1.40	0.50	4.20	0.006757
3000	73	223	13.699	12.670	1.56	0.16	4.04	0.002192
4000	71	294	14.085	12.981	1.81	0.25	3.79	0.003521
5000	73	367	13.699	12.670	1.95	0.14	3.65	0.001918
6000	77	444	12.987	12.092	2.24	0.29	3.36	0.003766
7000	71	515	14.085	12.981	2.38	0.14	3.22	0.001972
8000	70	585	14.286	13.142	2.70	0.32	2.90	0.004571
9000	70	655	14.286	13.142	2.76	0.06	2.84	0.000857
10000	71	726	14.085	12.981	2.95	0.19	2.65	0.002676
11000	77	803	12.987	12.092	3.25	0.30	2.35	0.003896
12000	72	875	13.889	12.824	3.45	0.20	2.15	0.002778
13000	70	945	14.286	13.142	3.67	0.22	1.93	0.003143
14000	71	1016	14.085	12.981	3.77	0.10	1.83	0.001408
15000	75	1091	13.333	12.374	3.83	0.06	1.77	0.000800
16000	70	1161	14.286	13.142	4.03	0.20	1.57	0.002857

17000	73	1234	13.699	12.670	4.08	0.05	1.52	0.000685
18000	71	1305	14.085	12.981	4.20	0.12	1.40	0.001690
19000	71	1376	14.085	12.981	4.25	0.05	1.35	0.000704
20000	74	1450	13.514	12.520	4.40	0.15	1.20	0.002027
21000	70	1520	14.286	13.142	4.50	0.10	1.10	0.001429
22000	70	1590	14.286	13.142	4.63	0.13	0.97	0.001857
23000	71	1661	14.085	12.981	4.74	0.11	0.86	0.001549
24000	77	1738	12.987	12.092	4.83	0.09	0.77	0.001169
25000	76	1814	13.158	12.231	4.93	0.10	0.67	0.001316
26000	77	1891	12.987	12.092	5.13	0.20	0.47	0.002597
27000	71	1962	14.085	12.981	5.20	0.07	0.40	0.000986
28000	70	2032	14.286	13.142	5.26	0.06	0.34	0.000857
29000	70	2102	14.286	13.142	5.36	0.10	0.24	0.001429
30000	75	2177	13.333	12.374	5.60	0.24	0.00	0.003200
			13.352	12.337		0.181		0.002466

Minimum wear rate	0.000685
Average wear rate	0.002466
Maximum wear rate	0.011842
Total time	2177

Sample J								
Test date								
Type	Vectus							
Water flow rate (L/hr)	340							
Water flow rate (g/s)	94.418							
Operating pressure (kPa)								
Sample thickness (mm)	5.8							
Impact angle (deg)	90							
Particle batch size	0.6-1.2							
D50 distribution (mm)	0.85							
Particle impact velocity (m/s)	3.34							
Sand mass (g)	Time increment (s)	Elapsed time (s)	Sand flow-rate (g/s)	Sand to water wt%	Hole depth (mm)	Wear (mm)	Sample wall thickness (mm)	Sample wear rate (mm/s)
0	0	0	0.000	0.000	0.00	0.00	5.80	0.000000
1000	78	78	12.821	11.955	0.31	0.31	5.49	0.003974
2000	73	151	13.699	12.670	0.50	0.19	5.30	0.002603
3000	80	231	12.500	11.691	0.73	0.23	5.07	0.002875
4000	70	301	14.286	13.142	0.88	0.15	4.92	0.002143
5000	72	373	13.889	12.824	0.91	0.03	4.89	0.000417
6000	73	446	13.699	12.670	1.40	0.49	4.40	0.006712
7000	74	520	13.514	12.520	1.68	0.28	4.12	0.003784
8000	70	590	14.286	13.142	1.91	0.23	3.89	0.003286
9000	71	661	14.085	12.981	2.17	0.26	3.63	0.003662

10000	70	731	14.286	13.142	2.43	0.26	3.37	0.003714
11000	71	802	14.085	12.981	2.55	0.12	3.25	0.001690
12000	71	873	14.085	12.981	2.77	0.22	3.03	0.003099
13000	71	944	14.085	12.981	2.96	0.19	2.84	0.002676
14000	75	1019	13.333	12.374	3.14	0.18	2.66	0.002400
15000	70	1089	14.286	13.142	3.30	0.16	2.50	0.002286
16000	70	1159	14.286	13.142	3.43	0.13	2.37	0.001857
17000	73	1232	13.699	12.670	3.60	0.17	2.20	0.002329
18000	74	1306	13.514	12.520	3.75	0.15	2.05	0.002027
19000	70	1376	14.286	13.142	3.80	0.05	2.00	0.000714
20000	71	1447	14.085	12.981	3.90	0.10	1.90	0.001408
21000	70	1517	14.286	13.142	3.96	0.06	1.84	0.000857
22000	80	1597	12.500	11.691	4.20	0.24	1.60	0.003000
23000	80	1677	12.500	11.691	4.44	0.24	1.36	0.003000
24000	75	1752	13.333	12.374	4.58	0.14	1.22	0.001867
25000	76	1828	13.158	12.231	4.70	0.12	1.10	0.001579
26000	72	1900	13.889	12.824	4.90	0.20	0.90	0.002778
27000	70	1970	14.286	13.142	5.07	0.17	0.73	0.002429
28000	71	2041	14.085	12.981	5.13	0.06	0.67	0.000845
29000	74	2115	13.514	12.520	5.28	0.15	0.52	0.002027
30000	70	2185	14.286	13.142	5.80	0.52	0.00	0.007429
			13.311	12.303		0.187		0.002563

Minimum wear rate	0.000417
Average wear rate	0.002563
Maximum wear rate	0.003714
Total time	2185

Sample K								
Test date								
Type	Flowtite							
Water flow rate (L/hr)	250							
Water flow rate (g/s)	69.425							
Operating pressure (kPa)								
Sample thickness (mm)	5.55							
Impact angle (deg)	90							
Particle batch size	0.6-1.2							
D50 distribution (mm)	0.85							
Particle impact velocity (m/s)	2.46							
Sand mass (g)	Time increment (s)	Elapsed time (s)	Sand flow-rate (g/s)	Sand to water wt%	Hole depth (mm)	Wear (mm)	Sample wall thickness (mm)	Sample wear rate (mm/s)
0	0	0	0.000	0.000	0.00	0.00	5.55	0.000000
1000	74	74	13.514	16.293	0.10	0.10	5.45	0.001351
2000	77	151	12.987	15.759	0.32	0.22	5.23	0.002857
3000	76	227	13.158	15.933	0.35	0.03	5.20	0.000395
4000	72	299	13.889	16.671	0.53	0.18	5.02	0.002500

5000	73	372	13.699	16.480	0.65	0.12	4.90	0.001644
6000	70	442	14.286	17.066	0.82	0.17	4.73	0.002429
7000	77	519	12.987	15.759	1.01	0.19	4.54	0.002468
8000	70	589	14.286	17.066	1.11	0.10	4.44	0.001429
9000	71	660	14.085	16.866	1.20	0.09	4.35	0.001268
10000	76	736	13.158	15.933	1.30	0.10	4.25	0.001316
11000	70	806	14.286	17.066	1.44	0.14	4.11	0.002000
12000	71	877	14.085	16.866	1.52	0.08	4.03	0.001127
13000	71	948	14.085	16.866	1.54	0.02	4.01	0.000282
14000	70	1018	14.286	17.066	1.56	0.02	3.99	0.000286
15000	75	1093	13.333	16.111	1.60	0.04	3.95	0.000533
16000	71	1164	14.085	16.866	1.61	0.01	3.94	0.000141
17000	74	1238	13.514	16.293	1.70	0.09	3.85	0.001216
18000	74	1312	13.514	16.293	1.77	0.07	3.78	0.000946
19000	70	1382	14.286	17.066	1.80	0.03	3.75	0.000429
20000	70	1452	14.286	17.066	1.88	0.08	3.67	0.001143
21000	70	1522	14.286	17.066	1.95	0.07	3.60	0.001000
22000	71	1593	14.085	16.866	2.01	0.06	3.54	0.000845
23000	70	1663	14.286	17.066	2.05	0.04	3.50	0.000571
24000	73	1736	13.699	16.480	2.10	0.05	3.45	0.000685
25000	70	1806	14.286	17.066	2.15	0.05	3.40	0.000714
26000	71	1877	14.085	16.866	2.21	0.06	3.34	0.000845
27000	76	1953	13.158	15.933	2.30	0.09	3.25	0.001184

28000	77	2030	12.987	15.759	2.39	0.09	3.16	0.001169
29000	77	2107	12.987	15.759	2.48	0.09	3.07	0.001169
30000	71	2178	14.085	16.866	2.58	0.10	2.97	0.001408
31000	70	2248	14.286	17.066	2.61	0.03	2.94	0.000429
32000	70	2318	14.286	17.066	2.69	0.08	2.86	0.001143
33000	71	2389	14.085	16.866	2.73	0.04	2.82	0.000563
34000	70	2459	14.286	17.066	2.80	0.07	2.75	0.001000
35000	77	2536	12.987	15.759	2.92	0.12	2.63	0.001558
36000	70	2606	14.286	17.066	3.02	0.10	2.53	0.001429
37000	76	2682	13.158	15.933	3.10	0.08	2.45	0.001053
38000	70	2752	14.286	17.066	3.13	0.03	2.42	0.000429
39000	73	2825	13.699	16.480	3.18	0.05	2.37	0.000685
40000	70	2895	14.286	17.066	3.21	0.03	2.34	0.000429
41000	72	2967	13.889	16.671	3.29	0.08	2.26	0.001111
42000	74	3041	13.514	16.293	3.35	0.06	2.20	0.000811
43000	77	3118	12.987	15.759	3.40	0.05	2.15	0.000649
44000	78	3196	12.821	15.588	3.40	0.00	2.15	0.000000
45000	77	3273	12.987	15.759	3.56	0.16	1.99	0.002078
46000	72	3345	13.889	16.671	3.59	0.03	1.96	0.000417
47000	77	3422	12.987	15.759	3.65	0.06	1.90	0.000779
48000	70	3492	14.286	17.066	3.71	0.06	1.84	0.000857
49000	78	3570	12.821	15.588	3.75	0.04	1.80	0.000513
50000	77	3647	12.987	15.759	3.78	0.03	1.77	0.000390

51000	72	3719	13.889	16.671	3.83	0.05	1.72	0.000694
52000	78	3797	12.821	15.588	3.90	0.07	1.65	0.000897
53000	77	3874	12.987	15.759	3.96	0.06	1.59	0.000779
54000	70	3944	14.286	17.066	3.98	0.02	1.57	0.000286
55000	70	4014	14.286	17.066	4.00	0.02	1.55	0.000286
56000	71	4085	14.085	16.866	4.07	0.07	1.48	0.000986
57000	70	4155	14.286	17.066	4.10	0.03	1.45	0.000429
58000	70	4225	14.286	17.066	4.14	0.04	1.41	0.000571
59000	75	4300	13.333	16.111	4.19	0.05	1.36	0.000667
60000	70	4370	14.286	17.066	4.25	0.06	1.30	0.000857
61000	71	4441	14.085	16.866	4.34	0.09	1.21	0.001268
62000	70	4511	14.286	17.066	4.36	0.02	1.19	0.000286
63000	70	4581	14.286	17.066	4.46	0.10	1.09	0.001429
64000	70	4651	14.286	17.066	4.54	0.08	1.01	0.001143
65000	70	4721	14.286	17.066	4.58	0.04	0.97	0.000571
66000	70	4791	14.286	17.066	4.61	0.03	0.94	0.000429
67000	71	4862	14.085	16.866	4.67	0.06	0.88	0.000845
68000	70	4932	14.286	17.066	4.70	0.03	0.85	0.000429
69000	70	5002	14.286	17.066	4.72	0.02	0.83	0.000286
70000	70	5072	14.286	17.066	4.74	0.02	0.81	0.000286
71000	70	5142	14.286	17.066	4.81	0.07	0.74	0.001000
72000	71	5213	14.085	16.866	4.83	0.02	0.72	0.000282
73000	70	5283	14.286	17.066	4.93	0.10	0.62	0.001429

74000	70	5353	14.286	17.066	5.23	0.30	0.32	0.004286
75000	70	5423	14.286	17.066	5.55	0.32	0.00	0.004571
			13.668	16.410		0.073		0.001009

Minimum wear rate	0.000141
Average wear rate	0.001009
Maximum wear rate	0.004571
Total time	5423

Sample L								
Test date								
Type	Vectus							
Water flow rate (L/hr)	250							
Water flow rate (g/s)	69.425							
Operating pressure (kPa)								
Sample thickness (mm)	5.7							
Impact angle (deg)	90							
Particle batch size	0.6-1.2							
D50 distribution (mm)	0.85							
Particle impact velocity (m/s)	2.46							
Sand mass (g)	Time increment (s)	Elapsed time (s)	Sand flow-rate (g/s)	Sand to water wt%	Hole depth (mm)	Wear (mm)	Sample wall thickness (mm)	Sample wear rate (mm/s)

0	0	0	0.000	0.000	0.00	0.00	5.70	0.000000
1000	70	70	14.286	17.066	0.00	0.00	5.70	0.000000
2000	70	140	14.286	17.066	0.10	0.10	5.60	0.001429
3000	70	210	14.286	17.066	0.31	0.21	5.39	0.003000
4000	74	284	13.514	16.293	0.38	0.07	5.32	0.000946
5000	65	349	15.385	18.140	0.42	0.04	5.28	0.000615
6000	62	411	16.129	18.852	0.50	0.08	5.20	0.001290
7000	65	476	15.385	18.140	0.52	0.02	5.18	0.000308
8000	65	541	15.385	18.140	0.57	0.05	5.13	0.000769
9000	64	605	15.625	18.372	0.60	0.03	5.10	0.000469
10000	65	670	15.385	18.140	0.62	0.02	5.08	0.000308
11000	62	732	16.129	18.852	0.83	0.21	4.87	0.003387
12000	63	795	15.873	18.609	1.00	0.17	4.70	0.002698
13000	69	864	14.493	17.270	1.09	0.09	4.61	0.001304
14000	67	931	14.925	17.694	1.25	0.16	4.45	0.002388
15000	70	1001	14.286	17.066	1.36	0.11	4.34	0.001571
16000	65	1066	15.385	18.140	1.42	0.06	4.28	0.000923
17000	65	1131	15.385	18.140	1.49	0.07	4.21	0.001077
18000	64	1195	15.625	18.372	1.60	0.11	4.10	0.001719
19000	63	1258	15.873	18.609	1.64	0.04	4.06	0.000635
20000	63	1321	15.873	18.609	1.70	0.06	4.00	0.000952
21000	70	1391	14.286	17.066	1.85	0.15	3.85	0.002143
22000	69	1460	14.493	17.270	1.95	0.10	3.75	0.001449

23000	66	1526	15.152	17.915	2.07	0.12	3.63	0.001818
24000	65	1591	15.385	18.140	2.13	0.06	3.57	0.000923
25000	67	1658	14.925	17.694	2.17	0.04	3.53	0.000597
26000	63	1721	15.873	18.609	2.20	0.03	3.50	0.000476
27000	62	1783	16.129	18.852	2.23	0.03	3.47	0.000484
28000	66	1849	15.152	17.915	2.32	0.09	3.38	0.001364
29000	67	1916	14.925	17.694	2.38	0.06	3.32	0.000896
30000	62	1978	16.129	18.852	2.45	0.07	3.25	0.001129
31000	62	2040	16.129	18.852	2.48	0.03	3.22	0.000484
32000	63	2103	15.873	18.609	2.50	0.02	3.20	0.000317
33000	61	2164	16.393	19.102	2.57	0.07	3.13	0.001148
34000	62	2226	16.129	18.852	2.64	0.07	3.06	0.001129
35000	64	2290	15.625	18.372	2.72	0.08	2.98	0.001250
36000	70	2360	14.286	17.066	2.81	0.09	2.89	0.001286
37000	62	2422	16.129	18.852	2.83	0.02	2.87	0.000323
38000	64	2486	15.625	18.372	2.89	0.06	2.81	0.000938
39000	62	2548	16.129	18.852	2.93	0.04	2.77	0.000645
40000	64	2612	15.625	18.372	2.94	0.01	2.76	0.000156
41000	63	2675	15.873	18.609	2.96	0.02	2.74	0.000317
42000	66	2741	15.152	17.915	2.98	0.02	2.72	0.000303
43000	61	2802	16.393	19.102	3.00	0.02	2.70	0.000328
44000	62	2864	16.129	18.852	3.02	0.02	2.68	0.000323
45000	62	2926	16.129	18.852	3.06	0.04	2.64	0.000645

46000	62	2988	16.129	18.852	3.08	0.02	2.62	0.000323
47000	70	3058	14.286	17.066	3.11	0.03	2.59	0.000429
48000	61	3119	16.393	19.102	3.13	0.02	2.57	0.000328
49000	65	3184	15.385	18.140	3.17	0.04	2.53	0.000615
50000	61	3245	16.393	19.102	3.24	0.07	2.46	0.001148
51000	62	3307	16.129	18.852	3.25	0.01	2.45	0.000161
52000	67	3374	14.925	17.694	3.26	0.01	2.44	0.000149
53000	65	3439	15.385	18.140	3.30	0.04	2.40	0.000615
54000	66	3505	15.152	17.915	3.33	0.03	2.37	0.000455
55000	70	3575	14.286	17.066	3.38	0.05	2.32	0.000714
56000	74	3649	13.514	16.293	3.45	0.07	2.25	0.000946
57000	67	3716	14.925	17.694	3.55	0.10	2.15	0.001493
58000	67	3783	14.925	17.694	3.63	0.08	2.07	0.001194
59000	61	3844	16.393	19.102	3.65	0.02	2.05	0.000328
60000	62	3906	16.129	18.852	3.70	0.05	2.00	0.000806
61000	67	3973	14.925	17.694	3.73	0.03	1.97	0.000448
62000	62	4035	16.129	18.852	3.77	0.04	1.93	0.000645
63000	68	4103	14.706	17.480	3.82	0.05	1.88	0.000735
64000	63	4166	15.873	18.609	3.88	0.06	1.82	0.000952
65000	64	4230	15.625	18.372	3.92	0.04	1.78	0.000625
66000	70	4300	14.286	17.066	3.97	0.05	1.73	0.000714
67000	62	4362	16.129	18.852	4.01	0.04	1.69	0.000645
68000	70	4432	14.286	17.066	4.05	0.04	1.65	0.000571

69000	71	4503	14.085	16.866	4.07	0.02	1.63	0.000282
70000	64	4567	15.625	18.372	4.12	0.05	1.58	0.000781
71000	70	4637	14.286	17.066	4.15	0.03	1.55	0.000429
72000	61	4698	16.393	19.102	4.19	0.04	1.51	0.000656
73000	69	4767	14.493	17.270	4.27	0.08	1.43	0.001159
74000	70	4837	14.286	17.066	4.37	0.10	1.33	0.001429
75000	70	4907	14.286	17.066	4.46	0.09	1.24	0.001286
76000	71	4978	14.085	16.866	4.52	0.06	1.18	0.000845
77000	74	5052	13.514	16.293	4.54	0.02	1.16	0.000270
78000	72	5124	13.889	16.671	4.59	0.05	1.11	0.000694
79000	73	5197	13.699	16.480	4.68	0.09	1.02	0.001233
80000	67	5264	14.925	17.694	4.77	0.09	0.93	0.001343
81000	68	5332	14.706	17.480	4.81	0.04	0.89	0.000588
82000	67	5399	14.925	17.694	4.86	0.05	0.84	0.000746
83000	67	5466	14.925	17.694	4.88	0.02	0.82	0.000299
84000	67	5533	14.925	17.694	4.92	0.04	0.78	0.000597
85000	71	5604	14.085	16.866	4.95	0.03	0.75	0.000423
86000	64	5668	15.625	18.372	5.00	0.05	0.70	0.000781
87000	61	5729	16.393	19.102	5.05	0.05	0.65	0.000820
88000	67	5796	14.925	17.694	5.07	0.02	0.63	0.000299
89000	65	5861	15.385	18.140	5.11	0.04	0.59	0.000615
90000	67	5928	14.925	17.694	5.17	0.06	0.53	0.000896
91000	69	5997	14.493	17.270	5.70	0.53	0.00	0.007681

15.052	17.776		0.062		0.000933
--------	--------	--	-------	--	----------

Minimum wear rate	0.000149
Average wear rate	0.000933
Maximum wear rate	0.007681
Total time	5997

Sample M								
Test date								
Type	Flowtite							
Water flow rate (L/hr)	480							
Water flow rate (g/s)	133.296							
Oppering pressure (kPa)								
Sample thickness (mm)	5.4							
Impact angle (deg)	90							
Particle batch size	0.6-1.5							
D50 distribution (mm)	1.268							
Particle impact velocity (m/s)	4.72							
Sand mass (g)	Time increment (s)	Elapsed time (s)	Sand flow-rate (g/s)	Sand to water wt%	Hole depth (mm)	Wear (mm)	Sample wall thickness (mm)	Sample wear rate (mm/s)
0	0	0	0.000	0.000	0	0.00	5.40	0.000000
1000	85	85	11.765	8.110	2.17	2.17	3.23	0.025529

2000	81	166	12.346	8.477	3.03	0.86	2.37	0.010617
3000	83	249	12.048	8.289	4.08	1.05	1.32	0.012651
4000	80	329	12.500	8.574	4.70	0.62	0.70	0.007750
5000	75	404	13.333	9.093	5.40	0.70	0.00	0.009333
			10.332	7.091		0.900		0.010980

Minimum wear rate	0.007750
Average wear rate	0.010980
Maximum wear rate	0.025529
Total time	404

Sample N	
Test date	
Type	Vectus
Water flow rate (L/hr)	480
Water flow rate (g/s)	133.296
Operating pressure (kPa)	
Sample thickness (mm)	5.75
Impact angle (deg)	90
Particle batch size	0.6-1.5
D50 distribution (mm)	1.268
Particle impact velocity (m/s)	4.72

Sand mass (g)	Time increment (s)	Elapsed time (s)	Sand flow-rate (g/s)	Sand to water wt%	Hole depth (mm)	Wear (mm)	Sample wall thickness (mm)	Sample wear rate (mm/s)
0	0	0	0.000	0.000	0	0.00	5.75	0.000000
1000	88	88	11.364	7.855	1.26	1.26	4.49	0.014318
2000	75	163	13.333	9.093	2.47	1.21	3.28	0.016133
3000	78	241	12.821	8.774	3.19	0.72	2.56	0.009231
4000	73	314	13.699	9.319	3.68	0.49	2.07	0.006712
5000	75	389	13.333	9.093	4.27	0.59	1.48	0.007867
6000	70	459	14.286	9.680	4.75	0.48	1.00	0.006857
7000	75	534	13.333	9.093	5.75	1.00	0.00	0.013333
			11.521	7.864		0.719		0.009306

Minimum wear rate	0.006712
Average wear rate	0.009306
Maximum wear rate	0.016133
Total time	534